

AD-A166 286

AN INVESTIGATION OF TURBULENCE MECHANISMS IN V/STOL
UPWASH FLOW FIELDS. (U) GRUMMAN AEROSPACE CORP BETHPAGE
NY RESEARCH AND DEVELOPMENT C. B GILBERT 15 SEP 85

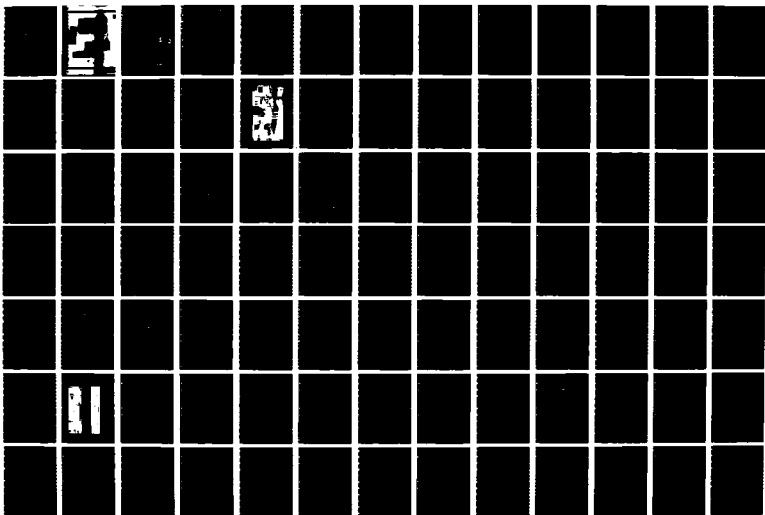
1/4

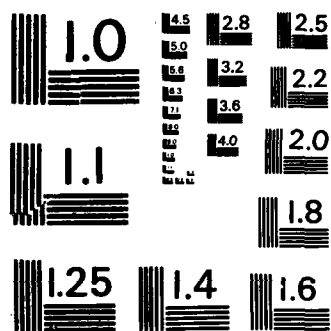
UNCLASSIFIED

RE-787 AFOSR-TR-86-0096 F49620-82-C-0025

F/G 20/4

NL





MICROCOPY RESOLUTION TEST CHART
NATIONAL BUREAU OF STANDARDS-1963-A

GRUMMAN AEROSPACE CORPORATION

4FOSR-TR- 83-0096

REPORT RE-707

AN INVESTIGATION OF TURBULENCE MECHANISMS
IN V/STOL UPWASH FLOW FIELDS

SEPTEMBER 1985


Approved for public release,
distribution unlimited

AD-A166 286

DTIC
ELECTE
S APR 03 1986
D

DTIC FILE COPY

RESEARCH & DEVELOPMENT CENTER

AIR FORCE OFFICE OF SCIENTIFIC RESEARCH (AFSC) 
NOTICE OF TRANSMITTAL TO DTIC
This technical report has been reviewed and is
approved for public release IAW AFM 190-12.
Distribution is unlimited.
MATTHEW J. KERNER
Chief, Technical Information Division

AFOSR-TR- 86 - 0096

REPORT RE-707

**AN INVESTIGATION OF TURBULENCE MECHANISMS
IN V/STOL UPWASH FLOW FIELDS**

SEPTEMBER 1985

Approved for public release,
distribution unlimited

prepared by

Barry L. Gilbert
Aerosciences Directorate

Corporate Research Center
Grumman Corporation
Bethpage, New York 11714

Final Report on
Contract F49620-82-C-0025
For the period March 15, 1982 through June 15, 1985

prepared for

Dr. James D. Wilson
External Aerodynamics and Fluid Mechanics
Air Force Office of Scientific Research
Bolling AFB, Washington D.C. 20332

**DTIC
ELECTE
APR 03 1986**
S D

Approved by


Richard A. Scheuing, V.P.
Corporate Research Center

UNCLASSIFIED

AD-A166286

REPORT DOCUMENTATION PAGE

1a. REPORT SECURITY CLASSIFICATION Unclassified			1b. RESTRICTIVE MARKINGS		
2a. SECURITY CLASSIFICATION AUTHORITY			3. DISTRIBUTION / AVAILABILITY OF REPORT Approved for public release, distribution unlimited Unrestrictive		
2b. DECLASSIFICATION / DOWNGRADING SCHEDULE			5. MONITORING ORGANIZATION REPORT NUMBER AFOSR-TR-86-0096		
4. PERFORMING ORGANIZATION REPORT NUMBER(S) RE-707			7a. NAME OF MONITORING ORGANIZATION Air Force Office of Scientific Research		
6a. NAME OF PERFORMING ORGANIZATION Grumman Aerospace		6b. OFFICE SYMBOL (if applicable)	7b. ADDRESS (City, State, and ZIP Code) Bolling AFB, Washington D.C. 20332		
6c. ADDRESS (City, State, and ZIP Code) Bethpage NY 11714		9. PROCUREMENT INSTRUMENT IDENTIFICATION NUMBER F49620-82-C-0025			
8a. NAME OF FUNDING SPONSORING ORGANIZATION Air Force Office of Scientific Research		8b. OFFICE SYMBOL (if applicable)	10. SOURCE OF FUNDING NUMBERS		
8c. ADDRESS (City, State, and ZIP Code) Bolling AFB, Washington D.C. 20332		PROGRAM ELEMENT NO 61102F	PROJECT NO 2307	TASK NO A1	WORK UNIT ACCESSION NO
11. TITLE (Include Security Classification) An Investigation of Turbulence Mechanisms in V/STOL Upwash Flow Fields					
12. PERSONAL AUTHOR(S) Barry Gilbert					
13a. TYPE OF REPORT Final		13b. TIME COVERED FROM 3/82 TO 6/85		14. DATE OF REPORT (Year, Month, Day) 1985, August 15 Sept.	
15. PAGE COUNT 70					
16. SUPPLEMENTARY NOTATION					
17. COSATI CODES			18. SUBJECT TERMS (Continue on reverse if necessary and identify by block number)		
FIELD	GROUP	SUB-GROUP	↓ This report presents results		
Were investigated					
19. ABSTRACT (Continue on reverse if necessary and identify by block number) Presented are the results of the first three years of an experimental investigation of the abnormally high turbulent mixing layer growth rate characteristics found in the upwash regions of V/STOL flows in ground effect. The approach adopted is to investigate the fundamental turbulent V/STOL upwash mechanisms in increasingly more complex flow configurations. Most of this study uses utilizes the two-dimensional upwash formed by the collision of opposed two-dimensional wall jets. Initial parameters used to characterize the upwash formation were identified as the maximum wall jet velocity and wall jet half velocity width. Upwash measurements were taken in flows formed from equal wall jets with the same maximum velocities and equal wall jets with the same half widths. Velocity profiles were obtained at seven locations in the upwash. All three components of velocity were measured as well as second, third and fourth moments. These higher moments are					
20. DISTRIBUTION / AVAILABILITY OF ABSTRACT <input checked="" type="checkbox"/> UNCLASSIFIED/UNLIMITED <input type="checkbox"/> SAME AS RPT <input type="checkbox"/> DTIC USERS			21. ABSTRACT SECURITY CLASSIFICATION Unclassified		
22a. NAME OF RESPONSIBLE INDIVIDUAL JAMES D WILSON			22b. TELEPHONE (Include Area Code) 202/ 767-4935		22c. OFFICE SYMBOL AFOSR/NA

UNCLASSIFIED

found as terms in the turbulent kinetic energy equation. These data are presented in similarity form. While mixing layer growth rates were larger than those found in a free two-dimensional jet, these values were less than those reported by previous investigators. An explanation based on non-similarity conditions in the flow is offered. The abnormally high turbulence levels reported by other investigators were not found. The increased growth rate seem to be a direct effect of the head-on collision process. There is an indication that in the far field the upwash growth characteristics are approaching those found in free jets. This has profound implications to the turbulence modelers. Measurements were taken in the upwash region formed by the collision of unequal wall jets. These results compare favorably to a simple theory. By choosing a coordinate system aligned with the upwash, these data can be characterized in a pattern similar to the equal wall jet case. Obstacles of various heights were placed at the collision point of equal wall jets. Away from the influences of the obstacle's wake, the upwash exhibited increasing decay rates with decreasing obstacle heights. This behavior asymptotes to the no-obstacle case for small obstacles and to twice the wall jet growth for large obstacles. A radial wall jet facility was constructed to create a more complex flow configuration. This facility employs a unique design that creates the radial wall jets from source jets below the instrumentation plate. Preliminary measurements were made in this new configuration and show increased growth rates found in the two dimension flows.

CONTENTS

<u>Section</u>	<u>Page</u>
ABSTRACT	
1. OVERVIEW.....	1
2. SIGNIFICANT ACCOMPLISHMENTS.....	5
2.1 Summary.....	5
2.2 Wall Jet.....	6
2.3 Equal Jet Upwash.....	14
2.4 Short Plate Equal Jet Upwash.....	28
2.5 Unequal Wall Jets.....	38
2.6 Unequal Jet Analysis.....	49
2.7 Centerline Obstacles.....	52
2.8 Additional Work.....	54
2.9 Radial Wall Jets.....	54
3. CONCLUSION.....	63
4. REFERENCES.....	65
APPENDIX A Case A: Short Plate, Full Speed.....	A-1
APPENDIX B Case B: Short Plate, 87% Speed.....	B-1



Accession For	
NTIS	CRA&I
DTIC	TAB
Unannounced	<input type="checkbox"/>
Justification	<input type="checkbox"/>
By <i>Per Mr. Wade</i> AFOSR	
Distribution /	
Availability Codes	
Dist	Avail and/or Special
A-1	

LIST OF ILLUSTRATIONS

<u>Figure</u>		<u>Page</u>
1	Diagram of Two-dimensional Jet Upwash Facility.....	7
2	Photograph of Two-dimensional Jet Upwash Facility.....	8
3	Coordinate System Nomenclature Conversion.....	9
4	Typical Jet Exit Velocity Profiles.....	10
5	Two-dimensional Wall Jet Characteristics.....	12
6	Wall Jet Mean Velocity Profiles in Similarity Form.....	13
7	Wall Jet Turbulence Intensity Profiles in Similarity Form....	13
8	Upwash Flow Field Vectors for Equal Wall Jets at Seven Heights.....	16
9	Spread Rate and Mean Velocity Decay in a Two-dimensional Upwash.....	18
10	Mean Velocity Profiles for Equal Wall Jet Upwash at Six Heights in Similarity Form.....	20
11	Component Turbulence Energy in the Mean Flow Direction at Six Heights.....	20
12	Component Turbulence Energy in the Cross Flow Direction at Six Heights.....	21
13	Component Turbulence Energy in the Third Orthogonal Direction at Six Heights.....	21
14	Total Turbulence Kinetic Energy in an Equal Wall Jet Upwash at Six Heights.....	22
15	Ratio of the Cross Component Turbulence Energy.....	22
16	Shear Stress Component in an Upwash at Six Heights.....	23
17	Intermittency Profiles in an Equal Jet Upwash.....	23
18	Comparisons of Mean and Turbulence Profiles for a Free 2-D Jet with a 2-D Upwash.....	25
19	Integral Scale Lengths Across 2-D Upwash.....	27
20	Taylor Micro-scale Lengths Across 2-D Upwash.....	27

<u>Figure</u>		<u>Page</u>
21	Wall Jet Mean Velocity Profiles in Similarity Form.....	30
22	Wall Jet Turbulence Intensity Profiles in Similarity Form....	30
23	Two-dimensional Wall Jet Characteristics.....	31
24	Wall Jet Mean Velocity Profiles at the Centerline for Four Source Velocities in Similarity Form.....	32
25	Wall Jet Turbulence Intensity Profiles at the Centerline for Four Source Velocities in Similarity Form.....	32
26	Mean Velocity Profiles for Equal Wall Jet Upwash at Six Heights in Similarity Form.....	33
27	Mean Velocity Profiles for Equal Wall Jet Upwash at Six Heights in Similarity Form.....	33
28	Spread Rate and Mean Velocity Decay in a Two-dimensional Upwash for Various Initial Conditions.....	35
29	Upwash Flow Field Vectors for Pressure Ratio = 1.0.....	40
30	Upwash Flow Field Vectors for Pressure Ratio = 1.2.....	41
31	Upwash Flow Field Vectors for Pressure Ratio = 1.4.....	42
32	Upwash Flow Field Vectors for Pressure Ratio = 1.6.....	43
33	Upwash Flow Field Vectors for Pressure Ratio = 1.8.....	44
34	Half Velocity Width Growth Rate in the Upwash of Unequal Wall Jets.....	45
35	Mean Velocity Decay in the Upwash of Unequal Wall Jets.....	45
36	Position of the Maximum Velocity Peak in the Upwash of Unequal Wall Jets.....	46
37	Turbulence Kinetic Energy in the Upwash of Unequal Wall Jets	47
38	Unequal Wall Jet Diagram.....	51
39	Diagram of Radial Wall Jet Design.....	56
40	Radial Wall Jet Exit Profiles.....	58
41	Radial Wall Jet Mean Velocity Decay Profile.....	59
42	Radial Wall Jet Momentum for Different Gap Heights.....	59

<u>Figure</u>		<u>Page</u>
43	Increased Mass Flow Rate for Radial Wall Jets.....	60
44	Radial Wall Jets Mean Velocity Profiles.....	60
45	Photograph of Radial Wall Jet Upwash Facility.....	61
A-1	Cross Stream Mean Velocity Profiles at Six Heights	A-2
A-2	Component Turbulent Energy in the Mean Flow Direction at Six Heights.....	A-2
A-3	Component Turbulence Energy in the Cross Flow Direction at Six Heights.....	A-3
A-4	Shear Stress Component in an Upwash at Six Heights.....	A-3
A-5	Total Turbulence Kinetic Energy in an Equal Wall Jet Upwash at Six Heights.....	A-4
A-6	Intermittency Profiles in an Equal Jet Upwash.....	A-5
A-7	Integral Scale Lengths Across 2-D Upwash.....	A-6
A-8	Taylor Micro-scale Lengths Across 2-D Upwash.....	A-7
A-9	Third Moments Across 2-D Upwash.....	A-8
A-10	Fourth Moments Across 2-D Upwash.....	A-10
B-1	Cross Stream Mean Velocity Profiles at Six Heights.....	B-1
B-2	Component Turbulent Energy in the Mean Flow Direction at Six Heights.....	B-1
B-3	Component Turbulence Energy in the Cross Flow Direction at Six Heights.....	B-2
B-4	Shear Stress Component in an Upwash at Six Heights.....	B-2
B-5	Total Turbulence Kinetic Energy in an Equal Wall Jet Upwash at Six Heights.....	B-3
B-6	Intermittency Profiles in an Equal Jet Upwash.....	B-4
B-7	Integral Scale Lengths Across 2-D Upwash.....	B-5
B-8	Taylor Micro-scale Lengths Across 2-D Upwash.....	B-6
B-9	Third Moments Across 2-D Upwash.....	B-7
B-10	Fourth Mements Across 2-D Upwash.....	B-9

LIST OF TABLES

<u>Table</u>		<u>Page</u>
1	Comparison of Initial Conditions for Three Equal Wall Jet Tests.....	34
2	Comparison of Theory with Experiments with Unequal Wall Jets	49
3	Summary of Centerline Obstacle Results.....	53

ABSTRACT

Results are presented from the first three years of an experimental investigation of the abnormally high turbulent mixing layer growth rate characteristics found in the upwash regions of V/STOL flows in ground effect. The overall objectives of this program are to examine the origin of the increased fluctuations, to characterize systematically the development and structure of the upwash, and to determine the parameters that influence these characteristics. The approach adopted is to investigate the fundamental turbulent V/STOL upwash mechanisms in increasingly more complex flow configurations.

Most of this study utilizes the two-dimensional upwash formed by the collision of opposed two-dimensional wall jets. Initial parameters used to characterize the upwash formation were identified as the maximum wall jet velocity and wall jet half velocity width. Upwash measurements were taken in flows formed from equal wall jets with the same maximum velocities and equal wall jets with the same half widths. Velocity profiles were obtained at seven locations in the upwash. All three components of velocity were measured as well as second, third and fourth moments. These higher moments are found as terms in the turbulent kinetic energy equation. These data are presented in similarity form. While mixing layer growth rates were larger than those found in a free two-dimensional jet, these values were less than those reported by previous investigators. The abnormally high turbulence levels reported by other investigators were not found. An explanation based on non-similarity conditions in the flow is offered. The increased growth rate seems to be a direct effect of the head-on collision process. There is an indication that in the far field the upwash growth characteristics are approaching those found in free jets. This has profound implications to the turbulence modelers.

As part of the study of the effect of various initial conditions, a series of measurements was taken in the upwash region formed by the collision of unequal wall jets. These results compare favorably to a simple theory. By choosing a coordinate system aligned with the upwash, these data can be characterized in a pattern similar to the equal wall jet case. Obstacles of various heights were placed at the collision point of equal wall jets. Away from the influences of the obstacle's wake, the upwash exhibited increasing

decay rates with decreasing obstacle heights. This behavior asymptotes to the no-obstacle case for small obstacles and to twice the wall jet growth for large obstacles. This shows that the increased mixing is due to the head-on collision turbulent interaction of the wall jets.

A radial wall jet facility was constructed to create a more complex flow configuration. This facility employs a unique design that creates the radial wall jets from source jets below the instrumentation plate. The upwash formed by the collision of these radial wall jets is not influenced by the presence of impinging jets. As in the two-dimensional case, this allows for the systematic investigation of the upwash phenomenon that are more representative of V/STOL flows without the additional complications introduced by the impinging jets on the ground plane and re-circulation zone between the impinging jets and the upwash. Preliminary one component measurements were made in this new configuration and show increased mixing layer growth rates. A new contract to study the upwash in a more representative flow using radial wall jets will use this facility.

1. OVERVIEW

A unique turbulent mixing phenomenon results from the collision of opposing jets. The mean velocity profile of the generated flow appears to be similar to those found in free and wall jet turbulent flows. However, the macroscopic properties of mixing layer growth rate and the corresponding mean velocity decay rate are significantly different. This combined effect means that there is a different distribution of average momentum in the flow. It also indicates that turbulence models currently employed to predict the flow behavior are inadequate. In all cases where this type of flow is found, it is important to understand properly the mixing process and the dynamics of the resulting flow.

One such flow has been identified due to the recent development of aircraft with vertical/short take-off and landing (V/STOL) capability. When a V/STOL aircraft is in ground effect, the exhaust from the aircraft lift jets interacts with the ground, producing an upwash flow directed towards the underside of the aircraft. This upwash flow (including fountains, in the case of more than two jets) has profound aerodynamic implications on the aircraft design by virtue of the additional lift force it imparts to the aircraft at its most critical point of operation, in hover. The induced aerodynamic effects due to upwash augmentation of lift forces and suckdown entrainment over the lower surfaces of only 5% of engine thrust may translate into as much as a 40% difference in mission payload or endurance (Ref. 1, 2). An understanding of the basic physical mechanisms acting in the flow field between the aircraft and the ground is vital to the successful development of a practical V/STOL aircraft.

The upwash flow is very difficult to analyze because of the much greater mixing layer growth rate compared to other types of turbulent flows (Ref. 3-9). The problem is made computationally difficult by the intrinsic three-dimensionality of the upwash and because the turbulence in this type of flow is not understood. Numerical codes require better definition of the turbulent structure in order to make reliable predictions of the fountain flow and, later, the fountain/aircraft interaction.

The objective of this research is to increase the basic understanding of the turbulent structure in the upwash and determine those parameters that

directly affect the upwash behavior. This study is primarily intended to provide a reliable data base for use in predictive computational models. The program we put forth is designed to investigate the mechanisms that control turbulence levels, mixing layer spread rate and mean velocity decay rate in the upwash fan, thereby determining the pertinent scaling parameters of the flow.

In this multi-year program, the investigation has proceeded from a simple two-dimensional flow geometry through geometries that more closely reproduce the essential characteristics of the V/STOL flow field. Although a number of investigations of overall flow in ground effect have been carried out, measurements in these highly unsteady flows are very difficult, and interpretations of these measurements vary widely (Ref. 3-9). Many experimental investigations have attempted to study the full V/STOL flow field with its full geometric complexity. Some of these have even made measurements with an aircraft planform. These are configuration specific studies that can mask the fundamental flow characteristics. The simple two-dimensional flow configuration and a simple radial flow configuration are the subjects of the current study.

In an earlier contract phase, the complex V/STOL upwash flow geometry was simplified. The lifting jet impingement region with the ground was eliminated. The radially spreading wall jets were replaced by the much simpler two-dimensional wall jets. This part of the study had the goal of isolating the specific characteristics contributing to the increased mixing rate. The upwash turbulence structure was examined in fine detail, providing for the first time a detailed data base. During the current contract phase, this initial investigation was extended to a geometry more closely related to the V/STOL flow situation. The two-dimensional wall jet was replaced by a radially spreading wall jet. The mechanisms found to affect the upwash are being tested with this geometry to study the influence of the radial upwash fan geometry. This work will be continued in the follow-on contract.

During the first year's effort, the experimental apparatus used to produce a two-dimensional upwash was designed and constructed. After the facility was running and sufficient measurements were obtained to assure two-dimensionality and uniformity of the exit profiles, detailed measurements of the wall jet profiles were obtained. These measurements are very important

since these two-dimensional wall jets represent the initial flow conditions for the formation region of the upwash. A single wire anemometer was used to measure one-component mean and turbulence profiles at six locations in the upwash. These provided a comparison set of data to the relatively small sample of upwash measurements that exist in the current literature. These data appear in the first annual report (Ref. 10).

The second year's effort included the continuation of the 2-D upwash measurements. Measurements were taken at seven heights between 1 and 8 characteristic lengths in an equal wall jet upwash using an X-wire hot film anemometer. Repeating these measurement positions with the probe rotated 90° , we determined all three velocity components. In addition, higher order turbulent moments were measured. Energy spectra and autocorrelation and crosscorrelation measurements, computed with digital fast Fourier transforms, were utilized to determine relevant length scales.

Several experiments were conducted to determine the effect of the collision position on the upwash. Using symmetry plates at the position of the collision of equal wall jets, we tested the effects of the stability of the collision point. A study was conducted on the effects of unequal wall jets on the position and turbulence structure in the upwash. These data are reported in the second annual report (Ref. 11).

The third (current) year's effort completed the investigation of the 2-D upwash geometry. Initial parameters used to characterize the upwash formation were identified as the maximum wall jet velocity and wall jet half velocity width. Upwash measurements were taken in flows formed from equal wall jets with the same maximum velocities and equal wall jets with the same half widths. Besides increasing the parameter range covered by our baseline data set, these additional tests suggest an explanation for the differences in results obtained by other investigations.

The final task was the design, construction and initial testing of a new experimental apparatus that increases the geometric complexity of the flow. A unique design was employed to produce accurately controlled radial wall jets. Two such wall jets are caused to collide and produce a radial flowing upwash. Plans for future research include use of this new facility in upwash experiments similar to those described for the 2-D upwash.

2. SIGNIFICANT ACCOMPLISHMENTS

2.1 SUMMARY

The data reported in this report represent the results of the first three years of an experimental investigation of the abnormally high turbulent mixing layer growth rate characteristics found in the upwash regions of V/STOL flows in ground effect. The first year's accomplishments were reported in detail in the first annual report (Ref. 10), and many of these results were presented at the AIAA 16th Fluid & Plasma Dynamics Conference, Danvers, MA, July 1983. The second year's accomplishments are detailed in the second annual report (Ref. 11). This year's study completes the measurements of the two-dimensional upwash formed by the collision of opposed two-dimensional wall jets. The results of this study are summarized here and expanded in the following subsections.

In the current year, we extended the data set started last year in order to determine those parameters that directly affect the upwash growth rate and turbulence structure. We have generated detailed surveys of the three components of velocity and their statistical moments for several types of wall jet collision regions. The interpretation of these data show for the first time the influence of initial starting conditions on the upwash turbulence characteristics and growth rate. By comparison with existing data by other investigators on similar flows, some of the variation in measured turbulence properties can be explained. During this year a radial wall jet facility was constructed to create a more complex flow configuration. This facility employs a unique design that creates the radial wall jets from source jets below the instrumentation plate. The upwash formed by the collision of these radial wall jets is not influenced by the presence of impinging jets. As in the two-dimensional case, this allows for the systematic investigation of the upwash phenomenon without the additional complications introduced by the impinging jets and re-circulation zone. Preliminary measurements are currently being made in this new configuration.

In previous contract years, extensive measurements have been made in the two-dimensional wall jet to establish the starting conditions of the upwash. Evaluation of these measurements has shown classical wall jet behavior, and fully developed mean and turbulence profiles at the collision zone. A unique

set of velocity profiles was obtained at seven locations in the upwash. While mixing layer growth rates were larger than those found in a free two-dimensional jet, these values were less than those reported by previous investigators. An explanation is offered later. The abnormally high turbulence levels reported by other investigators were not found. These data are presented in similarity form. Higher moments and some of the terms in the turbulence kinetic energy equation were also measured.

A series of measurements was taken in the upwash region formed by the collision of unequal wall jets. These are compared favorably to a simple theory. These data can be characterized in a pattern similar to the equal wall jet case. Obstacles of various heights were placed at the collision point of equal wall jets. Away from the influences of the obstacle's wake, the upwash exhibited increasing decay rates with decreasing obstacle heights. As expected, this behavior asymptotes to the no-obstacle case for small obstacles and to twice the wall jet growth for large obstacles.

These measurements of the turbulent characteristics found in the flow resulting from the collision of wall jets are being taken for the first time to form a detailed data base. The increased mixing found in this type of flow seems to be a direct result of the head-on collision process. The collision that forms the upwash is localized to a turning region of the order of two local wall jet heights. This is the first time that an origin region has been identified.

2.2 WALL JET

The wind tunnel facility designed and constructed for most of the first two years' effort is diagrammed in Fig. 1, and the test section is shown in Fig. 2. It is described in the first annual report (Ref. 10). To facilitate comparing the data with traditional wall and free jet data, a coordinate system was chosen that allows the X direction to be the mean direction of the largest velocity component. That is, X tracks some centerline streamline and Y is always perpendicular to it. This results in a 90° rotation of X from the wall jet to the upwash as shown in Fig. 3. For clarity, wall jet parameters are indicated with the subscript 'w'. U and u' are the mean and rms fluctuation components in the X direction. V and v' are the same components in the Y direction.

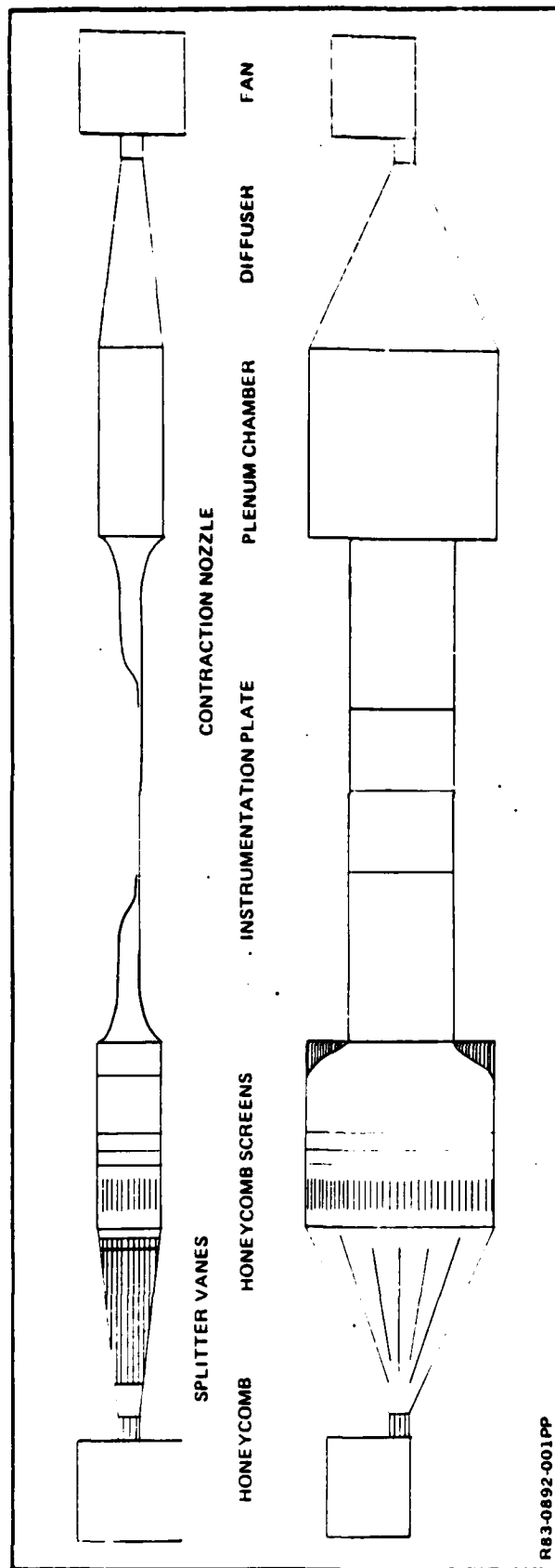


Fig. 1 Diagram of Two-dimensional Jet Upwash Facility

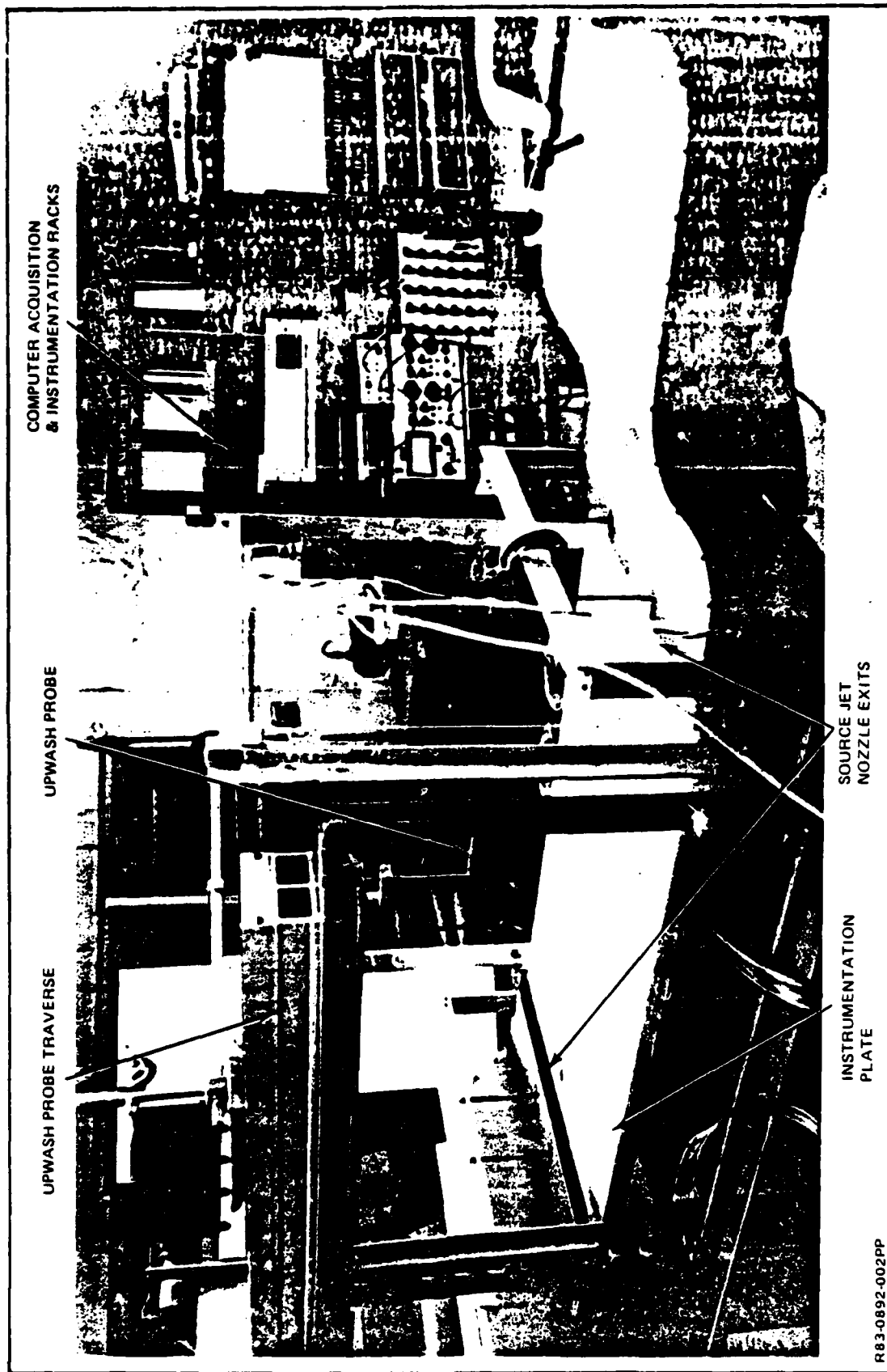


Fig. 2 Photograph of Two-dimensional Jet Upwash Facility

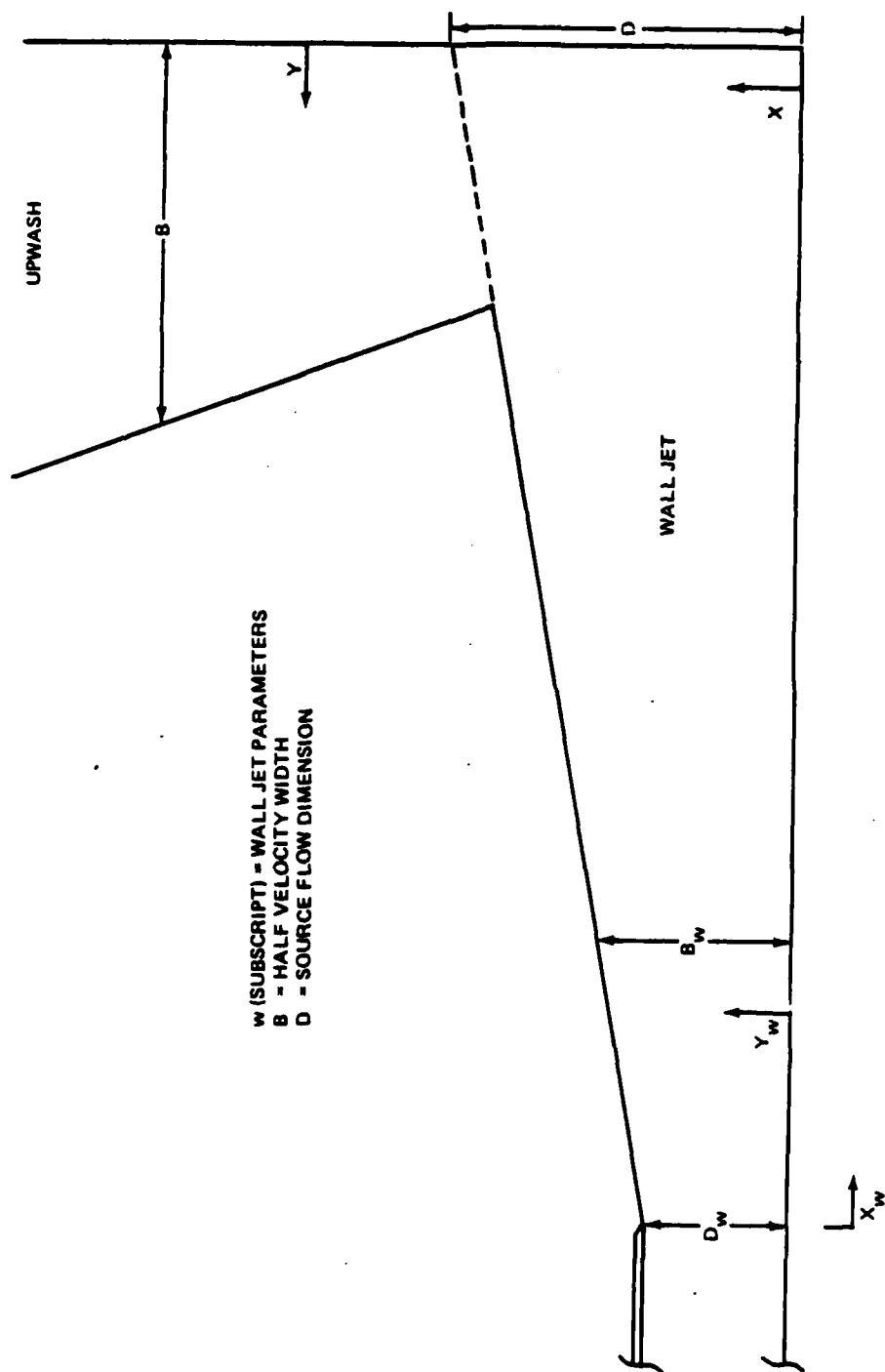


Fig. 3 Coordinate System Nomenclature Conversion

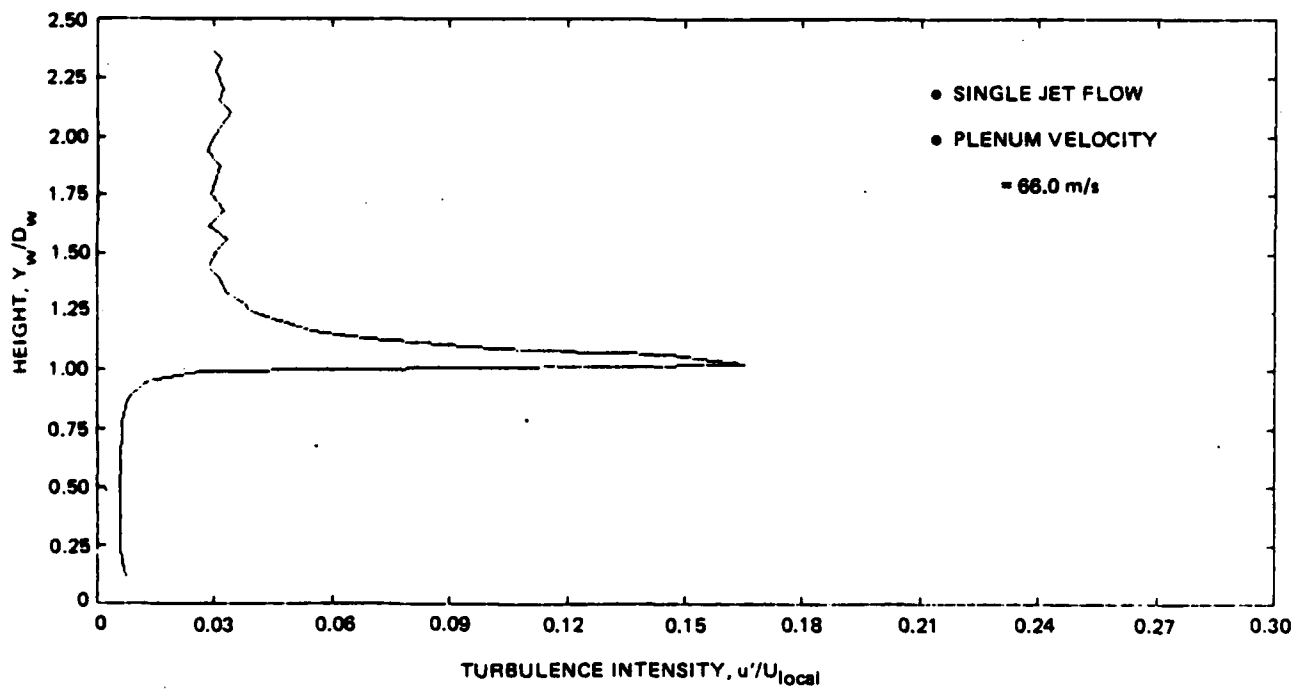
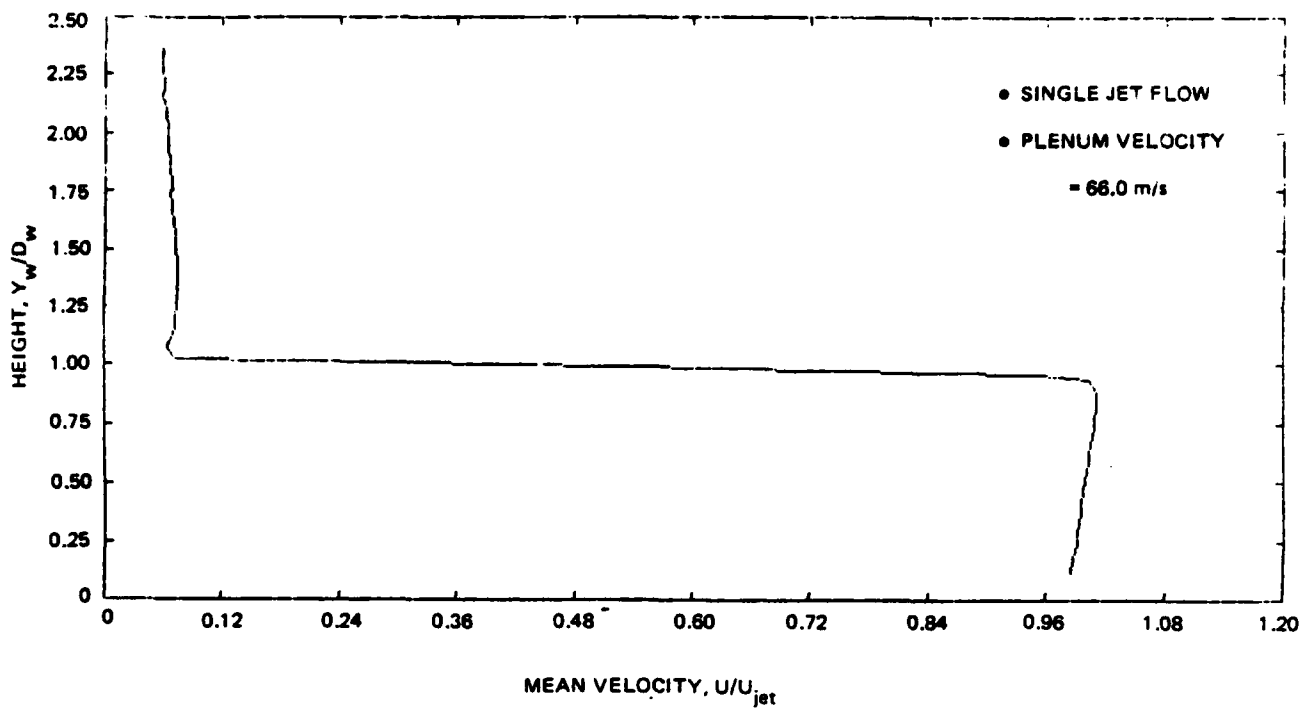
R83-0892-003PP

Figure 4 shows hot film anemometry measurements of a typical exit plane velocity profile taken vertically across the nozzle exit and includes the entrained flow velocity over the top of the nozzle. If the boundary layer is disregarded, the mean velocity is uniform to 0.75%, controllable to 67 m/s, with turbulent intensities u'/U of about 0.6%. The single jet external entrainment velocity increases from about 6.6% of the mean exit velocity to 9.7% when both wall jets are used to form an upwash. The instrumentation plate is 84 cm long (nozzle to nozzle).

Wall jet mean and turbulence profiles were taken at 20 locations from the jet exit nozzle to the instrumentation plate centerline. These measurements were made at equal distances along the plate in increments of approximately two nozzle heights. Each profile contains 24 data points. The data acquisition and positioning of the single element hot film probe were accomplished under the total control of the automatic digital data system.

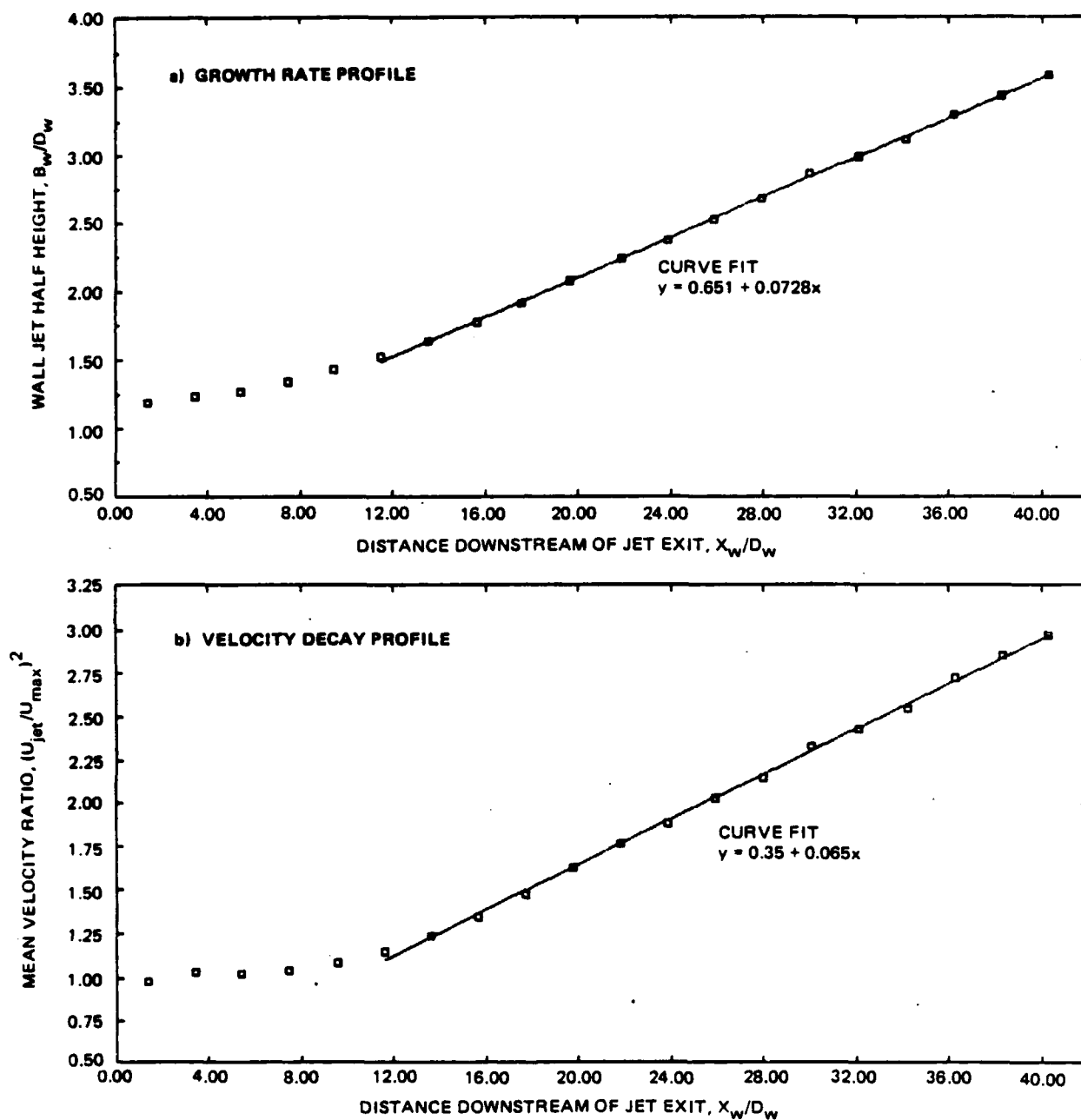
A plot of the wall jet growth rate as characterized by the half velocity height vs the distance downstream is given in Fig. 5a. A linear least squares curve fit of the data from stations 6 through 20 ($X_w/D_w > 10$) gives a growth rate of 0.0728. This is exactly the growth rate established as the "correct" value for self-preserved two-dimensional wall jets on plane surfaces at the 1980-81 AFOSR-HTTM Stanford Conference (Ref. 12) of 0.073 ± 0.002 . The first five stations were eliminated from the curve fit because they are in the development region. Figure 5b shows the linear decay of the maximum velocity squared vs distance. This relationship is required by conservation of momentum considerations. The data were normalized by the characteristic half height dimension and the 10 alternate profiles were plotted. Figure 6 shows that the mean velocity similarity exists as early as $X_w/D_w = 10$, much sooner than the 50 slot heights quoted at Stanford. Figure 7 shows the 10 alternate turbulence profiles normalized by the half velocity width. These show similarity at X_w/D_w of about 20.

The wall jet characteristics at the centerline may be determined at $X_w/D_w = 42$. The wall jet parameters when no collision occurs are appropriate based on our data to be used to normalize upwash data in a manner similar to using the wall jet nozzle height as an initial characteristic dimension. At the centerline, the wall jet half height is $B_w/D_w = 3.702 = D$ for the upwash and $U_{max}/U_{jet} = 0.571$.



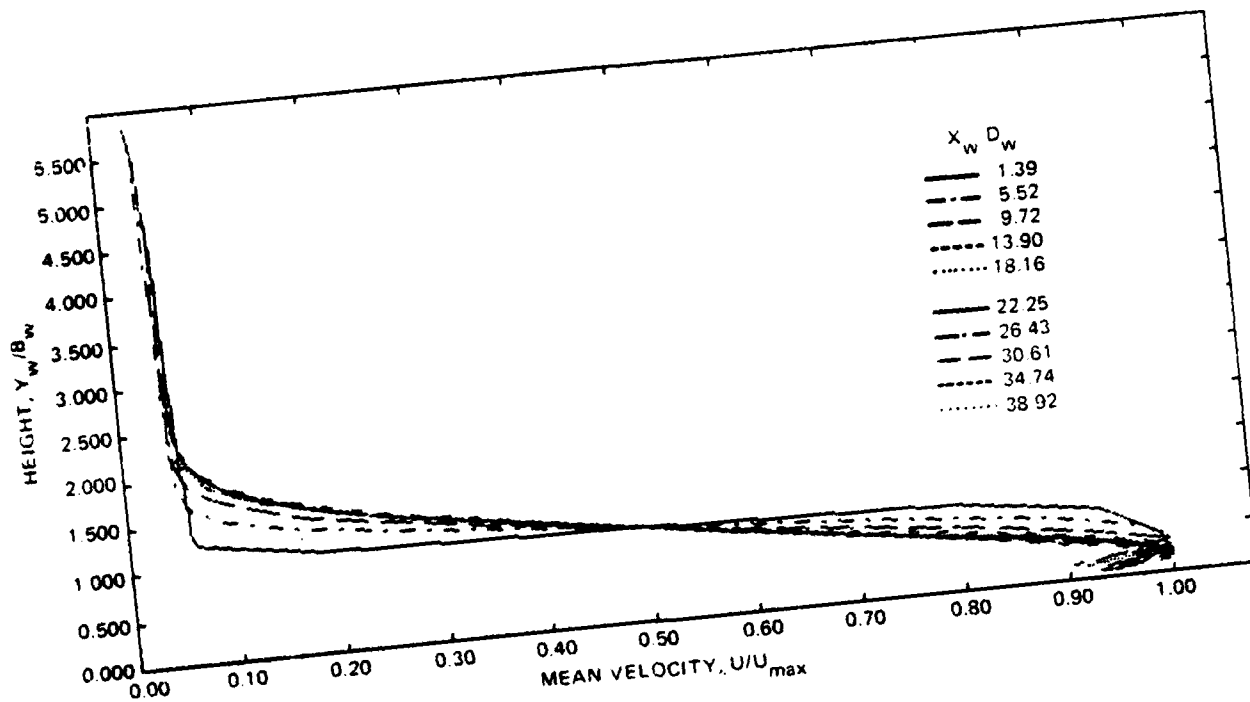
R83-0892-004PP

Fig. 4 Typical Jet Exit Velocity Profiles



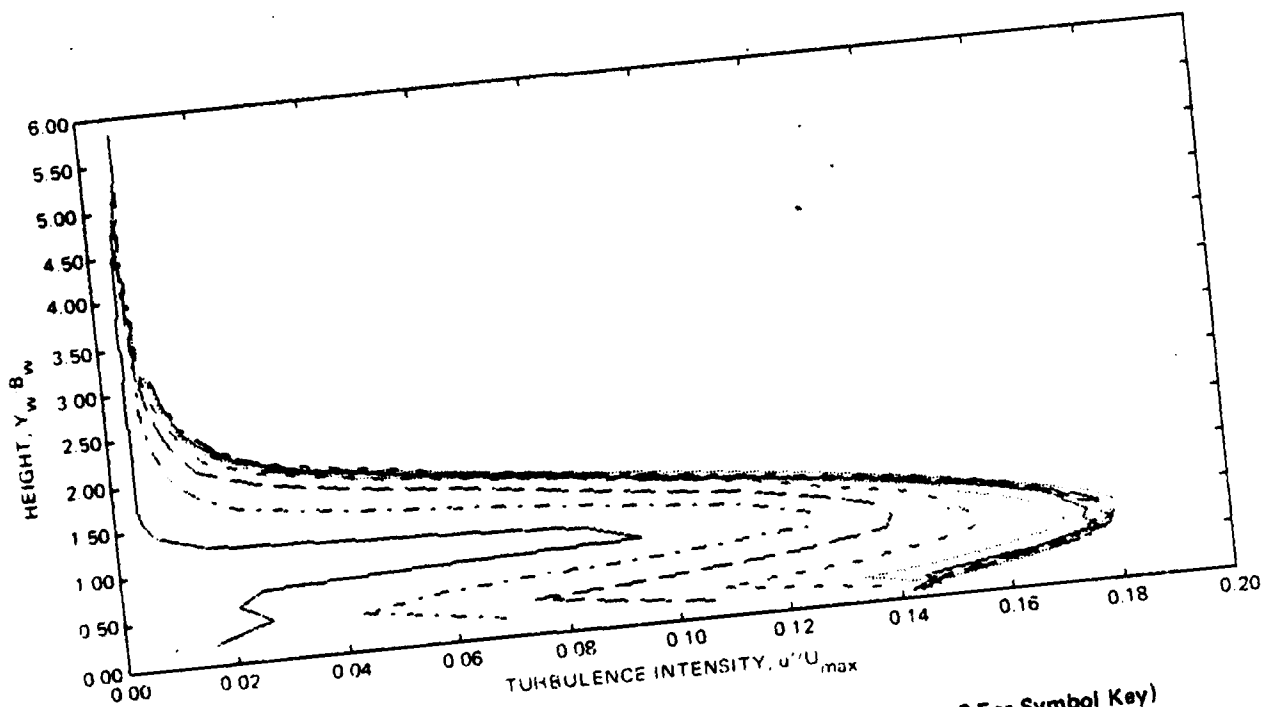
R83-0892-007PP

Fig. 5 Two-dimensional Wall Jet Characteristics



R83-0892-008PP

Fig. 6 Wall Jet Mean Velocity Profiles in Similarity Form



R83-0892-010PP

Fig. 7 Wall Jet Turbulence Intensity Profiles in Similarity Form (See Fig. 6 For Symbol Key)

2.3 EQUAL JET UPWASH

The upwash formed from the collision of two equal wall jets was probed extensively. The baseline set of measurements was taken at seven heights ($X/D = 2, 3, 4, 5, 6, 8$ and 1). At $X/D = 1$ the flow is still turning and is not yet fully in the upwash direction. This should be expected from the fact that D is the wall jet half velocity height, and therefore significant flow along the wall is above this point. These equal wall jet data were taken repeatedly and always produced the same results.

The data were taken using an X-wire hot film anemometer probe. An X-probe measures two components of the velocity simultaneously. After the mean flow and one cross flow component are measured, rotating the probe 90° about its axis provides a repeat of the mean flow and the other cross flow component. The data acquisition process was controlled by a digital computer. The program positioned the probe, acquired the data, performed the appropriate processing, and stored the processed raw data on disk. The profile information is constructed from 60 points, each 5.9 mm apart. That is, initially $\Delta y/D = 0.16$. Of course, as one continues up the upwash, the characteristic dimension gets larger and the relative data spacing gets smaller. At each point, 32,768 data pairs were taken in blocks of 4096 representing a time series of 13.4 s. There are two forms of the data analysis program. One does a complete turbulence analysis; the other computes only means, turbulence energy, and one component Reynolds stress. The complete program, in addition, computes third and fourth moments, autocorrelations and crosscorrelations, Taylor microscales and integral scales. These allow calculation of various terms in the turbulent kinetic energy equation, and intermittency. The length scales are calculated by computing the turbulence energy spectra from the time series by using fast Fourier transforms and then computing the correlation using the inverse transform. The Taylor scales were also computed from the derivative of the time series for comparison. Because taking derivatives inherently adds noise, these values are not as reliable as those obtained from the correlation except at the centerline, where the intermittency is one and the values agreed well.

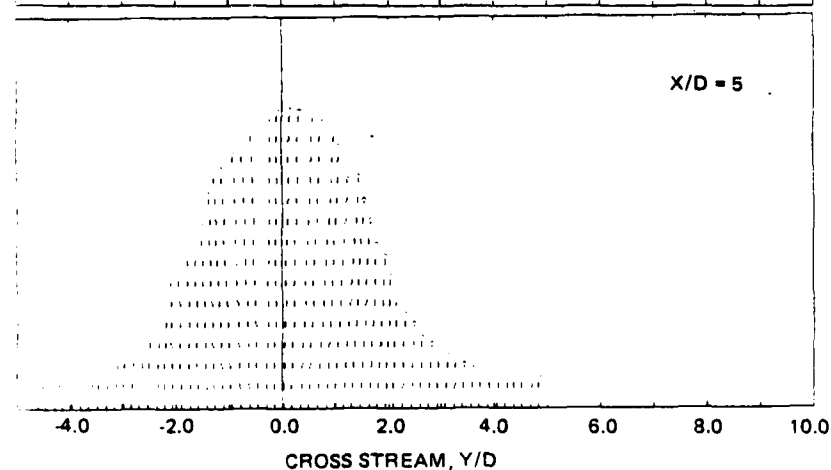
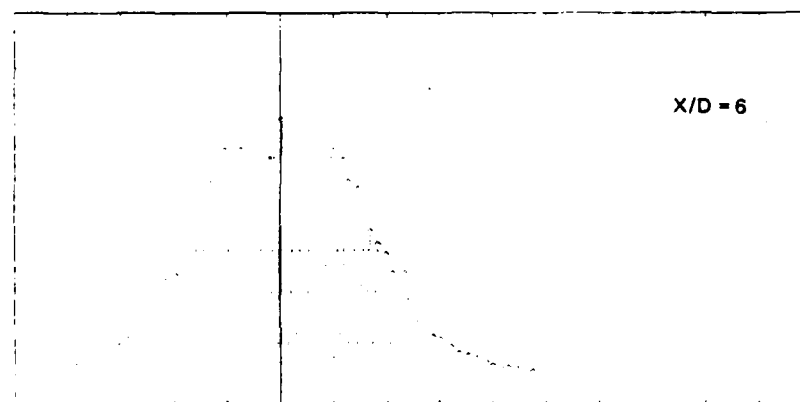
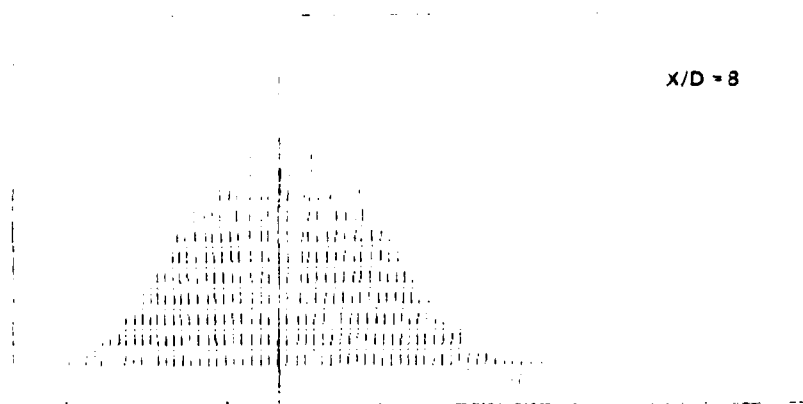
The upwash velocity vectors are shown in Fig. 8. The residual velocities in the tails are similar to other studies (Ref. 5-9). The flow in the tails

is the entrainment flow, which has been verified from smoke flow visualization studies. The mean velocity profiles are symmetric, and, beyond $X/D = 2$, the turbulence profiles have symmetric peaks. By comparison, Kotansky does not give these turbulent profile data (Ref. 7); Witze (Ref. 6) and Foley (Ref. 8) show only one-sided turbulence measurements, that is, they do not show the symmetric data; only Kind and Suthanthiran (Ref. 5) show the complete profiles and their data are not symmetric.

The mean velocity profiles in the upwash direction were curve fit with a least square curve of the form $U = A + C \exp [-(Y - Y_0)^2/2S^2]$. This curve fit gives the symmetry coordinate y_0 , the maximum velocity $(A + C)$, and the standard deviation S . Using the generally accepted definition of half velocity width, $B(U = U_{\max}/2) = 1.177 S$. It should be emphasized that our technique is far superior to the usual determination of half width. That procedure usually entails finding U_{\max} and interpolating between data points to determine B . The latter method suffers severely from scatter in the data at both U_{\max} and particularly at the half velocity point. Also, it rarely gives symmetric half velocity positions. A least squares curve fit avoids these problems. The results for the half velocity growth so defined are shown in Fig. 9a.

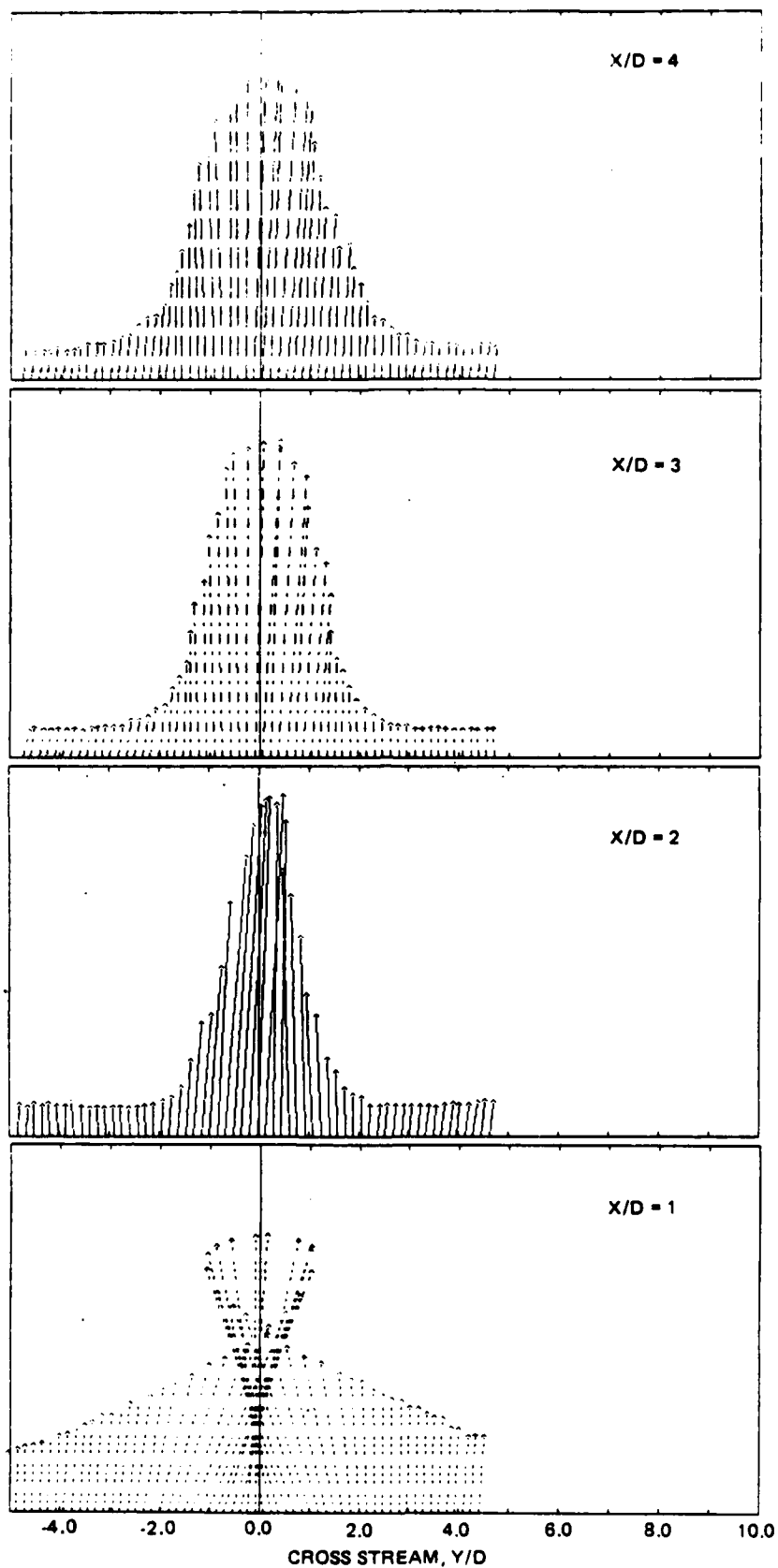
The growth rate is about 0.23, which doesn't agree with previously reported results (Ref. 5-9), but values between 0.22 and 0.23 were repeatedly obtained in these experiments. This value is more than twice the free jet value. A closer look at these other data shows inconsistency, and, in some cases, plotted data disagree with written statements. A possible explanation for this difference is given in the next section. The proper mean velocity decay characteristic is shown in Fig. 9b for X/D greater than 2.0. This is the form for the mean velocity decay required by conservation of axial momentum in the upwash; a characteristic not usually found by others. Between $X/D = 1.0$ and 2.0, the mean velocity actually increases and the mixing width decreases correspondingly. This is a strong indication that the extent of the collision zone is of the order of 2.0 D .

The mean velocity profiles at six heights are shown in Fig. 10. The profiles have been shifted to their symmetry point and normalized by the local half velocity width and local maximum mean velocity as determined by the curve fit. These similarity profiles for X/D greater than 2.0 may be expressed as



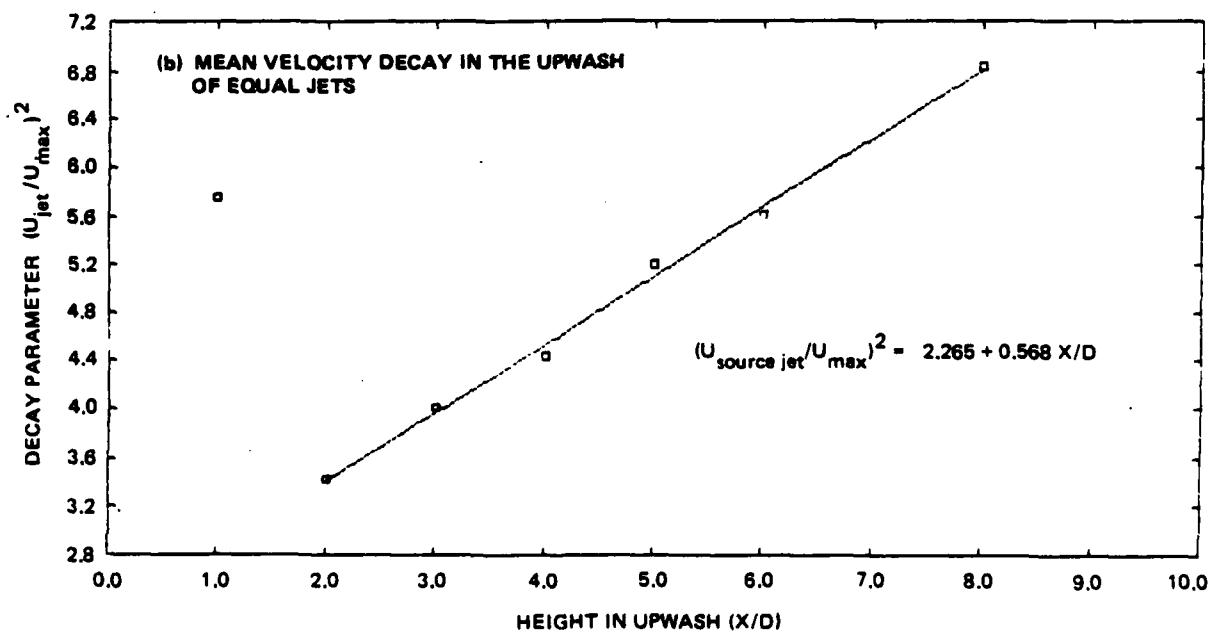
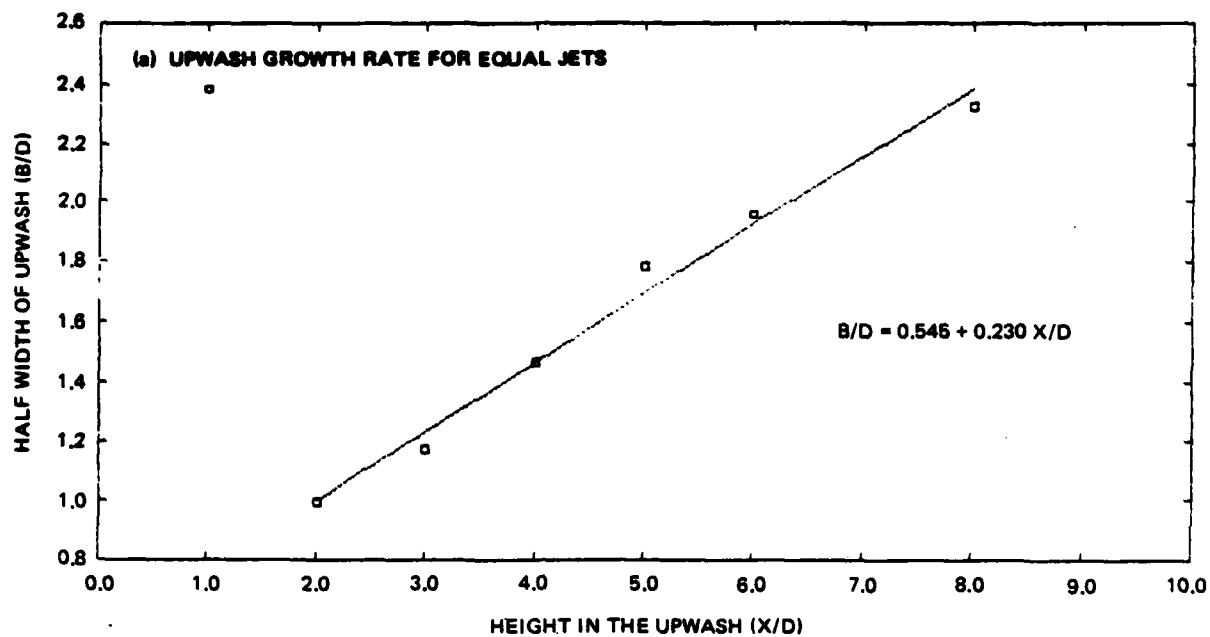
1335-001D

Fig. 8 Upwash Flow Field Vectors for Equal Wall Jets at Seven Heights (Sht. 1 of 2)



1335-001D

Fig. 8 Upwash Flow Field Vectors for Equal Wall Jets at Seven Heights (Sht. 2 of 2)



1335-002D

Fig. 9 Spread Rate and Mean Velocity Decay in a Two-dimensional Upwash

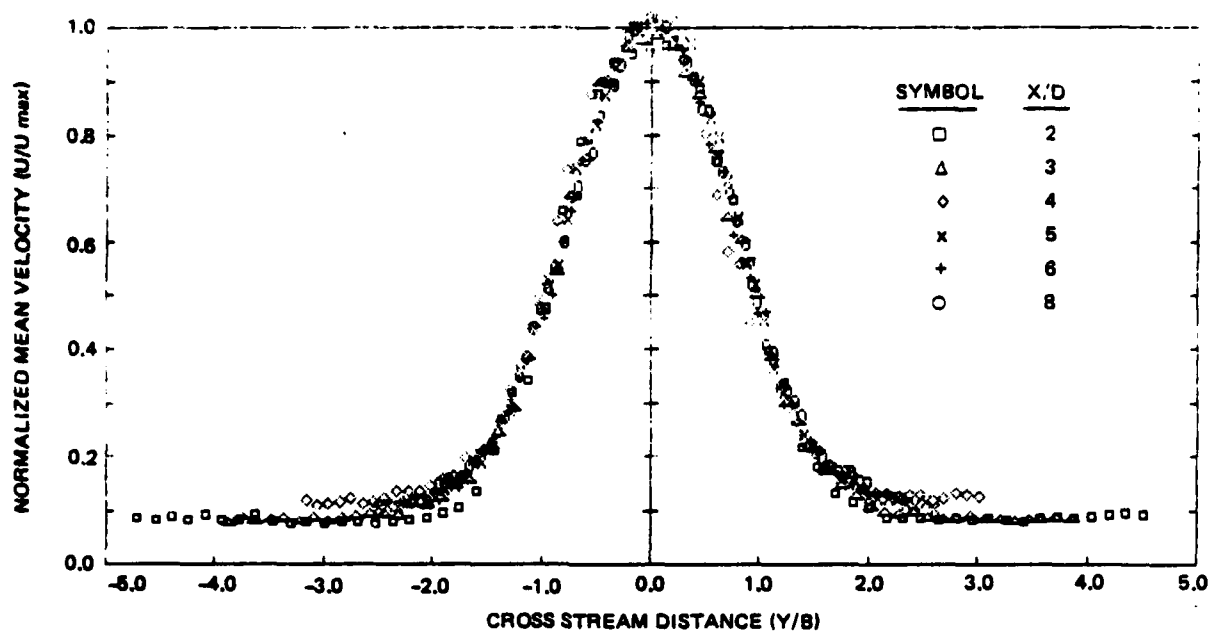
$$\frac{U}{U_{\max}} = \exp \{-0.693 \eta^2\} \text{ where } \eta = Y/B.$$

The component turbulence energy does not reach similarity as rapidly. The component in the mean flow direction is shown in Fig. 11. Similarity is reached at about $X/D = 5$, which is much faster than usually found in 2-D free jets. This may be due to the fact that there is no core region that needs to decay before the similarity jet can form. These profiles are normalized in a manner similar to the mean profiles. The magnitude and form of these profiles are exactly those expected to be found in a two-dimensional plane jet. The components in the other two cross stream directions, obtained by rotating the probe, are shown in Fig. 12 and 13. Again these show the expected form and values. Figure 14 shows the total turbulent kinetic energy profile at six heights, normalized as before. The total energy q^2 reaches similarity quite rapidly, showing that the slower development of the individual components is really due to a redistribution of turbulence among the various components as they approach local isotropy. Figure 15 shows the ratio w'^2/v'^2 . Throughout most of the center region, between $Y/B = -1$ to $+1$, this ratio is approximately 0.85. Therefore, calculations of q^2 when w data were not taken will be defined as $q^2 = (u'^2 + 1.85 v'^2)$.

Examination of the component turbulence energy and total kinetic energy levels found in the upwash shows these values to be exactly the same as those found in ordinary two-dimensional free jet flows. This is contrary to statements made by Foley (Ref. 8) and Witze (Ref. 6) that the turbulence intensity is a factor of three greater than the free jet case. However, examination of their data indicates ordinary levels. Only Kind and Suthanthiran (Ref. 5) show factors of three. Kotansky (Ref. 7) shows no turbulence data at all.

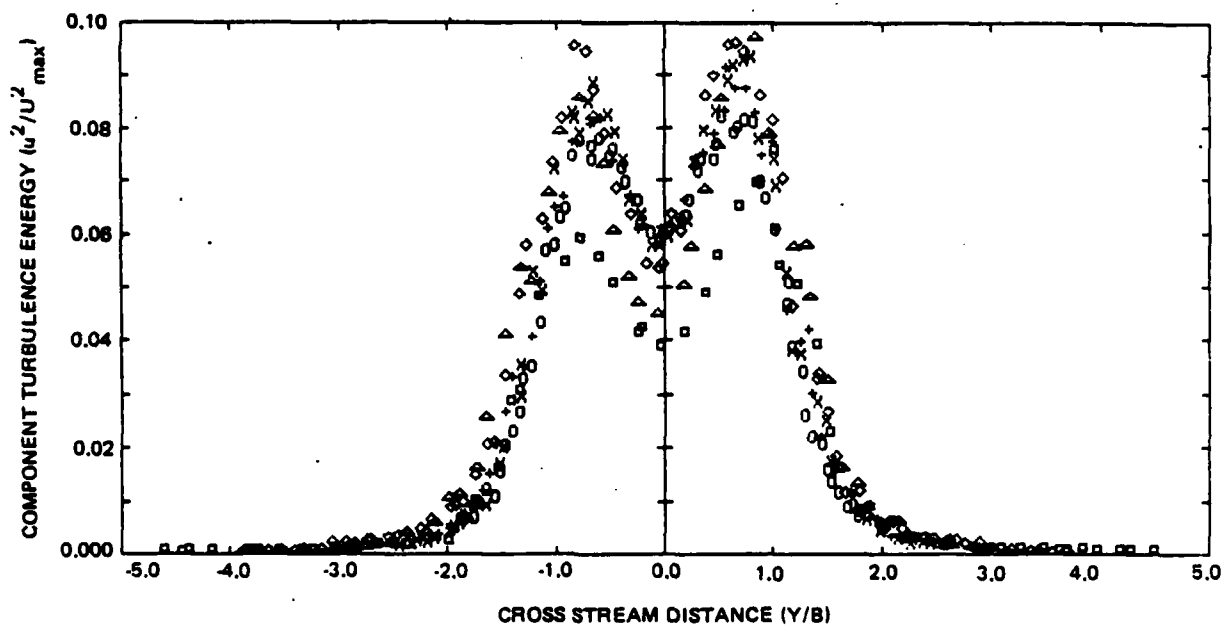
Figure 16 shows one component of the Reynolds stress, uv . Across the center region, the Reynolds stress profiles are anti-symmetric about the centerline passing through zero and have the same magnitude on either side. Since Reynolds stress measurements are particularly sensitive to measurement techniques, these plots are a good indication of the precision of the entire experiment. The form and magnitude are again exactly those expected in a two-dimensional jet.

In addition to growth rate, another departure from free jet characteristics is found in the intermittency. Figure 17 shows the normalized



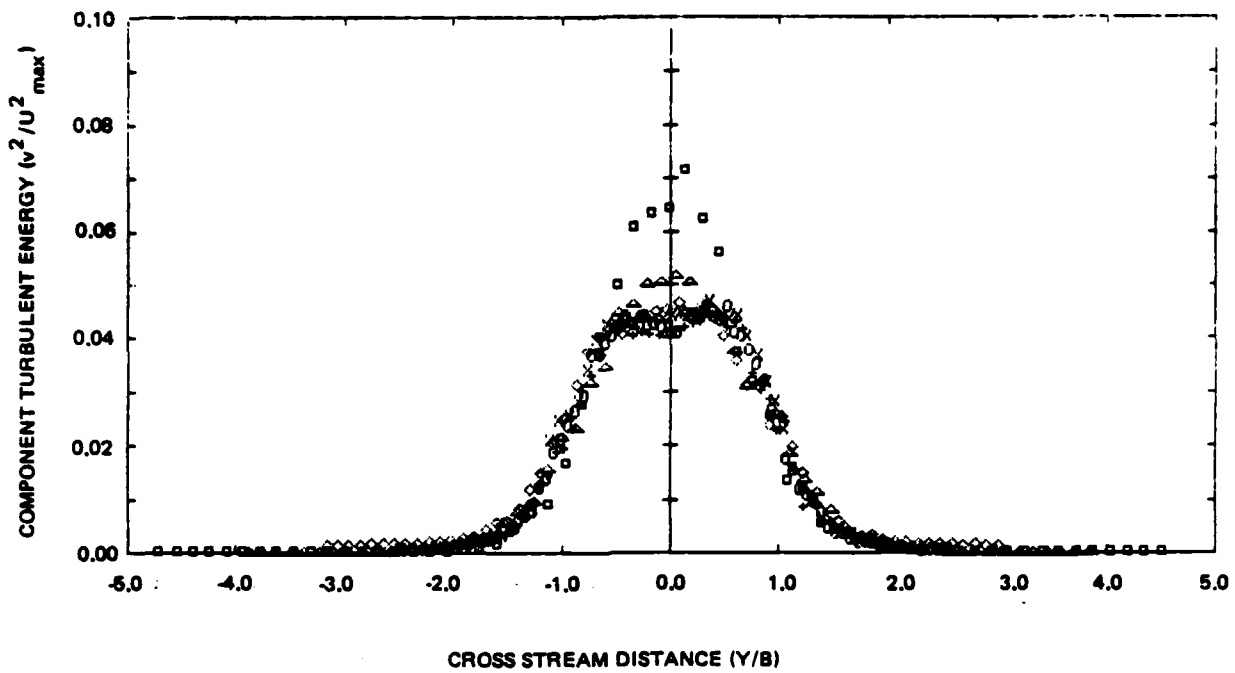
1335-003D

Fig. 10 Mean Velocity Profiles for Equal Wall Jet Upwash at Six Heights in Similarity Form



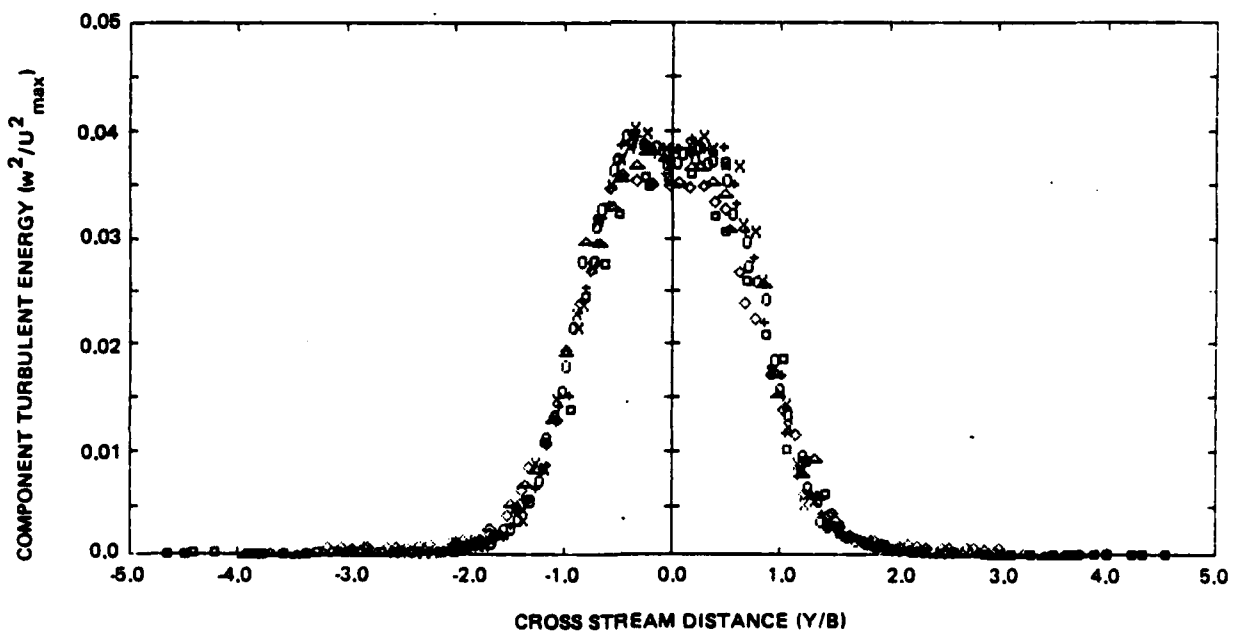
1335-004D

Fig. 11 Component Turbulence Energy in the Mean Flow Direction at Six Heights
(See Fig. 10 for Symbol Key)



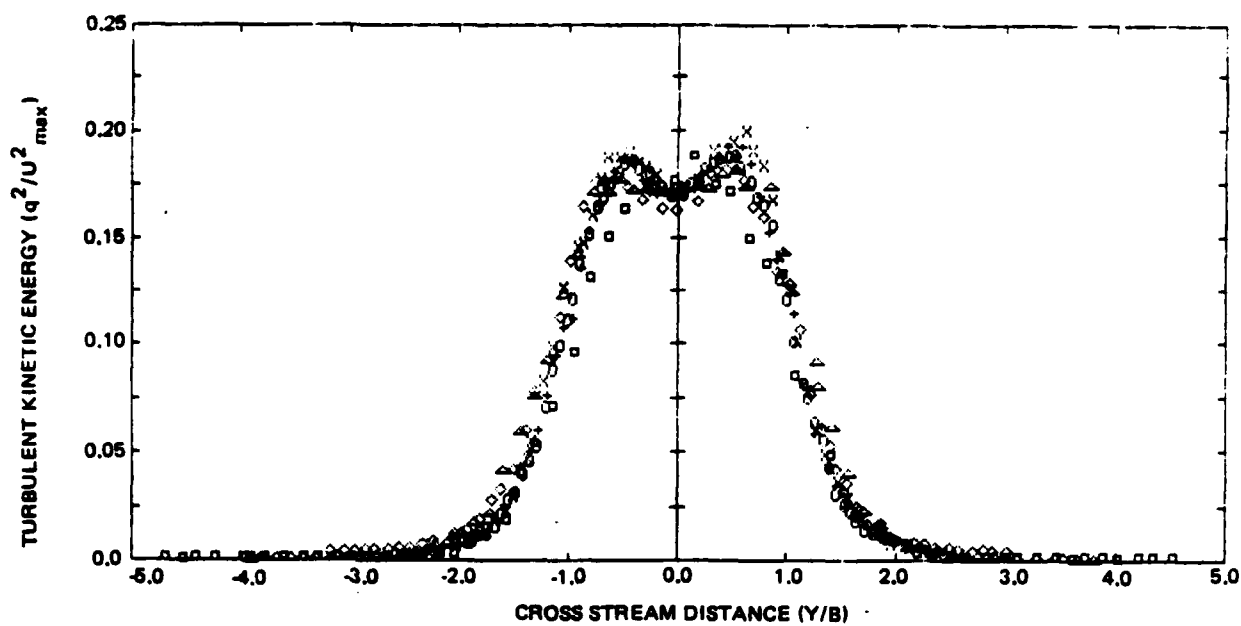
1335-005D

Fig. 12 Component Turbulence Energy in the Cross Flow Direction at Six Heights
(See Fig. 10 for Symbol Key)



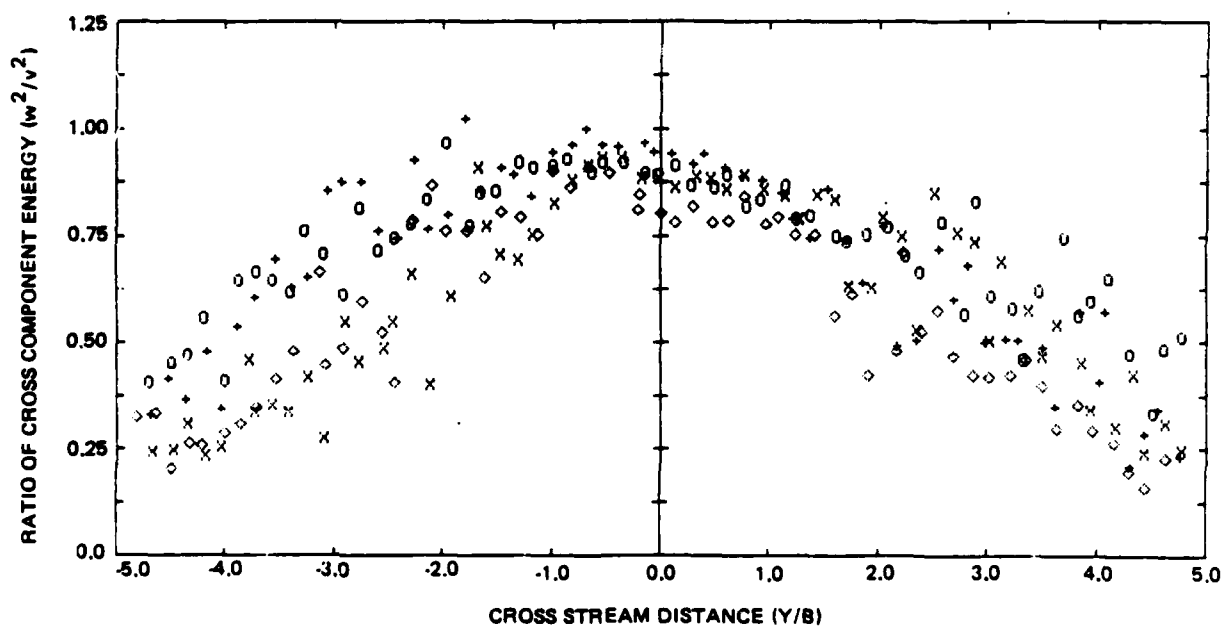
1335-006D

Fig. 13 Component Turbulence Energy in the Third Orthogonal Direction at Six Heights
(See Fig. 10 for Symbol Key)



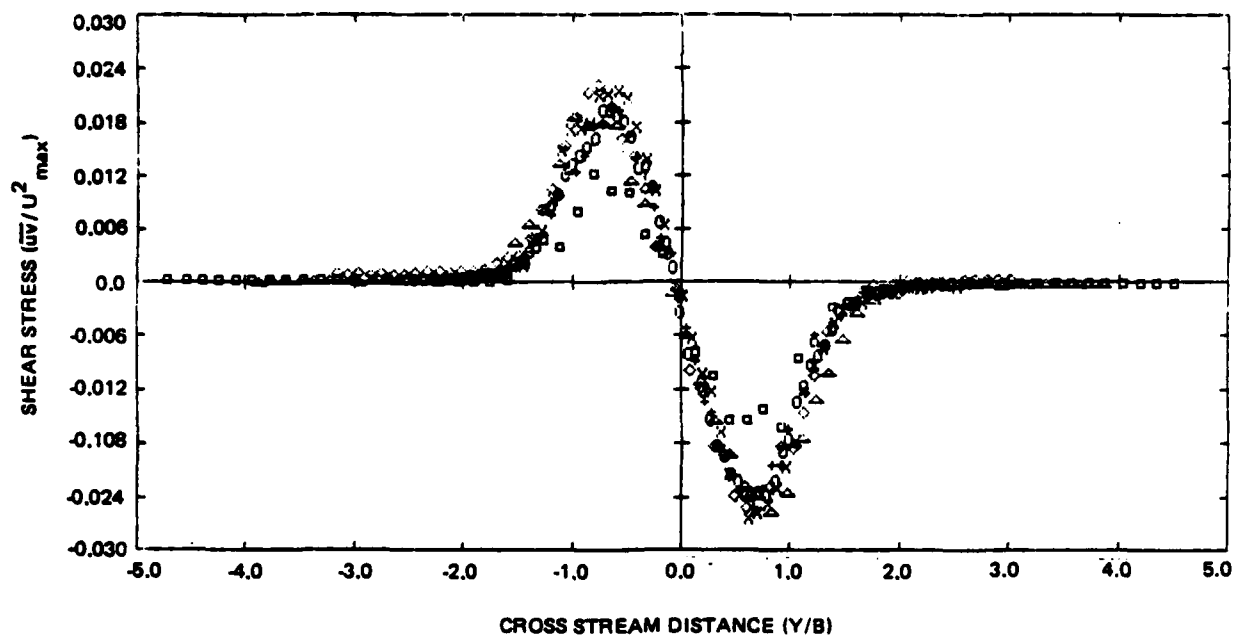
1335-007D

Fig. 14 Total Turbulence Kinetic Energy in an Equal Wall Jet Upwash at Six Heights
(See Fig. 10 for Symbol Key)



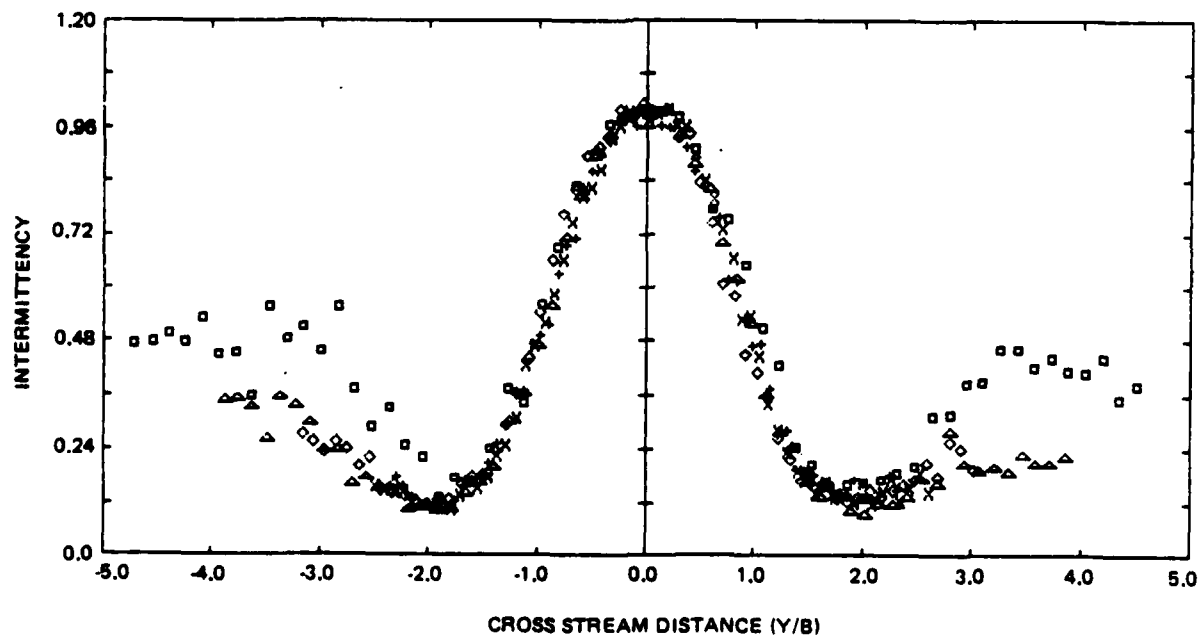
1335-008D

Fig. 15 Ratio of the Cross Component Turbulence Energy
(See Fig. 10 for Symbol Key)



1335-009D

Fig. 16 Shear Stress Component in an Upwash at Six Heights (See Fig. 10 for Symbol Key)



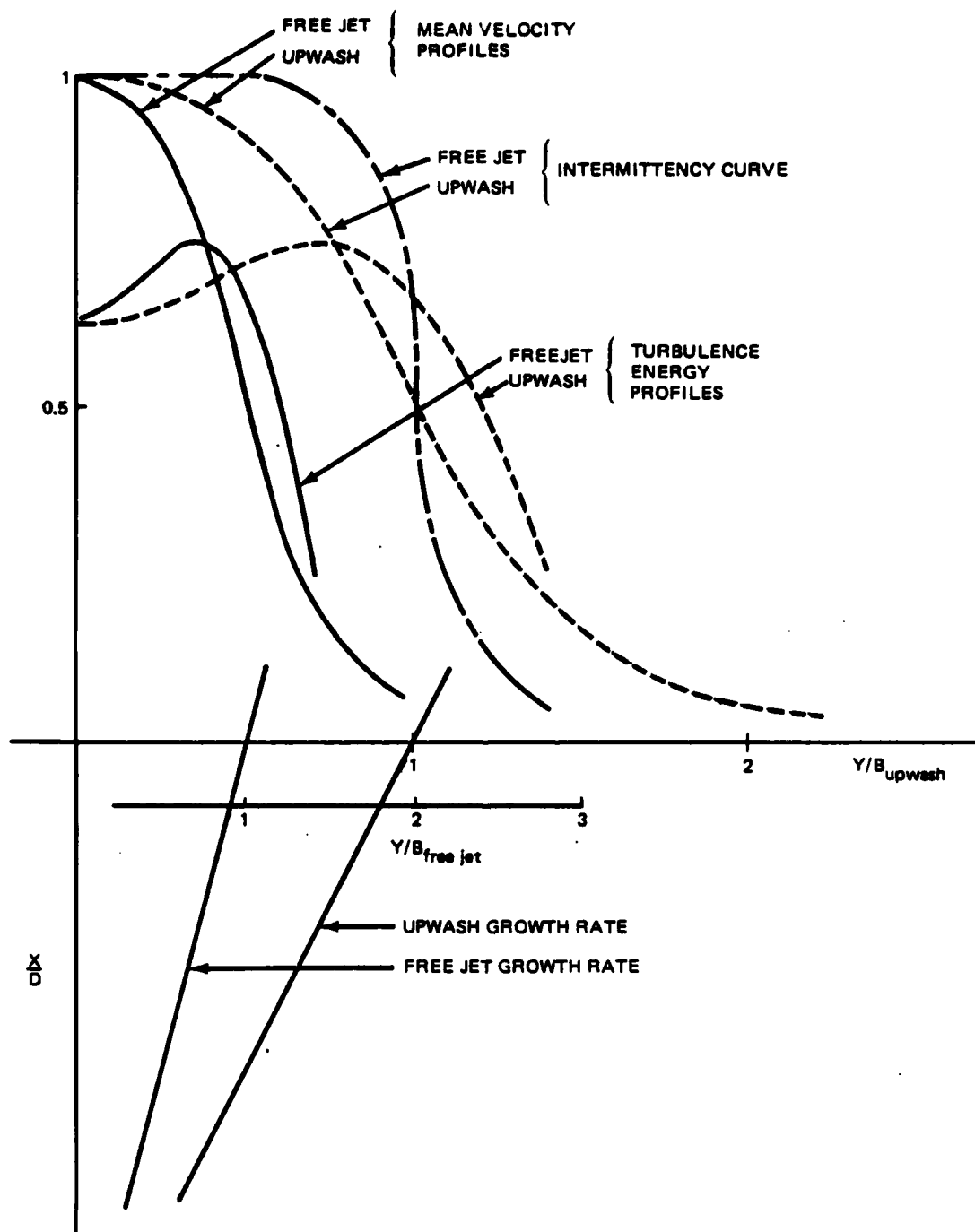
1335-010D

Fig. 17 Intermittency Profiles in an Equal Jet Upwash (See Fig. 10 for Symbol Key)

intermittency. The intermittency is determined by the flatness factor normalized by the centerline value. An intermittency factor of one indicates fully turbulent flow. The form of these curves is the expected normal distribution. However, in all free shear flows, the ratio of the intermittency half width to mean velocity half width is two (Ref. 13). Here, it is one. Remember, all of the profiles shown have been normalized by local mean velocity half widths. So, while the form looks absolutely correct, the widths of the profiles are about twice the free jet widths. Because of the method of normalization, this means that the intermittency profile is really very similar to the free jet profile. These are shown as the same curve on the diagram Fig. 18. Figure 18 also shows the relationship of the turbulence and mean profiles in free and upwash flows. The relative mixing layer growth rates are represented at the bottom of the figure. Because the upwash intermittency profile does not have a flat region at the centerline, the non-turbulent flow outside the upwash is penetrating nearly to the centerline. That is, the mixing layer must have a penetration length scale nearly equal to the half velocity width.

A useful concept to understand the organization of the turbulence motion are the length scales and their associated "eddies." An eddy can be thought of as a vortex filament or little swirl with an associated radii called its length scale. The turbulent motion can now be visualized as a collection of eddies of all different sizes. The distribution of energy among these eddies can be seen by taking the Fourier transform of the original turbulence signal. This gives the distribution of the energy contained at each frequency or, alternatively, at each length scale. This latter substitution is by Taylor's hypothesis, which states approximately that the temporal variation of the turbulence at a point in a "frozen" turbulent flow is equal to its spatial variation, such that one may replace $t = x/U$.

The turbulence spectra is continuous, that is, some energy is contained at every length scale. However, it is useful to identify specific length scales with specific characteristics of the spectra. Most of the energy contained in the turbulence is in the larger scales. These scales are responsible for the macro-structure of the turbulence; this includes the mixing processes. The smaller scale motions represent the scale where viscous dissipation of the turbulence energy occurs. Between these two extremes there



1335-0110

Fig. 18 Comparison of Mean and Turbulence Profiles for a Free 2-D Jet with a 2-D Upwash

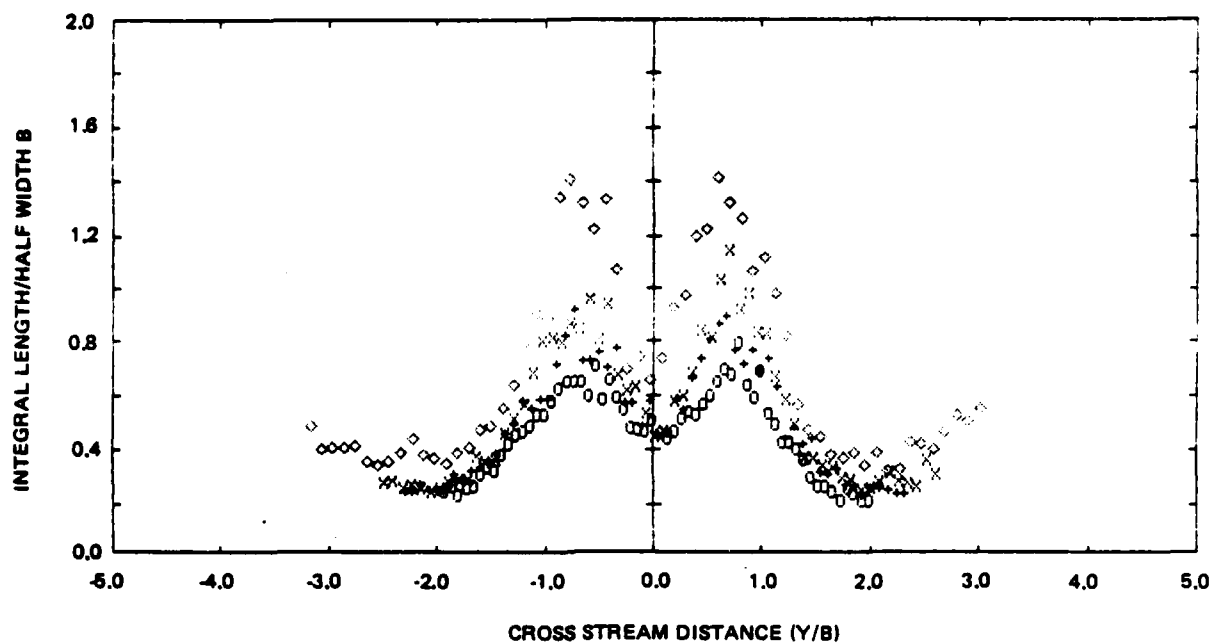
exists a range of eddy sizes that are not directly affected and transmit turbulent energy only from the larger scales where it is generated to the smaller scales where it is dissipated. If this range exists, it is called the equilibrium range and the flow is said to exhibit local isotropy.

Information about the influence of turbulent fluctuations on its surroundings can be found by examining the autocorrelation of the original time series. The autocorrelation can be thought of as a measure of the physical extent of the influence of a fluctuation at a point. A measure of this quantity then gives an idea of the length of mixing involvement. This scale is called the integral scale length because it is defined as the integral under the autocorrelation curve. Since the autocorrelation is also the inverse Fourier transform of the power spectral density function, it does not give any additional information about the flow. It does, however, give another physical interpretation to the length scales identified in the spectral representation.

An additional length scale often used to describe turbulence is the Taylor microscale. While the scale really has no physical significance, the Taylor microscale is related to the overall energy dissipation. If one considers that all of the energy is dissipated by eddies of one size, those eddies would be the size of the Taylor microscale. It is always much smaller than the integral scale.

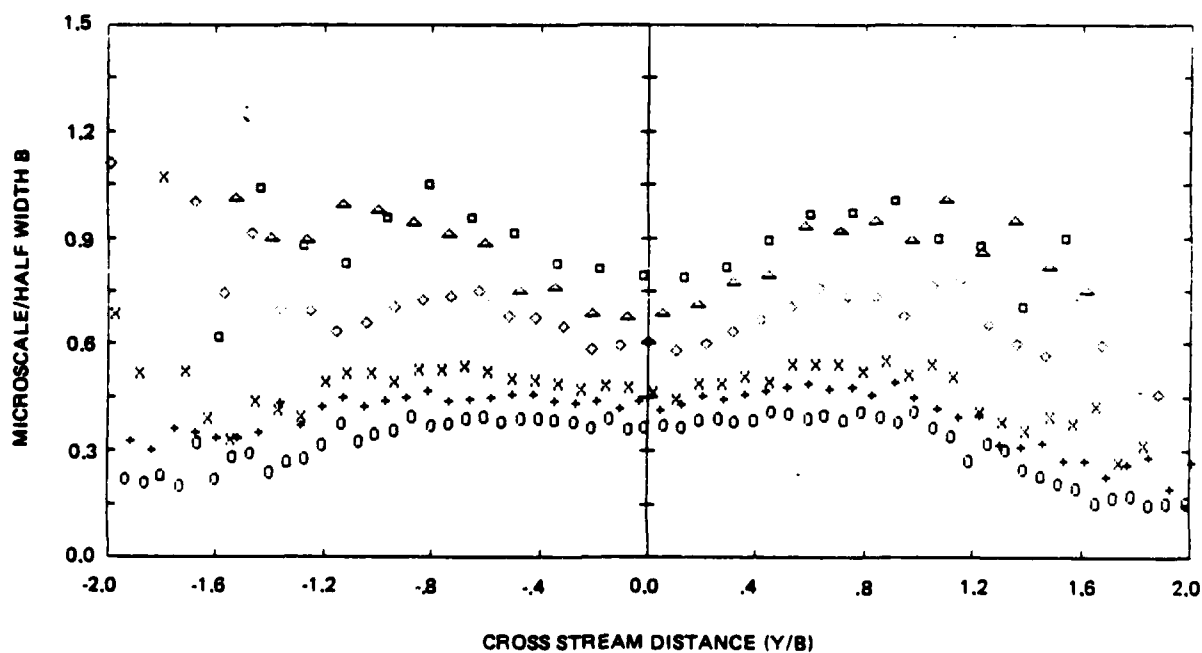
It is apparent from the length scale profiles shown in Fig. 19 that the large scale eddies at the half width position are at least as large as the upwash width itself. These integral scale lengths were obtained by integrating the area under the autocorrelation curve to the point of the first zero crossing. This length scale is representative of the size of the large scale motions responsible for mixing. Through the center region, it is seen that these are a significant percentage of the local mean velocity half width. These values are much larger than those found in a free jet flow, again by a factor of two!

The turbulent microscale is shown in Fig. 20. This scale, representative of the energy dissipation length, was calculated in two different ways. It was directly calculated from the derivative of the time series. This method suffers from the inherent noise increase by differentiation. In addition, due to the intermittency away from the centerline, the average values at a point



1335-0120

Fig. 19 Integral Scale Lengths Across 2-D Upwash (See Fig. 10 for Symbol Key)



1335-0130

Fig. 20 Taylor Micro-scale Lengths Across 2-D Upwash (See Fig. 10 for Symbol Key)

are prejudged towards lower values. The second method computes the scale from the second derivative of the autocorrelation function at the origin. At the centerline, these two methods give good agreement. Figure 20 utilizes the second method. The values are nearly constant across the mixing layer as assumed in some mixing length turbulence models. The values are unusually large, indicating greater than normal turbulence dissipation consistent with the increased mixing rate.

2.4 SHORT PLATE EQUAL JET UPWASH

In most ordinary turbulent flows, there are two characteristics that determine (at least in the near field) the macroscopic turbulent properties. These are usually a characteristic velocity scale and a characteristic length scale. For example, in a free jet, these are the initial free jet maximum velocity and initial jet diameter. It is well known that the influence of such factors as initial boundary layer thickness is secondary and in turbulent jets often negligible. In the far field, after the flow has attained a similarity form, the influence of even these factors appear only as shifts in virtual origins, or scaling factors. The usual length to similarity in free and wall jets is taken to be greater than 20 initial jet diameters. The upwash found in aircraft applications is at much shorter lengths, and so the experiments reported here are also performed in the near field.

An entirely new baseline set of complete turbulence measurements was taken and are reported in the last section. Two important questions about these data may be immediately asked. First, what is the influence of changes in the initial conditions found at the collision point, and second, why is there such a difference in the results reported by various investigators? In order to address both of these questions at the same time, another set of equal wall jet upwash experiments was designed. The initial conditions for these experiments are summarized in the following table. These experiments were performed using a shorter instrumentation plate than the baseline plate, giving a smaller characteristic wall jet half velocity height and, at maximum tunnel speed, a higher collision velocity. By lowering the tunnel speeds, the same collision velocity used in the baseline experiments could be repeated with the shorter instrumentation plate. The balance of the instrumentation and test procedures used in baseline experiments was repeated.

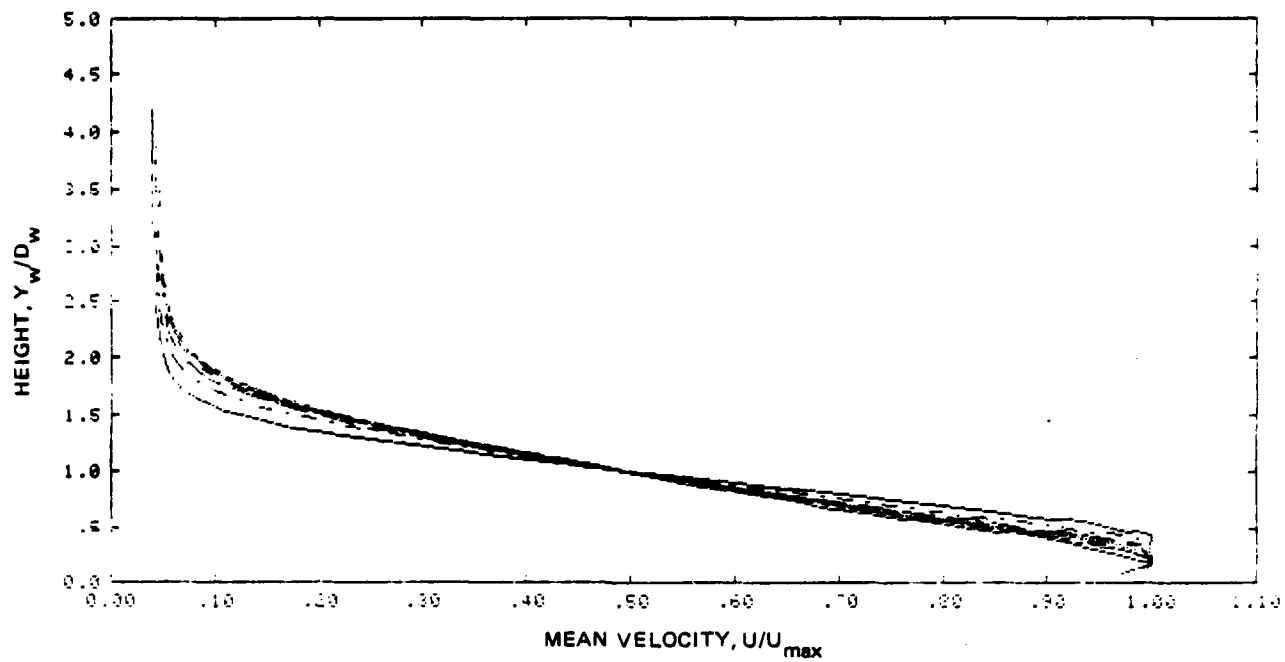
Wall jet mean and turbulence profiles were taken at 20 locations from

seven exit heights downstream of the nozzle past the centerline of the short instrumentation plate. These profiles were made to assure the same quality of wall jet flow that was obtained with the long plate. These profiles were made at equal distances along the plate of approximately 1.5 nozzle heights. Each profile contains 20 data points spaced about one quarter nozzle heights apart. Figure 21 shows the normalized wall jet profiles at 10 alternate downstream locations three nozzle heights apart. These profiles are identical to those shown in Fig. 6 for the long plate. Figure 22 shows the turbulence energy profiles normalized by the half velocity width at the same locations. These do not quite show that similarity in turbulence has been reached, but, comparing to Fig. 7, it is very close. This was the limiting characteristic in the choice of how short the plate could be made.

A plot of the wall jet growth rate as characterized by the half velocity height vs the distance downstream is given in Fig. 23a. As for the long plate shown in Fig. 5, a least squares curve fit gives a growth rate in the developed region of 0.072 vs 0.073 in the earlier case. Figure 23b shows the characteristic linear mean velocity decay relationship required by conservation of momentum.

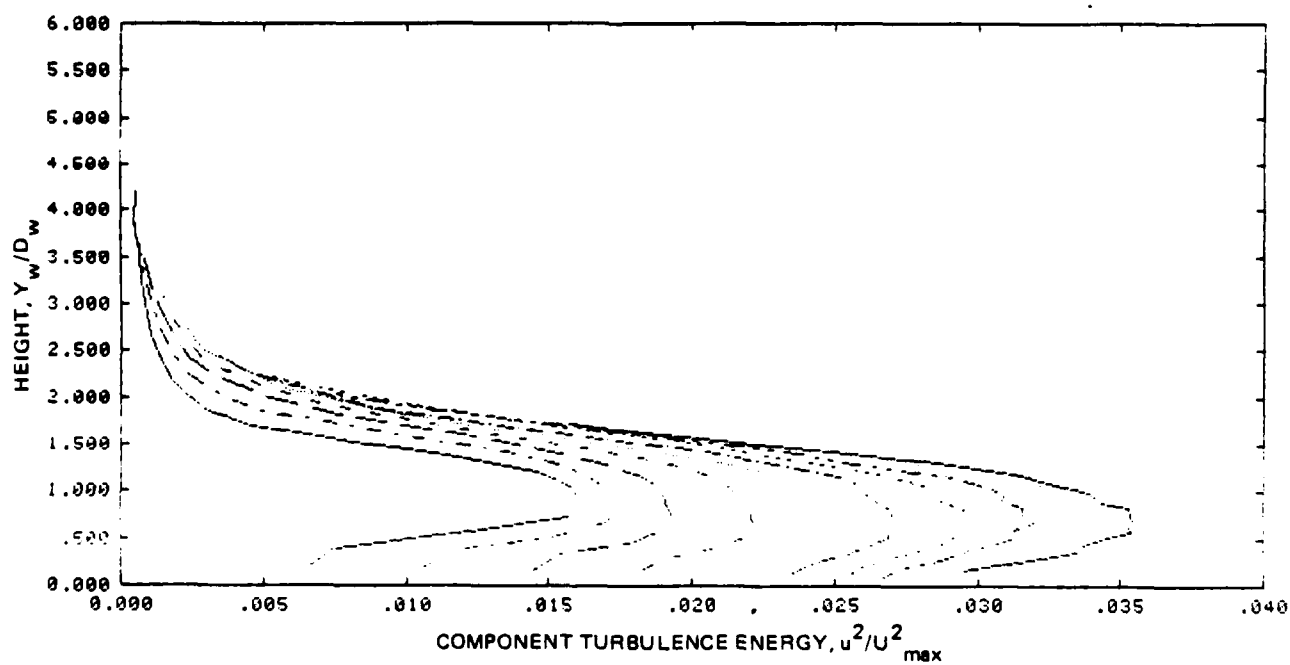
The centerline characteristics are shown on Table 1. Since the maximum velocity at the centerline is 63% of the source jet velocity, the second case was run at a source pressure of 0.75% of maximum to give a centerline maximum velocity equal to that used in the baseline case. The mean and turbulence velocity profiles were measured at the centerline for four different source jet pressures. These are shown in Fig. 24 and 25 for four pressures between 1.00 to 0.75 maximum. As expected, in every case the maximum velocity is 0.63 source velocity and the half velocity width is 2.72 nozzle heights. While the turbulence level was low in all cases, the highest speed wall jet had almost 50% higher turbulence energy. This may be the cause of secondary differences found.

The upwash formed by two equal two-dimensional wall jets, was probed and analyzed by the same methods developed and used in the baseline case. Measurements of all of the fundamental turbulence properties were taken at six heights through the upwash at heights of 2,4,6,8,10, and 12 local characteristic wall jet heights compared to 2,3,4,5,6, and 8 in the baseline case.



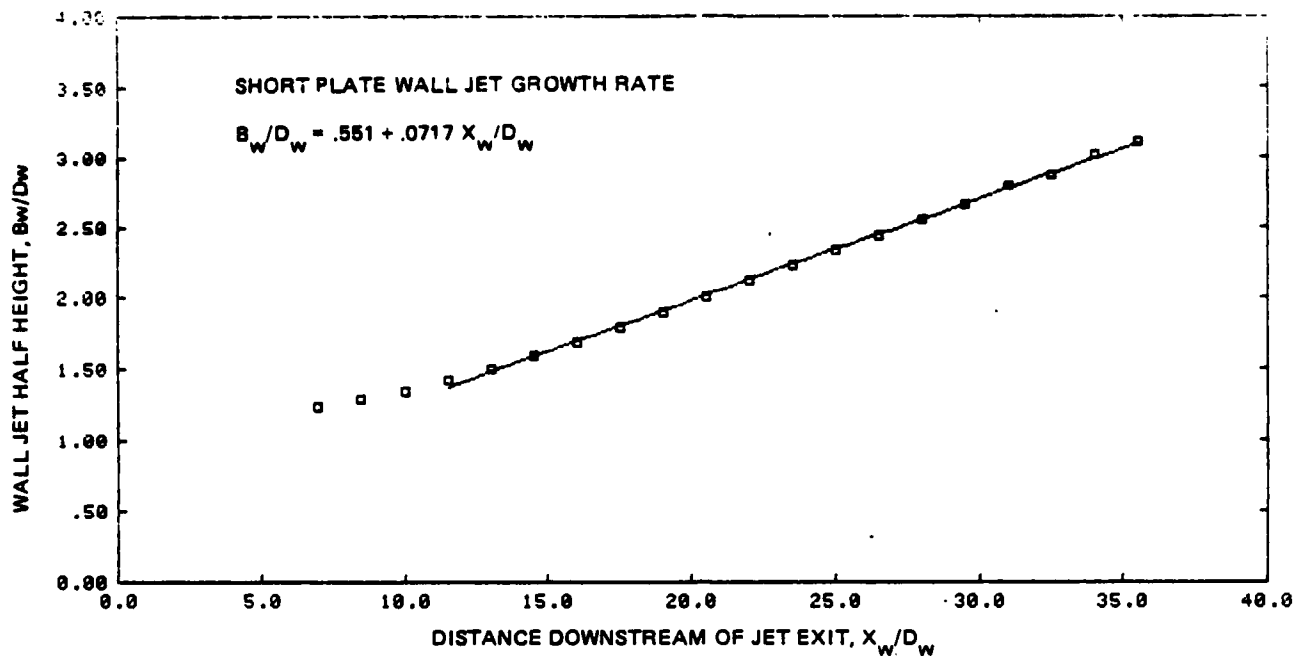
R85-1154-002B

Fig. 21 Wall Jet Mean Velocity Profiles in Similarity Form

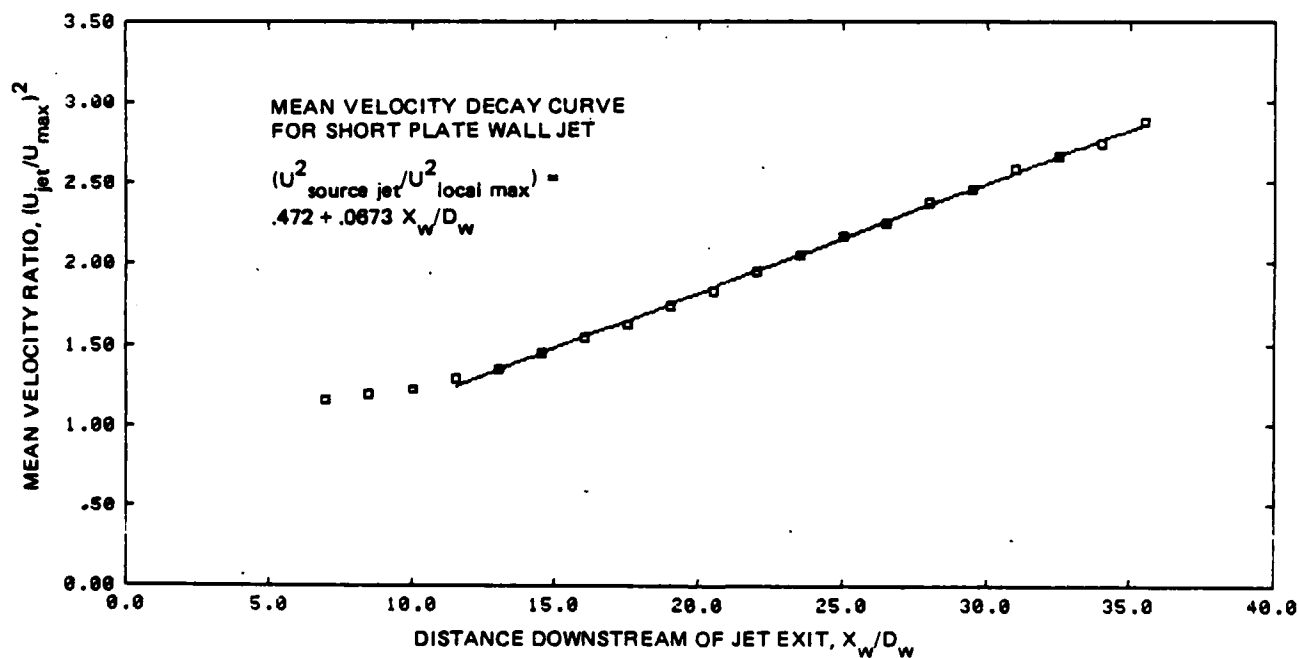


R85-1154-003B

Fig. 22 Wall Jet Turbulence Intensity Profiles in Similarity Form



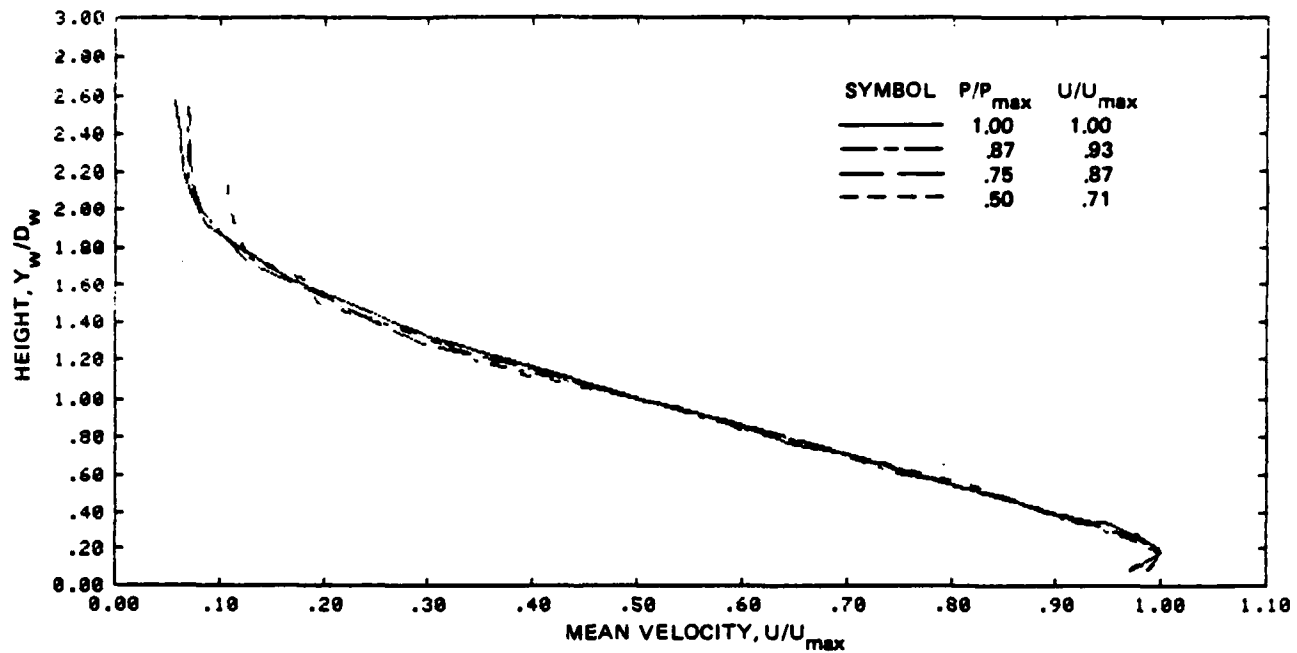
a) GROWTH RATE PROFILE



b) VELOCITY DECAY PROFILE

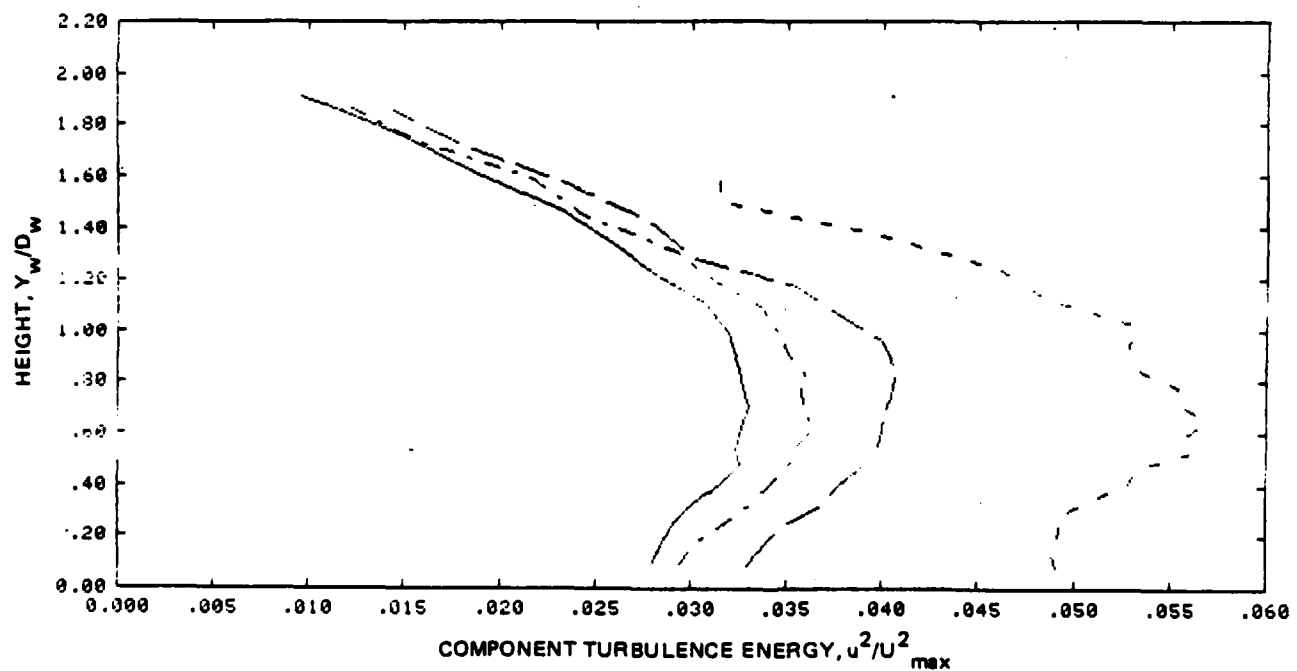
R85-1154-001B

Fig. 23 Two-dimensional Wall Jet Characteristics



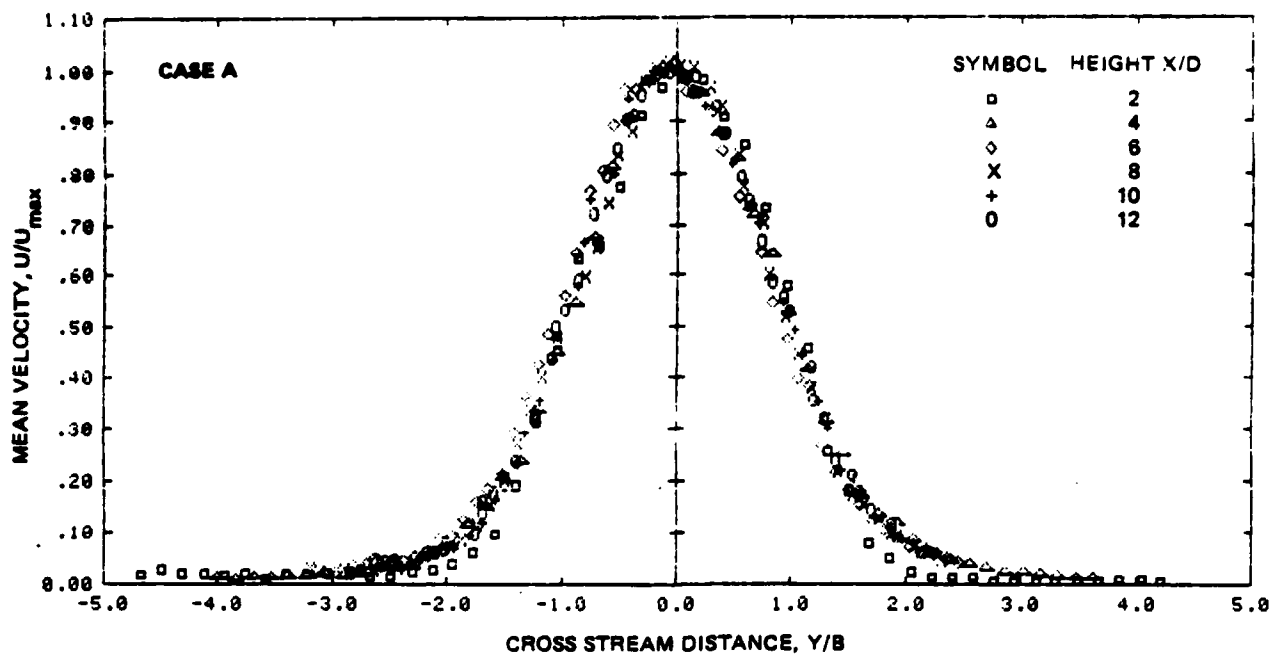
R85-1154-004B

Fig. 24 Wall Jet Mean Velocity Profiles at the Centerline for Four Source Velocities in Similarity Form



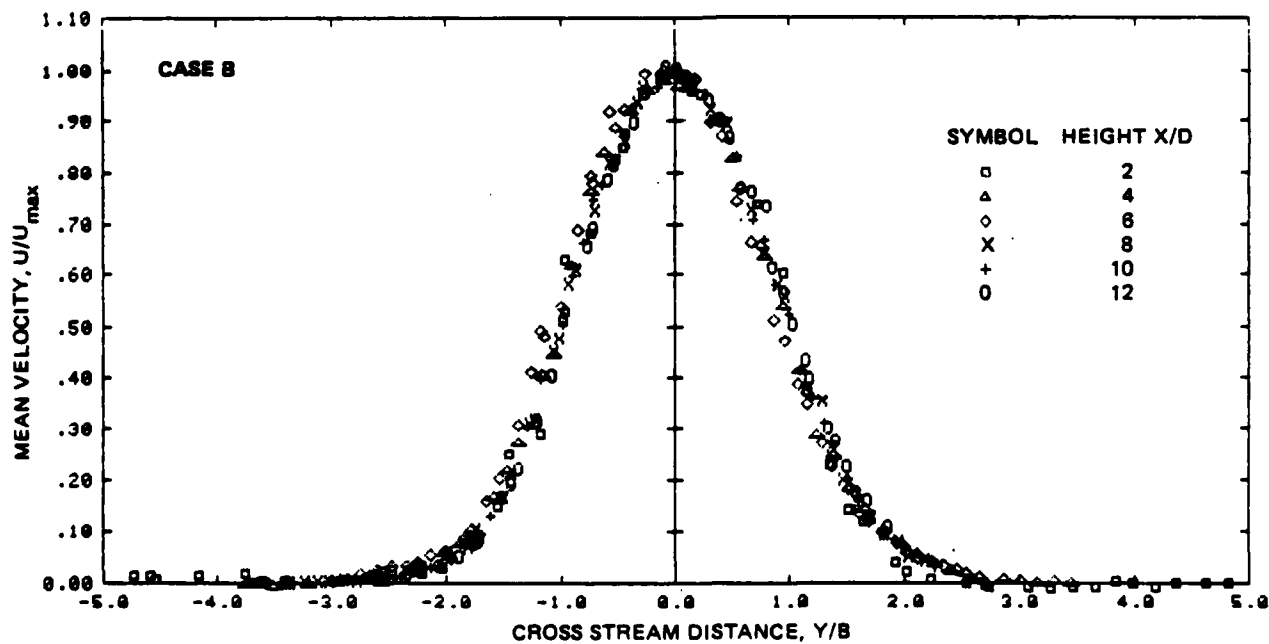
R85-1154-005B

Fig. 25 Wall Jet Turbulence Energy Profiles at the Centerline for Four Source Velocities in Similarity Form



R85-1154-023B

Fig. 26 Mean Velocity Profiles for Equal Wall Jet Upwash at Six Heights in Similarity Form



R85-1154-012B

Fig. 27 Mean Velocity Profiles for Equal Wall Jet Upwash at Six Heights in Similarity Form

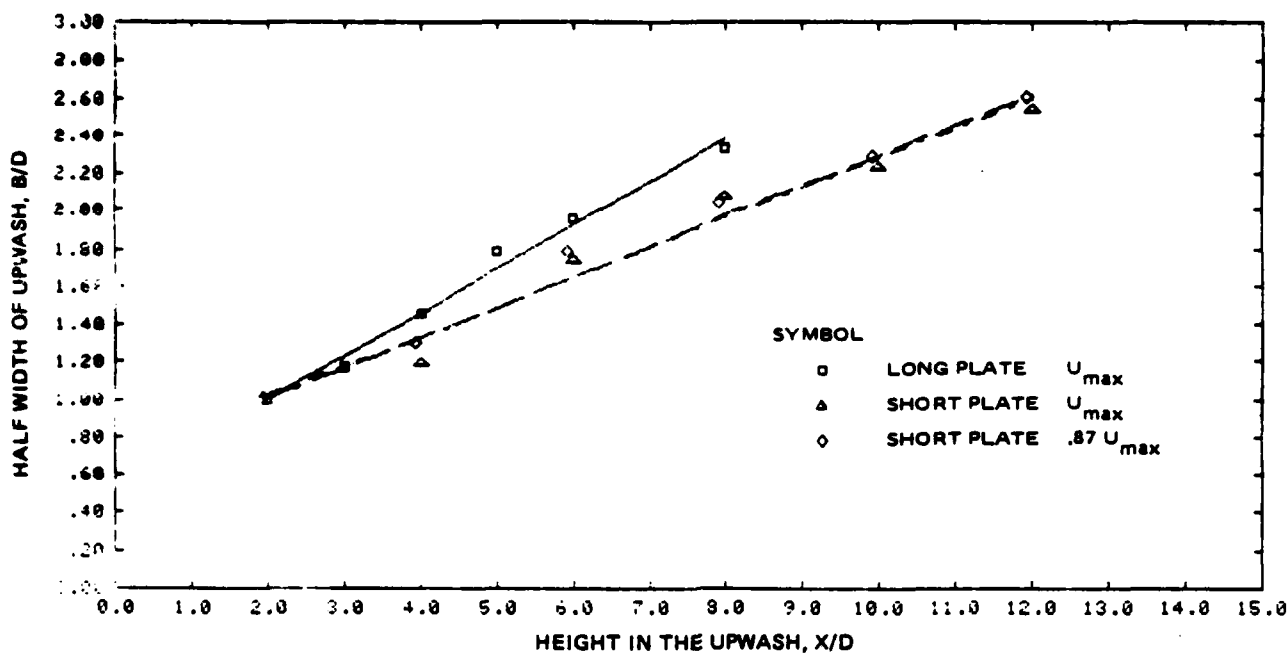
Table 1

COMPARISON OF INITIAL CONDITIONS FOR THE THREE EQUAL WALL JET TESTS

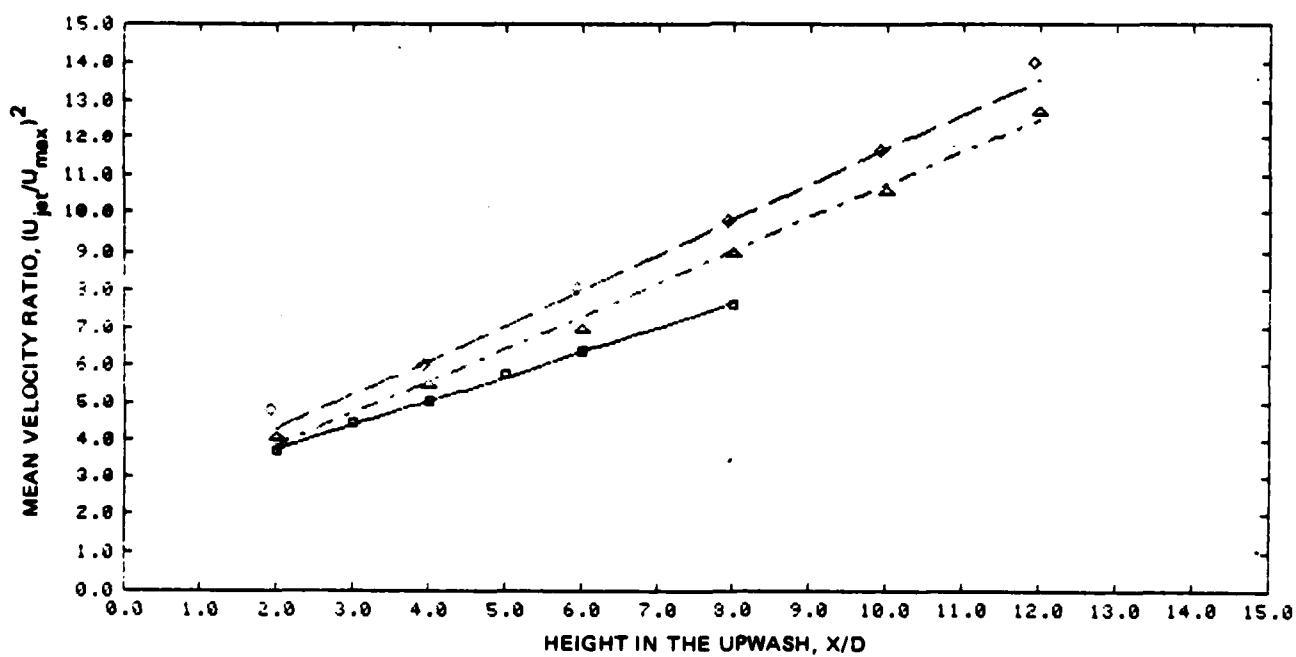
	Baseline	Case A	Case B
Plate length			
(X_w/D_w)	84	61	61
(X_w/X_{base})	1.00	0.73	0.73
Wall growth rate	0.073	0.072	0.072
Wall half velocity height at collision			
$(D=B_w/D_w)$	3.70	2.72	2.72
(D/D_{base})	1.00	0.74	0.74
Max. velocity at collision			
mps	36.7	41.6	36.2
(U/U_{jet})	0.57	0.63	0.63
(U/U_{base})	1.00	1.13	0.99
Max. turbulence energy $(u'/U)^2$	0.030	0.055	0.035
Max. height of measurement (X/D)	8	12	12

The mean velocity profiles in the upwash direction for the two new cases are shown in Fig. 26 and 27. These data were curve fit as before. The upwash half velocity growth rate and mean velocity decay rate are shown in Fig. 28a and 28b, for the three comparison cases. As pointed out earlier, the collision zone is of the order of two half velocity height so it is not surprising that at $X/D = 2$, the half width in all cases is one characteristic length. At first glance, the growth rate for the long plate seems to be much higher than that for the short plate. Since Case B has the same maximum velocity as the baseline case, it would appear that the length scale before the collision influences the growth rate in the upwash. This length is really only a function of running length, once similarity is obtained. Since both axes are normalized by this scale, it is unlikely that growth rate is a function of wall jet height.

A closer examination of these new data tells a different story and may throw some light on the differences in growth rate reported by different investigators. The new data extend 50% local characteristic dimensions farther downstream. The data between 2 and 8 heights downstream show growth



a) GROWTH RATE PROFILES



b) VELOCITY DECAY PROFILES

R85-1154-006B

Fig. 28 Spread Rate & Mean Velocity Decay in a Two-dimensional Upwash for Various Initial Conditions

rates more in line with the baseline set. In fact, the data should probably be plotted with a curve rather than a straight line. The fact that the slope of the growth rate is still changing indicates that the upwash is not a similarity flow although all of the turbulence properties seem to indicate that it is. In fact, the growth rate is continuing to decrease. One may well hypothesize that it will reach an asymptotic growth rate of about 0.1 found in the far field of a free jet.

With this explanation for the apparent differences found by previous investigators, these other reports may be re-examined. By recasting their data in terms of initial characteristic heights, Witze (Ref. 6) shows the normal growth rate for "constrained" jets of about 0.1. His tests with "impinging" jets show a much higher value of about 0.37, but it is not possible to tell what his initial characteristic length was. It is interesting that he does point out that there is a very quick transition from constrained to impinging jet flows. He makes the point that it is necessary to have a distance between jets of at least two core lengths, a situation similar to the one found here where the influence of the collision is felt at a distance of two local half heights. In his impinging case, Witze makes measurements only to R/Y of 1, though it is not possible to correlate that distance to half heights. It is probably near field data. His plot of growth rate versus constraint ratio should probably be replotted versus characteristic height. Kotansky (Ref. 7) found a growth rate of about 0.35 for data taken between X/D of 1.7 to 6.7, near field. Foley (Ref. 8) does not give enough data to make any statement. Kind (Ref. 5) obtained growth rates of about 0.3 for data also taken in the near field between X/D of 3.4 to 6. The data presented here are the only data to extend to at least 12 distances downstream. They clearly show a transition of growth characteristic from relatively high values in the very near field towards values more in line with those found in free jets. The data presented here are the only complete set to contain all the basic turbulence measurements. The current measurements contain higher moments and length scale information necessary for modifying turbulence models.

An examination of the shear stress profiles shown in Fig. 16 for the baseline case and Fig. A-4 and B-4 for the additional cases raises an interesting question. Consider the usual form of the momentum equation for

similarity flows given by

$$1/2 (B/x) U^2 + ((B/x) n U-V) dU/dn - \sigma \langle uv \rangle / \sigma n = 0$$

where the velocities have been normalized by the centerline velocity and $n = y/B(x)$.

All of these terms have been measured. Then at the centerline,

$$1/2 (B/x) = \left. \frac{d \langle uv \rangle}{dn} \right|_{\text{centerline}}$$

where B/x is the upwash mixing layer growth rate.

In a free jet $B/x \sim 0.1$ so the slope of the shear stress should be 0.05. In the experiments reported here, the shear stress slope at the centerline is also about 0.05 while the growth rate on the left hand side is twice the free jet value. The momentum equation when evaluated where the shear stress is maximum (slope = 0), does balance. The problem at the centerline was pointed out by Bradshaw (Ref. 14). The upwash experiments were repeated with great care to assure that the effect was not a measurement problem. In addition an examination of some well established free jet experiments also show some scatter in the shear stress slope at the centerline (Ref. 3 for example).

An explanation is available for the equation not balancing. As was pointed out earlier, the upwash measurements were taken in a region where the flow has not yet reached full similarity as indicated by the length scale development. The mixing layer growth rate continues to decrease thereby making the left hand side of the above equation more closely approach the shear stress slope.

Many of the turbulence models that have been enjoying some degree of success are two equation models. These models usually utilize a characteristic length scale or model a characteristic scale for their closure. The variation of the length scales as the flow develops is important to the overall macroscopic properties of the flow. It is obvious from the length scale data presented here that a simple form of this model will fail in its attempt to predict the turbulence properties found in the upwash. Some different variation in scale length in the near field is needed to reflect the change in growth rate from values of the order 0.35 to 0.10 as the flow

approaches similarity in length scale as well as in turbulence energy.

All of the turbulence properties measured have been plotted in similarity form. In this representation, there is very little to distinguish the data taken in one flow case versus another. These data are included in the Appendices for completeness and can be compared to the baseline data already presented.

The most interesting of these data are the length scale information given by the microscale and integral length scale development since these are the only normalized data still showing development throughout the upwash measurement range. The microscale shows a rate decrease in length from the lower stations approaching a constant value both cross as well as downstream of about a third of the half width dimension. The integral scale representing the largest eddies responsible for the macroscopic properties of the flow decrease from several times the half width to values of that order at the half width for stations where the growth rate is approaching the free jet value. As an interesting side point, the wall jet turbulence energy is much higher in Case A than in the baseline or Case B. However, this does not seem to affect the growth or turbulence characteristics in the upwash. As with the turbulent free jet, initial turbulence has only a secondary effect.

2.5 UNEQUAL WALL JETS

In an attempt to explain the increased turbulence mixing rate found in the upwash, several types of experiments were performed to examine the effect of the initial wall jet conditions on the upwash (Ref. 15-18). These include a series of experiments using unequal strength source wall jets, another series utilizing various height obstacles or fences located at the collision point of equal strength wall jets, and a series using tape boundary layer trips to assure turbulent wall jets.

A series of experiments was conducted using different source jet pressures. The pressure ratios were 1.0, 1.2, 1.4, 1.6 and 1.8, and profiles were taken at heights of 2, 4, 6 and 8 wall jet half heights used in the equal jet case. This combination of wall jet pressures and profile heights was selected because of the physical constraints of the test facility. The data acquisition and processing procedure was the same used in the equal jet case. The short version of the program was used.

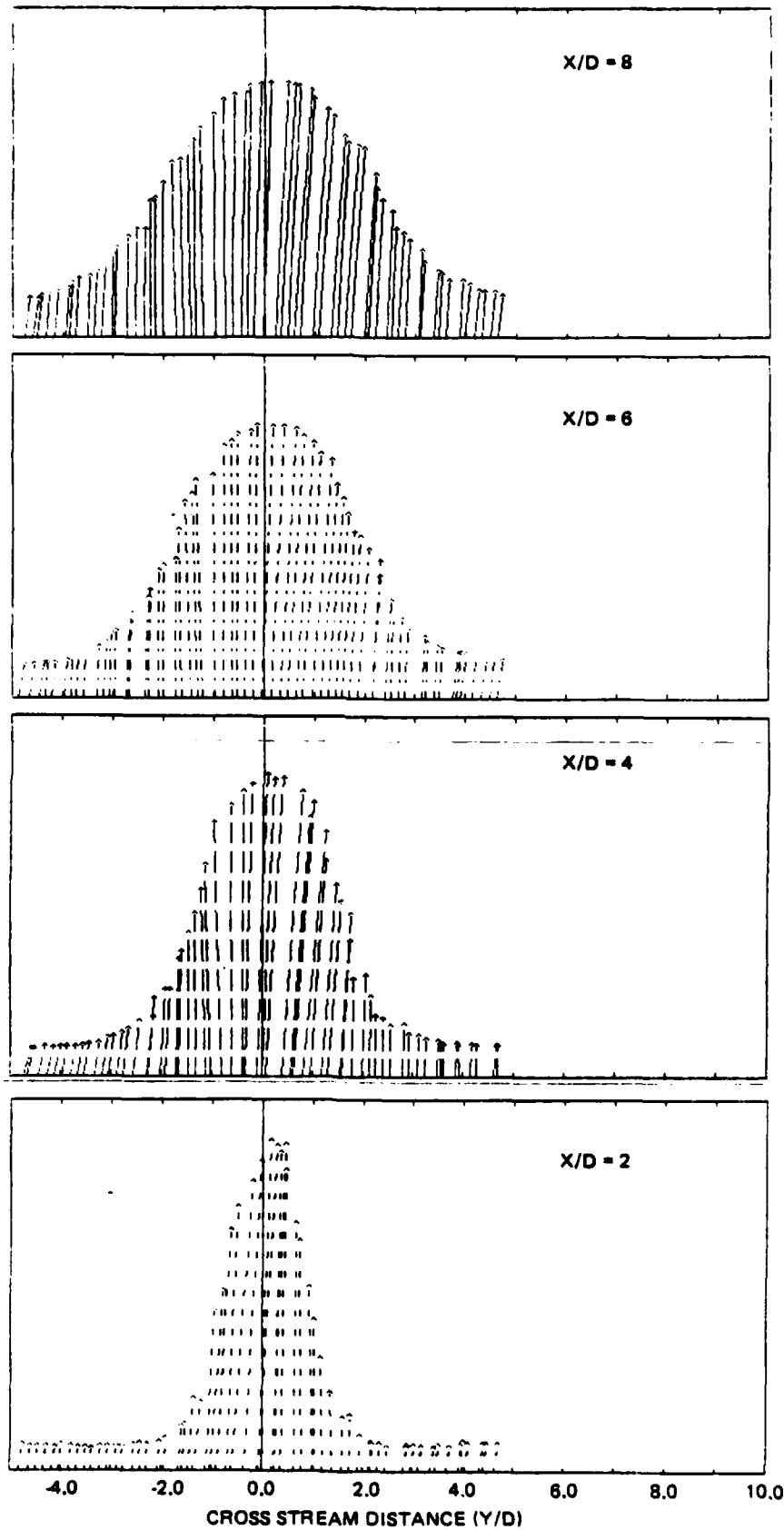
Figures 29 through 33 show the mean velocity vector profiles for these cases. Using the magnitude of the mean velocity, we again computed the half velocity growth rates from a Gaussian curve fit. These are shown in Fig. 34. It is interesting that all of these curves converge to approximately $B/D = 1$ at $X/D = 2$, implying that the extent of the collision zone is approximately two characteristic heights.

The required linear decay rates of the inverse maximum velocity squared curves are shown in Fig. 35. These curves are normalized by the maximum source jet velocity squared. For equal jets this is proportional to one half the total source momentum. By normalizing the curves by the average source momentum, the curves become almost identical with a slightly higher decay rate (larger slope) for the more unequal jet case.

Figure 36 shows the locus of the centerline points for each case examined. These are plotted with respect to the physical centerline of the apparatus. Linear curve fits give the slope of the upwash and the intercept point on the ground plate. A simple analysis, presented in the next section, gives an estimate of these values. The slopes are predicted very well in this simple analysis, but the intercept is, in all cases, underpredicted. This is easily explained when one considers that the upwash is formed from the top of the collision bubble and, necessarily, the extrapolation to the plate will underpredict (i.e., indicate a location closer to the centerline) the collision point. Many of the derived values are summarized in Table 2.

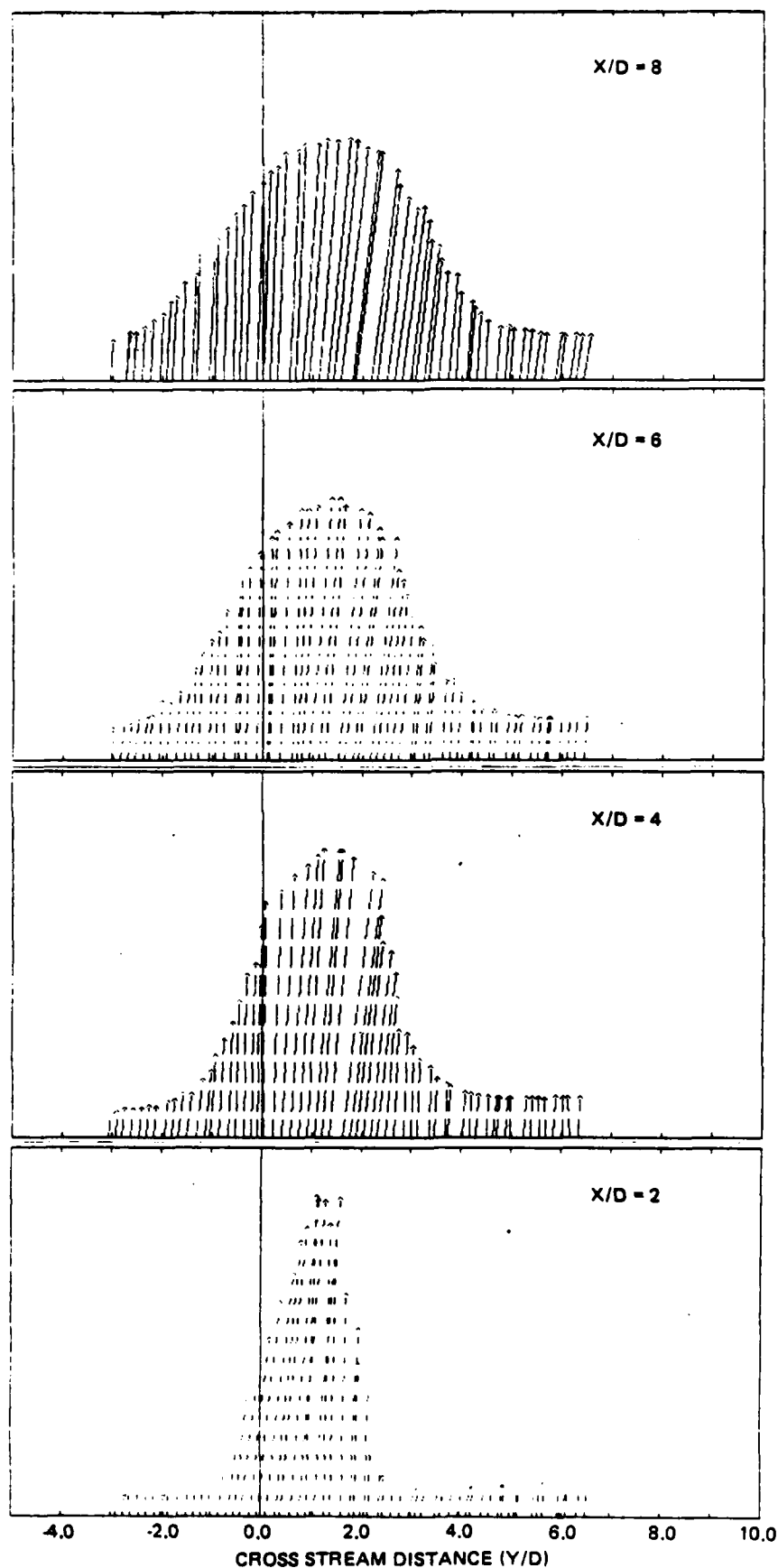
Figure 37 shows the turbulent kinetic energy normalized by the local maximum mean velocity. These profiles have been shifted in space so that they are all plotted with respect to their individual centerlines. This has the effect of plotting the profiles along a centerline in the direction of the upwash. The higher speed jet is from the left.

There are two features of these profiles that distinguish them from the equal jet case. While it is not obvious from the mean profiles, it was expected that the thinner wall jet from the right would produce a slightly higher shear rate right of center at the lower developing stations. The result of the greater shear is greater turbulence generation, which is seen in these profiles. In addition, due to the relatively smaller mass flow from the



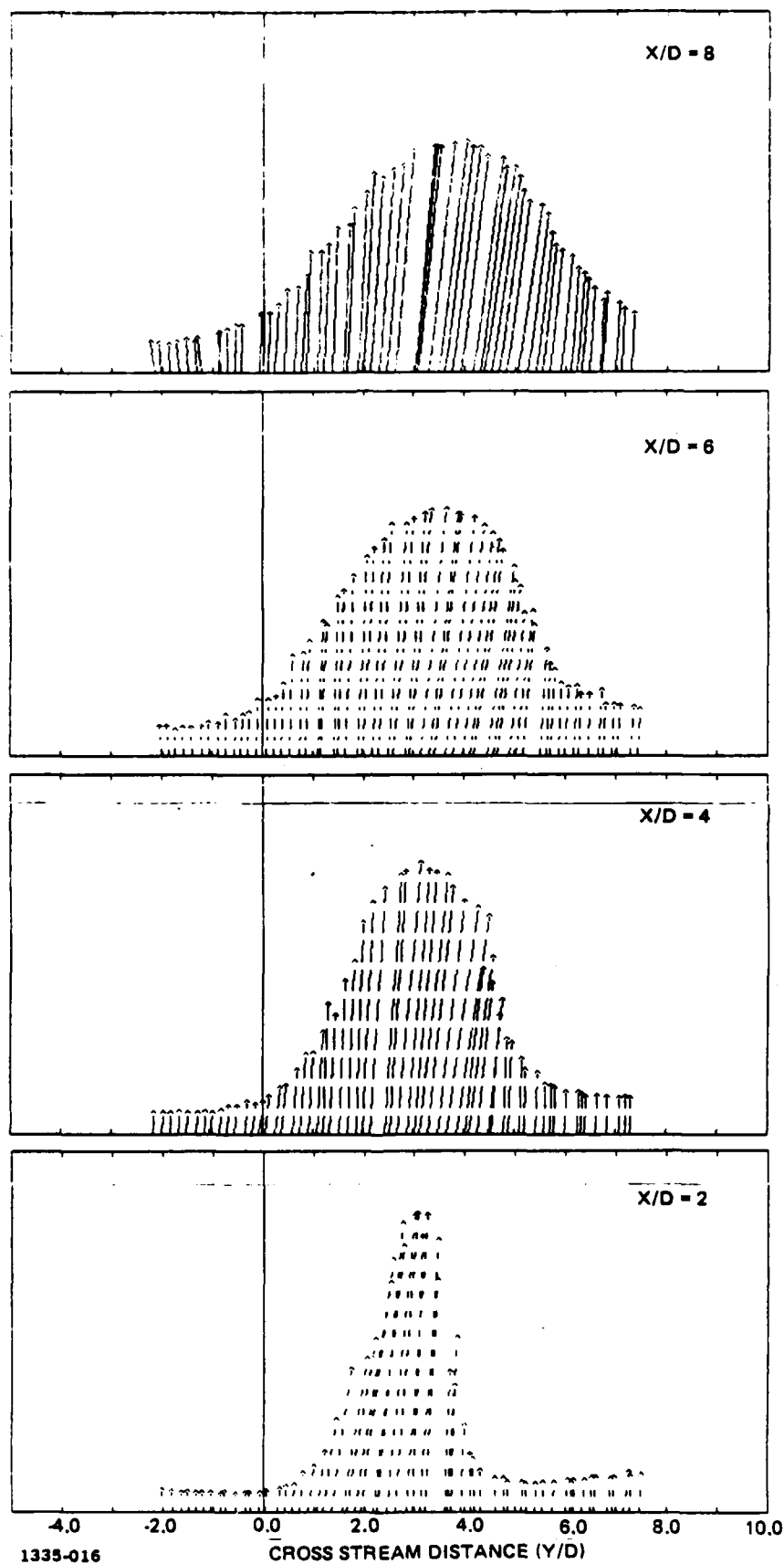
1335-014D

Fig. 29 Upwash Flow Field Vectors for Pressure Ratio = 1.0



1335-0150

Fig. 30 Upwash Flow Field Vectors for Pressure Ratio = 1.2



1335-016

Fig. 31 Upwash Flow Field Vectors for Pressure Ratio = 1.4

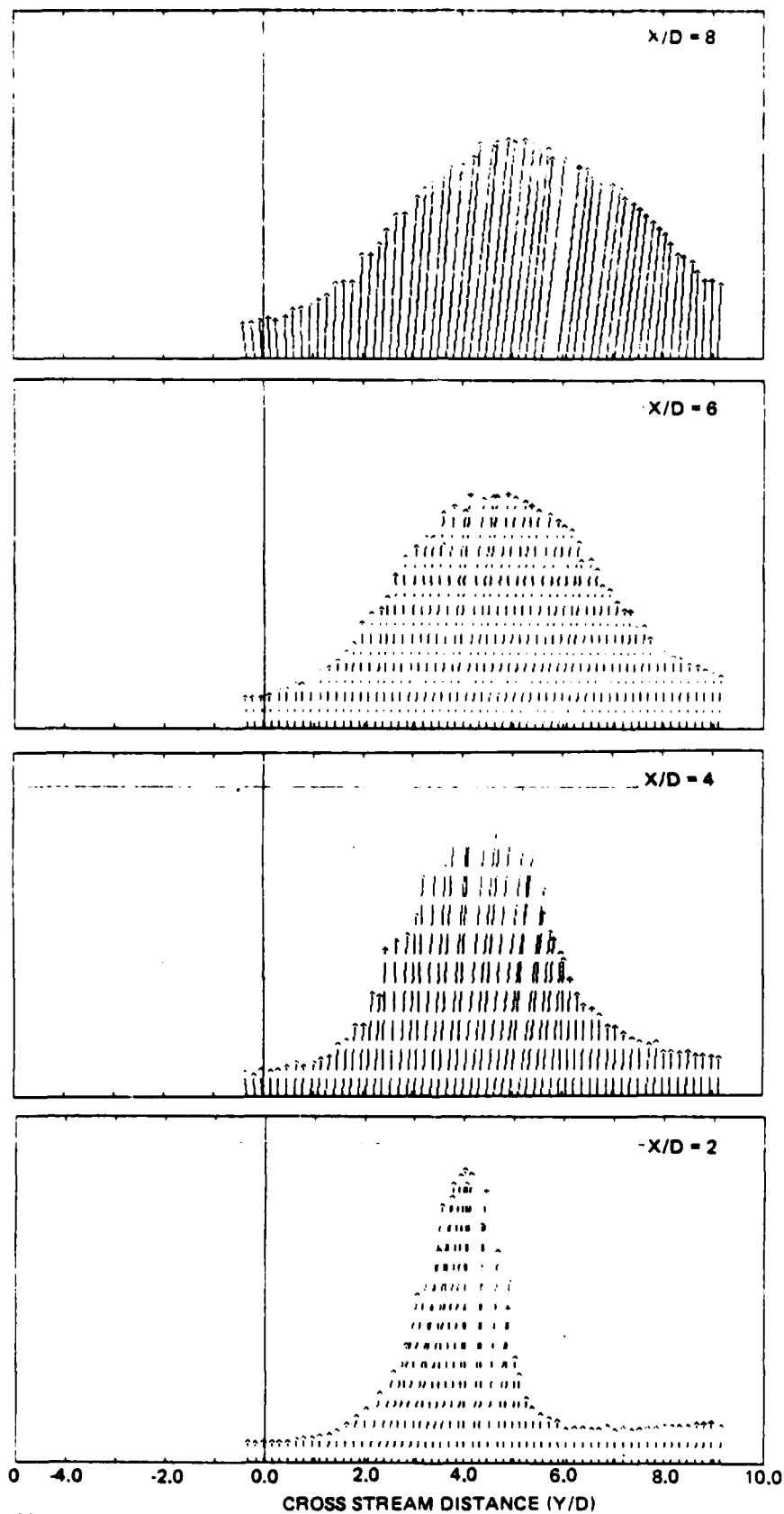


Fig. 32 Upwash Flow Field Vectors for Pressure Ratio = 1.6

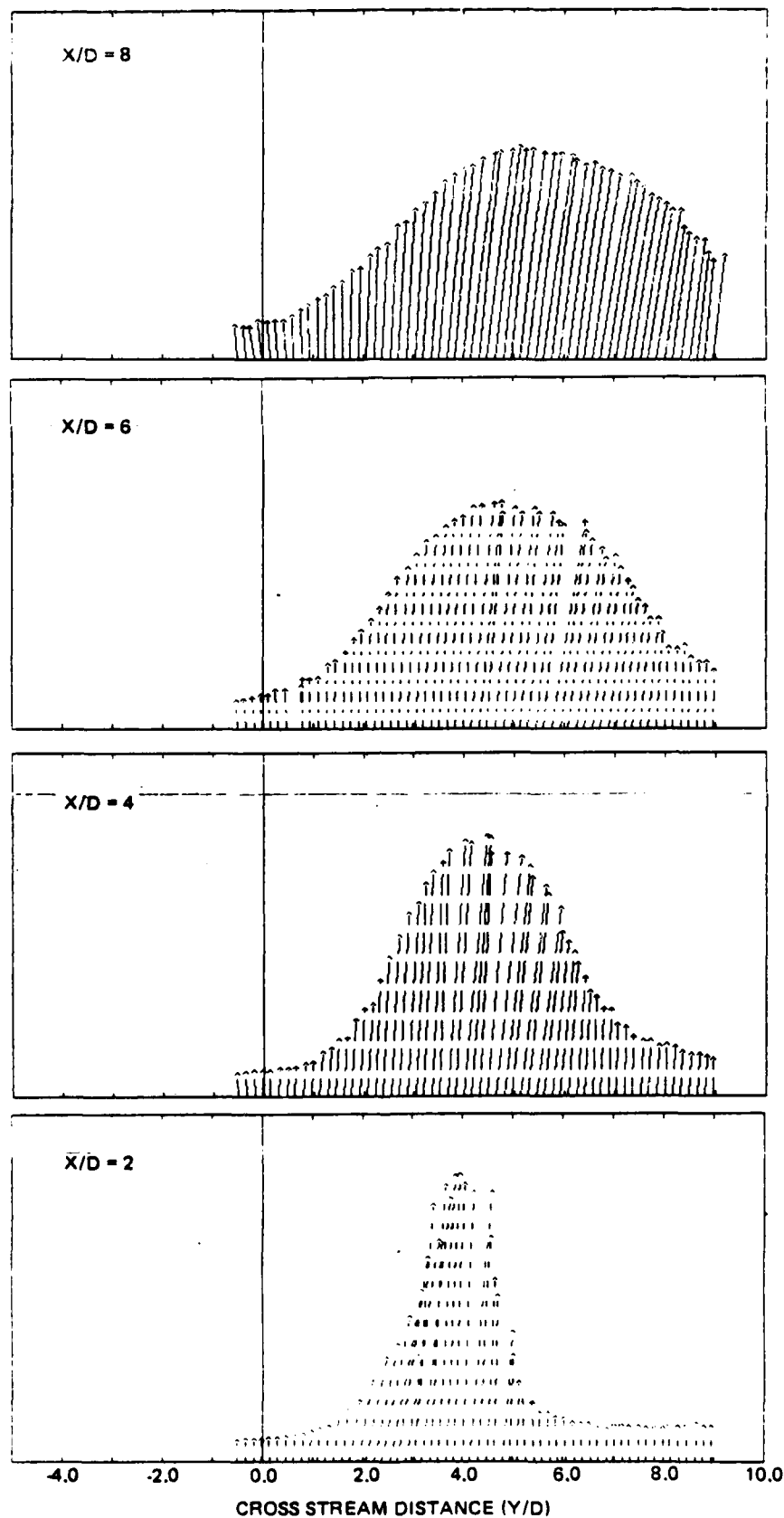
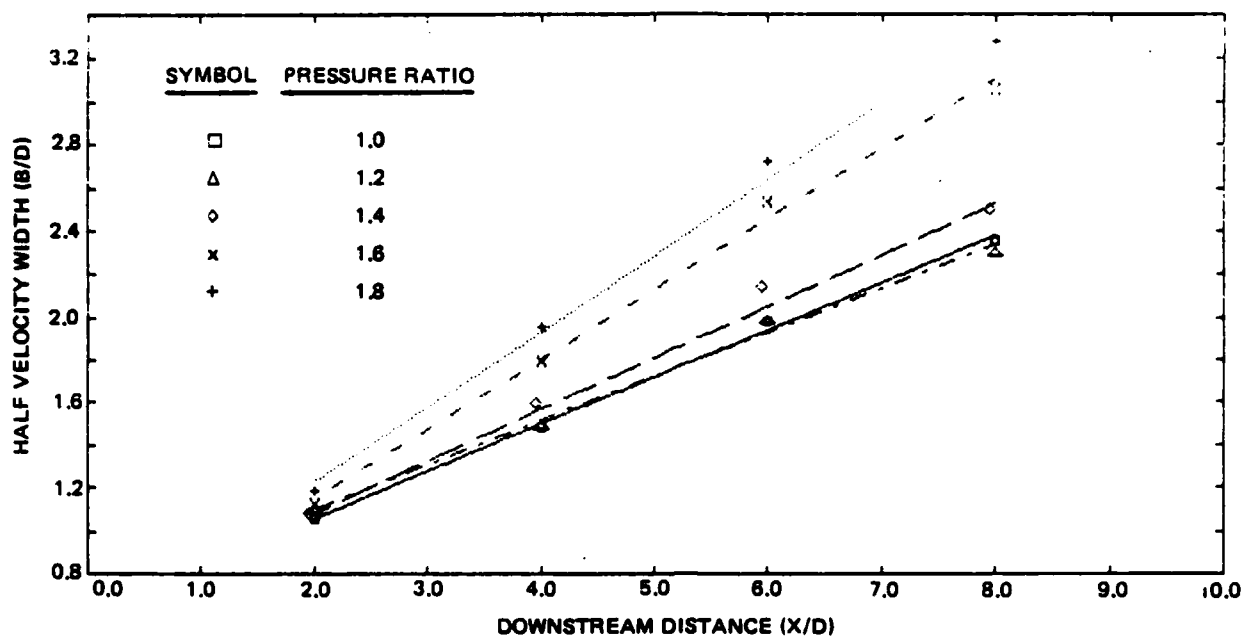
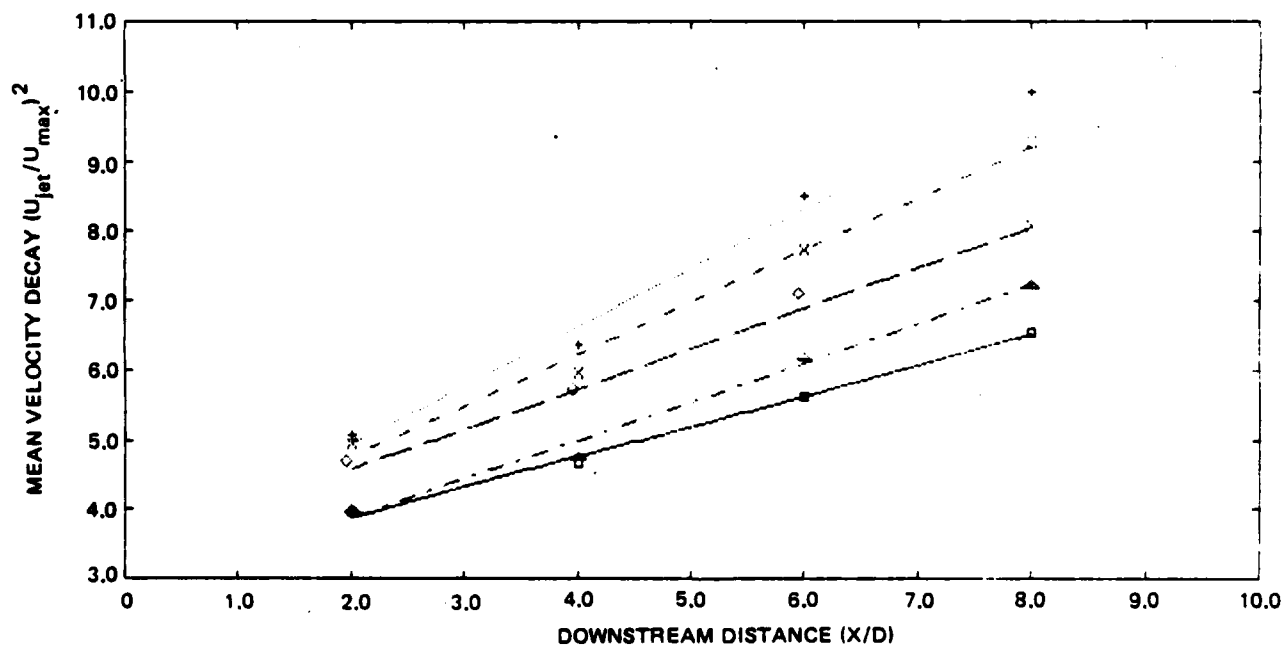


Fig. 33 Upwash Flow Field Vectors for Pressure Ratio = 1.8



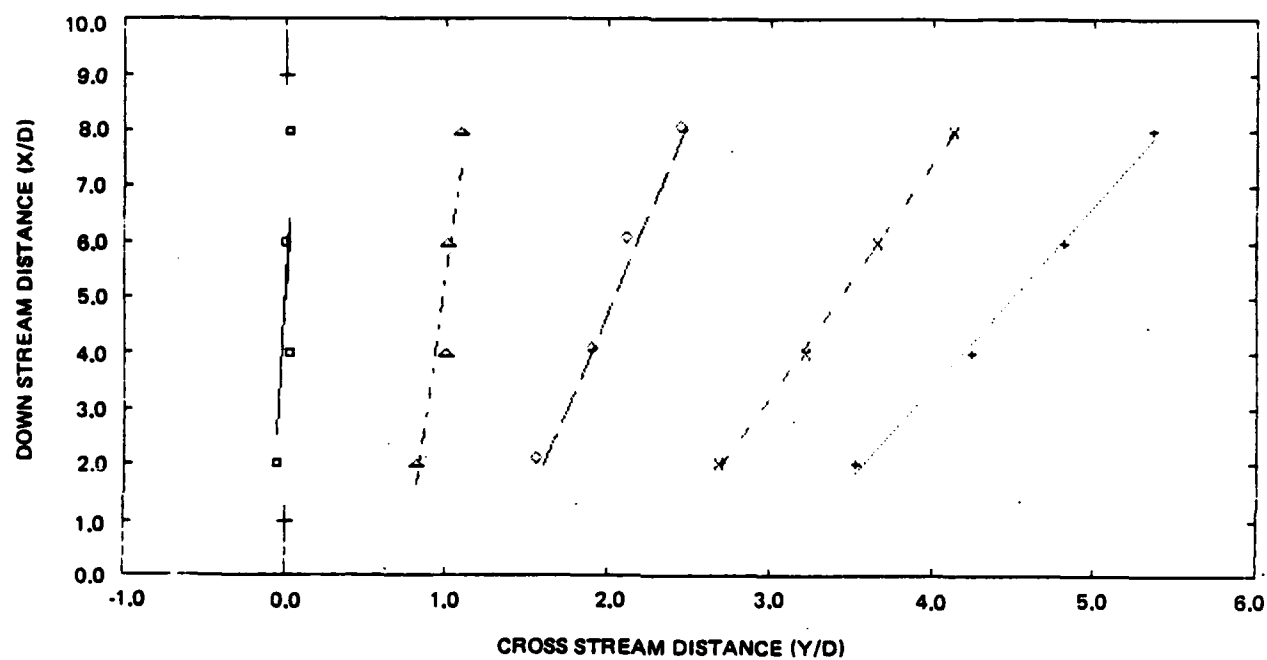
1335-019D

Fig. 34 Half Velocity Width Growth Rate in the Upwash of Unequal Wall Jets



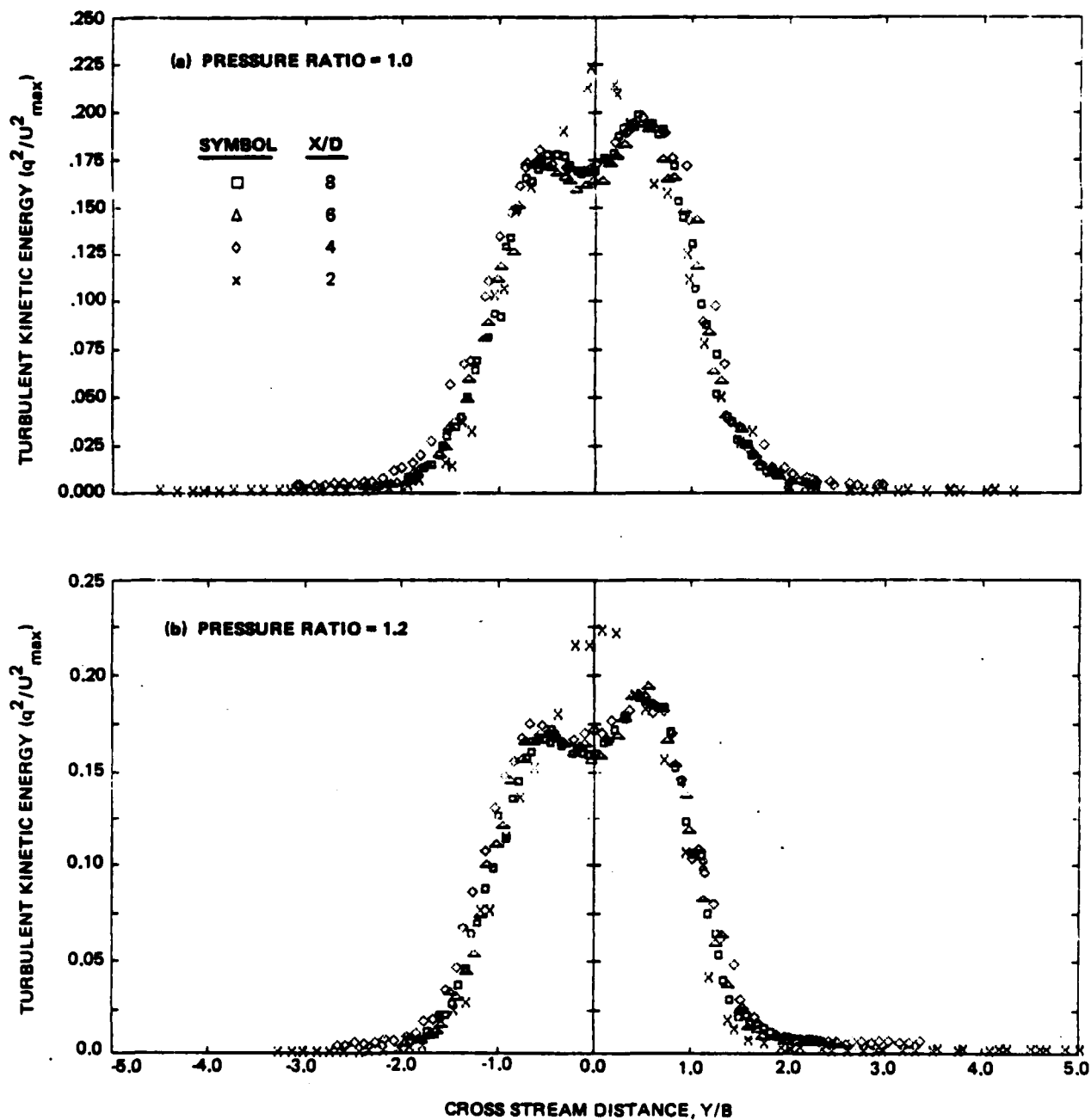
1335-020D

Fig. 35 Mean Velocity Decay in the Upwash of Unequal Wall Jets
(See Fig. 34 for Symbol Key)



1335-021D

Fig. 36 Position of the Maximum Velocity Peak in the Upwash of Unequal Wall Jets
(See Fig. 34 for Symbol Key)



1335-022D(1/2)

Fig. 37 Turbulence Kinetic Energy in the Upwash of Unequal Wall Jets (Sheet 1 of 2)

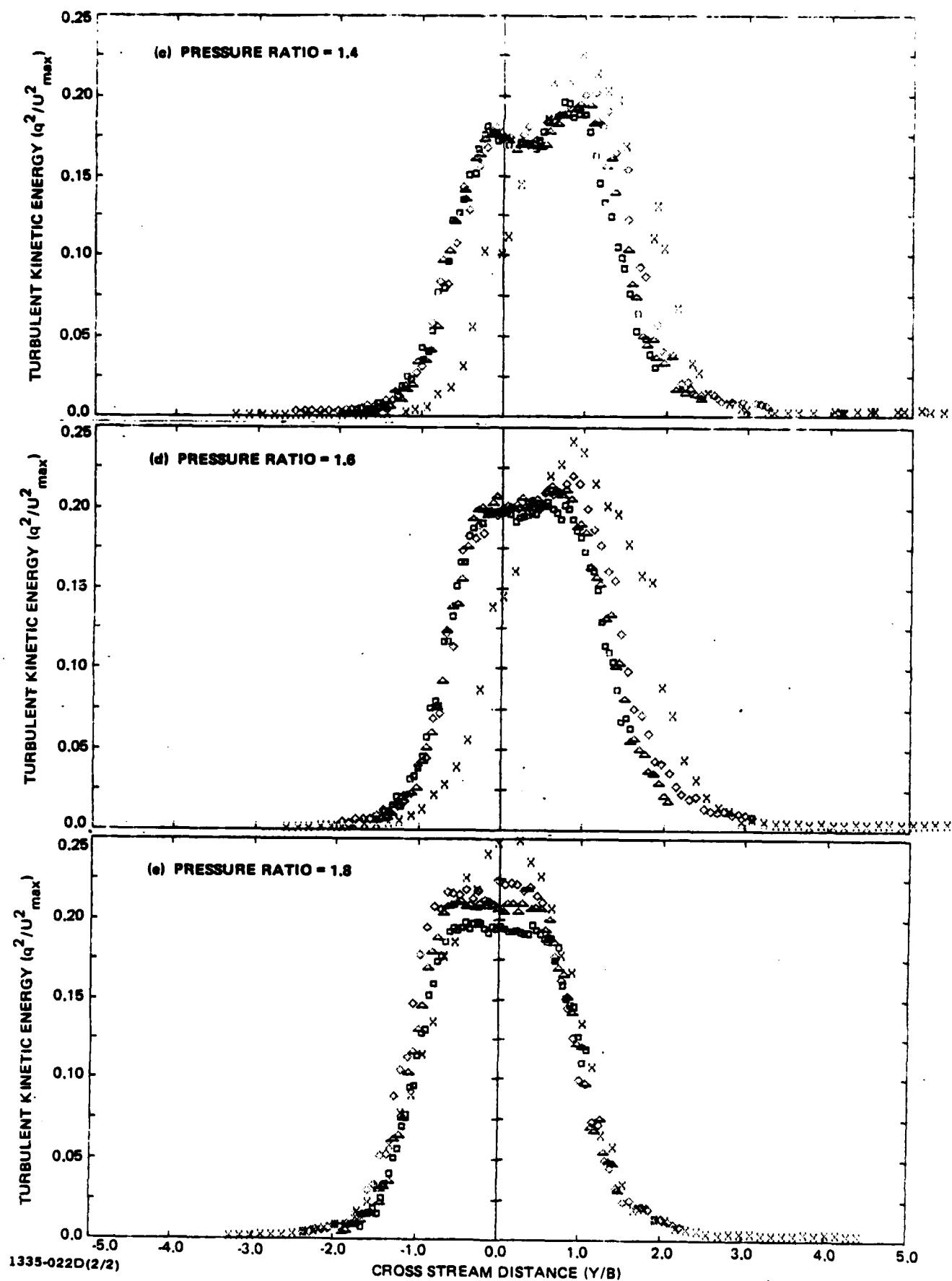


Fig. 37 Turbulence Kinetic Energy in the Upwash of Unequal Wall Jets (Sheet 2 of 2)

Table 2

COMPARISON OF THEORY WITH EXPERIMENTS WITH UNEQUAL WALL JETS

Pressure Ratio, K	Distance from CL to Collision (Δ/D)*		Upwash Angle		Growth Rate	Decay Rate	Normalized Decay Rate
	Predicted	Measured	Predicted	Measured			
1.0	0	-0.05	90.0	88.7	0.220	0.443	0.443
1.2	1.11	0.77	85.4	87.2	0.207	0.558	0.513
1.4	2.04	1.31	81.4	81.7	0.240	0.577	0.498
1.6	2.99	2.23	77.4	76.5	0.326	0.741	0.600
1.8	3.69	2.97	74.4	73.1	0.353	0.843	0.655

*See Fig. 38

right, it was expected that the maximum velocity point would be right of the symmetry point but would migrate towards the center as the flow developed. The data confirm this expectation. The small data scatter at the lowest station is due to increased weighing of the v component in the energy calculation (see Fig. 11-14). The Reynolds stress data, not shown here, exhibit the typical zero crossing at the centerline with decreasing maxima with increasing pressure ratio. At the lowest station, the left hand side shows a noticeable decrease in shear stress. This is a behavior contrary to simple mixing length theory and is in our view due primarily to the large cross stream turbulent energy component remaining from the collision process.

2.6 UNEQUAL JET ANALYSIS

A very simplified analysis may be used to estimate the position of collision and the angle the upwash makes with the ground plane. This analysis employs integral mass and momentum balances about a control surface around the collision point. Denoting flow from the left as 1, the right as 2, and exiting as 3 (as shown in Fig. 38) gives mass

$$m_1 + m_2 = m_3 \quad (1)$$

and momentum

$$h_1 u_1^2 - h_2 u_2^2 = h_3 u_3^2 \cos \theta. \quad (2)$$

Now assume, based on observation, that the point of collision is where the total pressures from each side are equal, that is,

$$\begin{aligned} 1/2 \rho u_1^2 &= 1/2 \rho u_2^2 \\ u_1^2 &= u_2^2 \end{aligned} \quad (3)$$

Since this is a simple analysis, the following proportionalities will be used:

$$\begin{aligned} u_1 &\sim u_{1,\max} \\ h_1 &\sim b_1 \text{ (the half velocity height)} \end{aligned}$$

introducing K = ratio of the initial momenta

$$= (u_{j1}/u_{j2})^2 \quad (4)$$

and taking $K > 1$, implying the stronger jet is from the left, and substituting

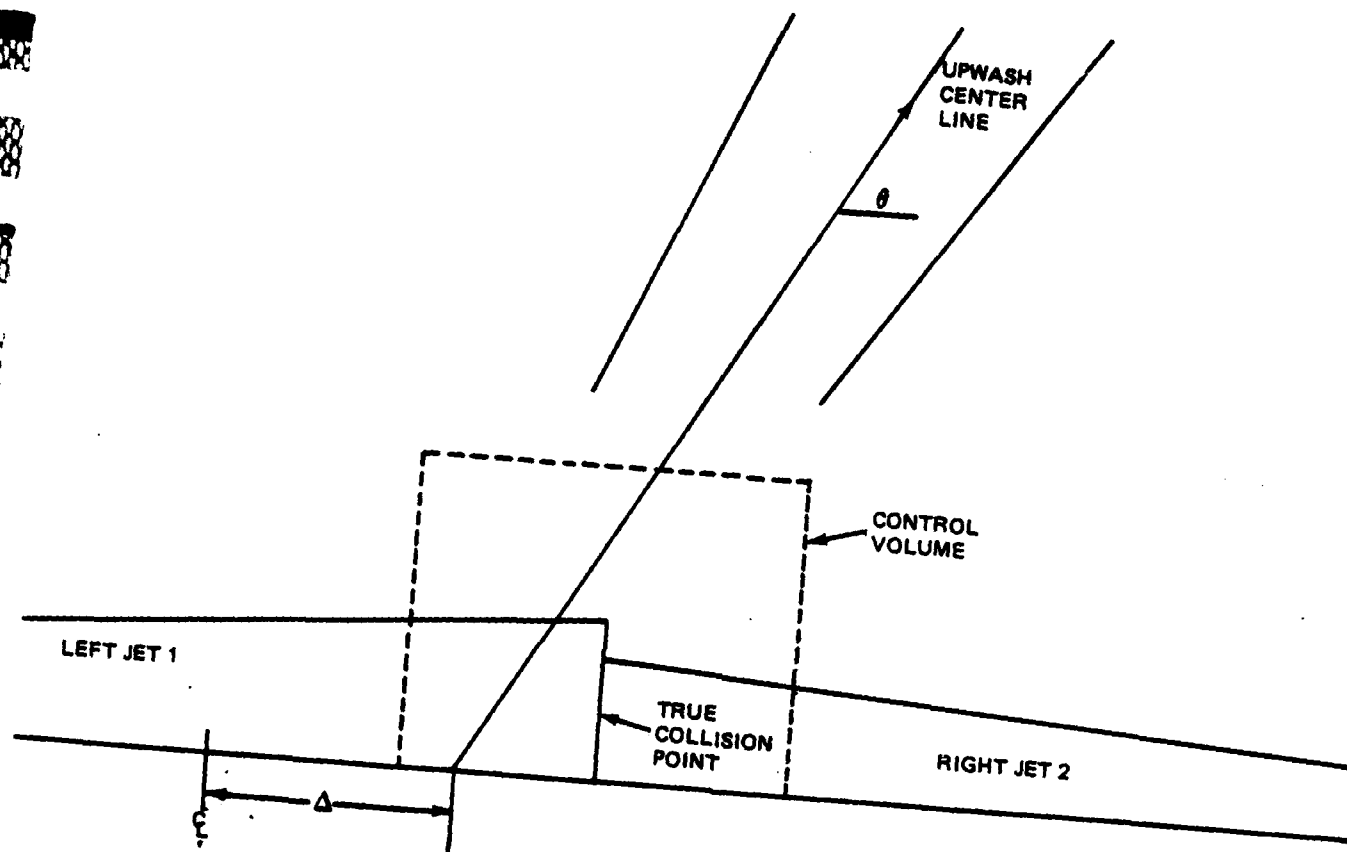


Fig. 38 Unequal Wall Jet Diagram

into (3) gives

$$\left(\frac{u_{j1}}{u_1}\right)^2 = K \left(\frac{u_{j2}}{u_2}\right)^2 \quad (5)$$

at the collision point. Now using (4) and (2) with $u_1 = u_2$ at the collision and $u_1 = u_3$ from Bernoulli's equation gives

$$b_1 - b_2 = b_3 \cos \theta \quad \text{from (2)}$$

$$b_1 + b_2 = b_3 \quad \text{from (1)}$$

so

$$\cos \theta = \frac{b_1 - b_2}{b_1 + b_2} \quad (6)$$

Now (5) and (6) can be used to determine the position and angle of the upwash flow. The wall jet relationships given in Ref. 10 for growth

$$b/D = 0.651 + 0.0728 X/D$$

and for decay

$$(U_j/U_{\max})^2 = 0.35 + 0.065 X/D$$

are used in the calculations shown in Table 2.

2.7 CENTERLINE OBSTACLES

One explanation that has been advanced for the large mixing rate and intermittency factors found in the upwash is a lateral movement of the entire upwash jet. If this were the case, it would be expected that a small object located at the collision point would pin the upwash and thereby reduce the mixing rate. We used six splitter plates located at the collision point. These obstacles are 1/4, 1/2, 1, 2, 3 and 4 characteristic wall jet heights and were tested with both jets operating.

All of the profiles are similar to those already shown for equal jets. The only noticeable difference in some of the profiles is the presence of a small centerline dip, due to the wake of the splitter plate, at the lowest location. The results of the curve fit are given in Table 3.

Table 3

SUMMARY OF CENTERLINE OBSTACLE RESULTS

Obstacle Height	Growth Rate	Heights Measured
0	0.230	8,6,4,2
1/4 D	0.182	8,6,4,2
1/2 D	0.174	8,6,4,2
1 D	0.144	8,6,4,2
2 D	0.131	8,6,4,2.1
3 D	0.131	8,6,4,3.1
4 D	0.130	8,6,5
sand	0.226	8,6,4,3

It is apparent that an increased growth rate is inherent to two-stream mixing jets where these streams have some head-on component velocities. The increased mixing in the upwash is due directly to the two-stream mixing process. Even with large splitter plates, where the wall jet flow has been turned into the vertical direction, there is still an increased mixing rate over the classical free jet value. For large splitters, the wall jets are nearly re-established before the vertical wall jets meet. At this point, the turning turbulence has started to die out. The resulting growth rate of 0.130 is much less than the upwash jet value of 0.220 but is still more than 0.10 for free jets. However, it is twice the wall jet (one from each side of the plate) value of 0.068. As the plates become smaller, the two-jet influence is more pronounced. It is obvious that lateral solid body motion of the upwash is not necessary for an increased mixing to be observed.

The case labeled "sand" is a test in which sandpaper trips were installed halfway between the jet exit and the centerline. This was done to insure a fully turbulent boundary layer. Since the wall jet dominates the upwash formation, there is no effect in the upwash due to the boundary layer changes. The linear half velocity growth develops a very short distance downstream of the splitter plate. Since physical limitations of the apparatus preclude going more than 8 D above the plate, a change in these growth characteristics is possible, but unlikely, with increased distance.

2.8 ADDITIONAL WORK

One possible explanation for the large mixing region is that the entire upwash is waving (Ref. 19). A method of detecting waving in the upwash is the measurement of cross correlation velocities at various points in the flow. If waving exists, positive (in-phase) correlations should be apparent when the two probes are on the same side of the upwash and negative (out-of-phase) correlation when they are on opposite sides. A set of experiments was conducted utilizing two X-probe anemometers. One probe was held stationary while the other was traversed across the upwash. Ten distinct auto and cross-velocity correlations were computed at each point for the various u and v components. These were conducted with the fixed probe at two heights and at two cross stream positions in the upwash. No indication of waving was detected.

Finally, a significant amount of time was devoted to trying to obtain good flow visualization of the mixing interface of the upwash with its surroundings. Attempts were made to photograph seeded flow illuminated by a laser sheet. Shadowgraph and schlieren were also tried. These were seeded with helium to increase the density differential. These all proved to be of little value because of the large interface and rapid turbulence mixing. Video tapes were made of ordinary smoke visualization. These showed very graphically that the entrainment flow extended from very large distances from the upwash. They also showed the non-regular intermittent nature of the upwash boundary. This again points up the importance of using a radial flow configuration that avoids the additional complications introduced by the presence of impinging jets.

2.9 RADIAL WALL JETS

It is our approach to study the upwash effects in increasingly more complex flow geometries. After completion of the two-dimensional upwash phase, we then required the construction of an apparatus to provide a radially spreading wall jet. The characteristics found in the two-dimensional upwash will be examined in this new radial upwash.

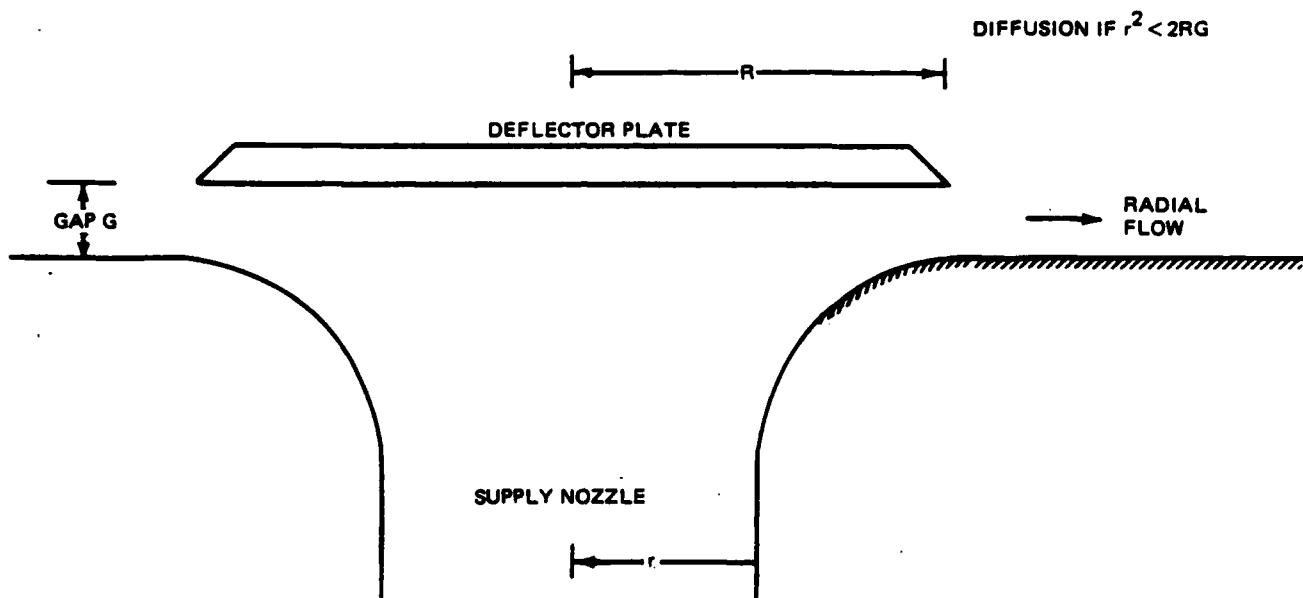
The usual method employed for the generation of this sort of wall jet is the impingement of the circular free jets into a ground plane. While this method undoubtedly creates a radial wall jet, in the case of the upwash, it

also introduces an additional complication: it is impossible to isolate the effects of the presence of circular free jets on the development of the upwash physically located between them. The downward flowing free jets set up a strongly coupled secondary rotating flow with the upward flowing upwash.

We had to ensure that we had a highly controllable upwash whose characteristics could be studied in a manner decoupled from other effects. Therefore, a study was undertaken to determine if a radically different geometry could be used to produce a suitable radial spreading wall jet. The geometry chosen was one that employed a circular source jet flowing through the ground plane from below. The circular jet was then diverted into the radial direction along the ground by impinging upon a circular deflector plate. It was found that using a much smaller gap than originally designed produced the desired flow. This design was then used in the full scale test facility that will be the primary apparatus used in the next follow-on phase. After we complete that phase, the full simulation of the V/STOL upwash will be examined in future follow-ons. This would use an upwash formed from the collision of impinging jets. Some of the development work on the new apparatus will now be reported.

The basic concept of the design is shown in Fig. 39. Several wall jet profiles were obtained from a conventional free jet impingement. These were used to compare with the wall jet profiles measured from the various geometries tested. Mean velocity decay curves and wall jet half height growth rate curves were also compared to assure that the wall jet obtained in the new geometry had the same characteristics as a conventional radial wall jet. Tests were conducted at several gap heights and with deflector plates of three different diameters. Decay and growth characteristics were computed from mean velocity profiles taken at the exit and at least six locations downstream.

In summary, it was found that if the gap was too large, the wall jet would form on the deflector plate, i.e., it would stick to the wrong surface. An example is shown in Fig. 40. Once this effect was identified, the choice of deflector plates was driven by the desire to minimize the internal diffusion effect as the flow changes direction. The largest radius of curvature supply nozzle available was chosen for the same reason. There is a net diffusion inside the turn if $RG > r^2/2$. In the small gap case, there is a minimum flow cross-sectional area at the nozzle lip, normal to the plate.



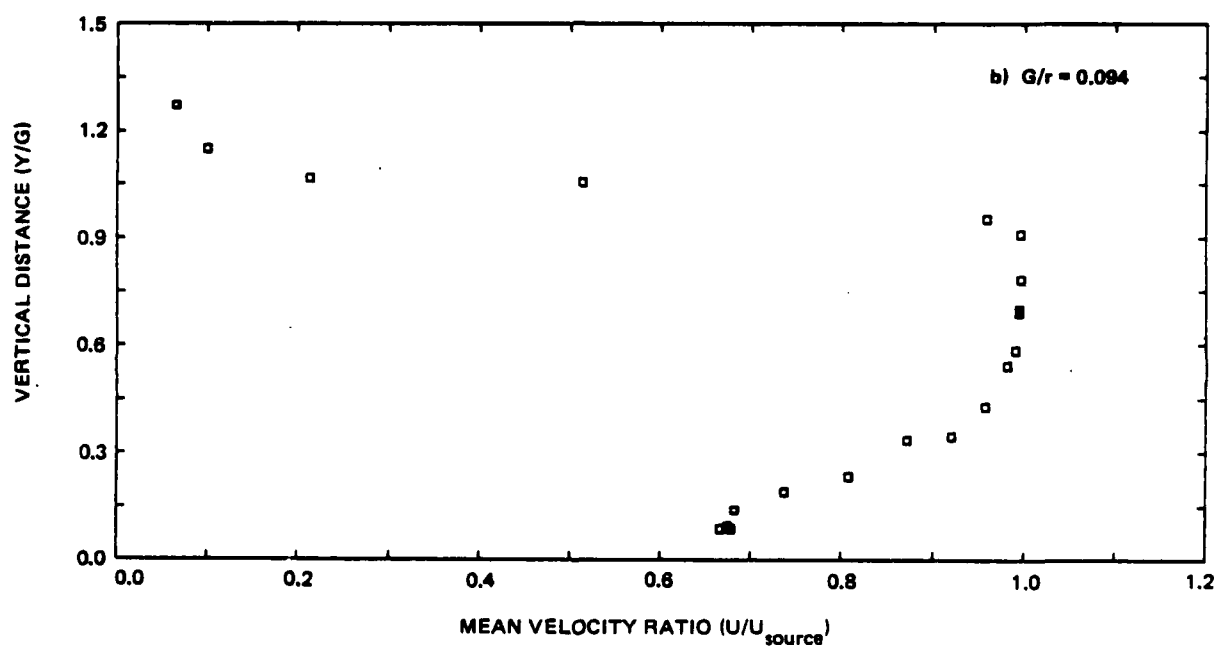
1335-024D

Fig. 39 Diagram of Radial Wall Jet Design

There is no net diffusion up to this point, only beyond. A separation bubble at the inner nozzle lip could promote downstream problems on the adjacent wall. In the large gap case, there is a minimum flow area in the nozzle, and diffusion area depends on the gap height. The plate was chosen such that the diffusion of the wall jet flow would take place outside of the turn.

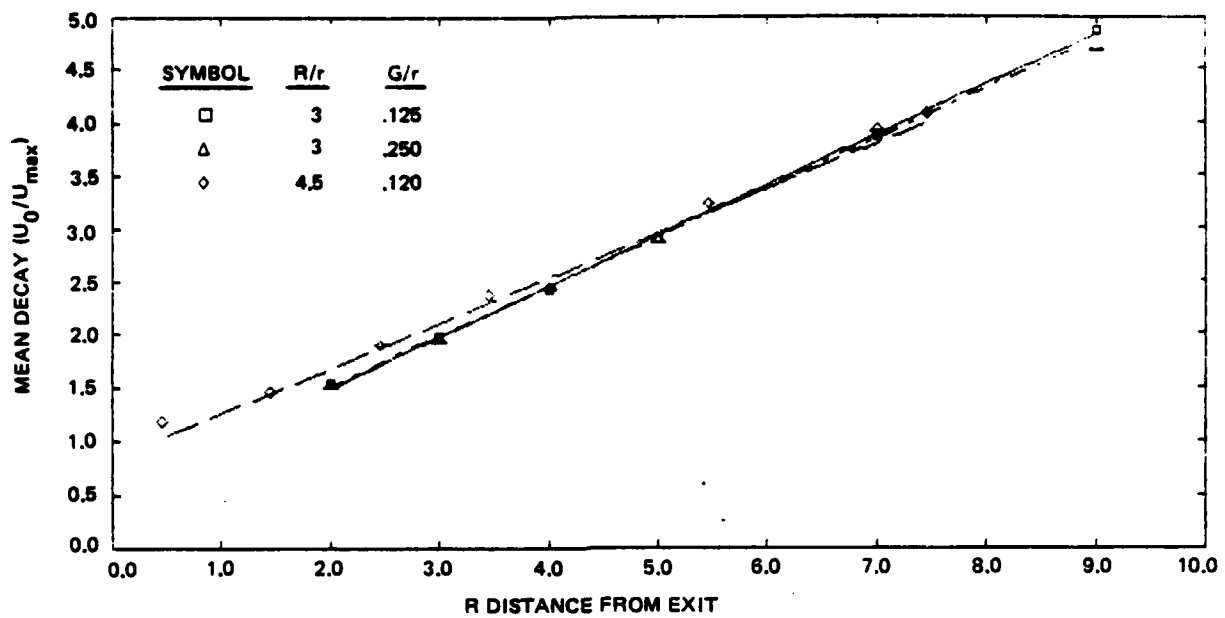
Figures 41 and 42 show the normalized mean velocity decay profiles and half width growth rate for acceptable flow geometries. In this form, the decay is independent of the specific arrangement. However, the effect of the internal diffusion on the flow rate is apparent in Fig. 43. The smaller gaps induce more flow. The smallest gap height was chosen for the full scale apparatus. Our selection was based on the best agreement with classical wall jet characteristics. Figure 44 shows the normalized downstream development of the mean velocity wall jet profiles.

Figure 45 shows the new radial wall jet test facility in our new Research Laboratory. This photograph shows the two source jets exhausting from the plenum chambers below the instrumentation plate. The source nozzles are coupled to the instrumentation plate via a flexible collar to provide vibration isolation. The plate is mounted on of the plenum chambers in such a way as to isolate the flow from any fan vibration that may be transmitted to the chambers. The deflection plates are mounted as already described. The gaps are adjustable by changing spacers. A simple hot film probe is shown mounted on a two-axis traverse, although only one axis is computer controlled. The circular disk in the center contains a series of eight static pressure taps. By rotating this disk, the entire static pressure field between the two source jets may be mapped. In comparison with the 2-D wall jets, the source gap is nominally 0.47 cm versus 1.0 cm, and the distance between lips is nominally 75 gap heights versus 84 and 61 for the long and short 2-D plates. Because the physical size of the gap is smaller, future experiments should be able to make measurements that extend farther downstream.



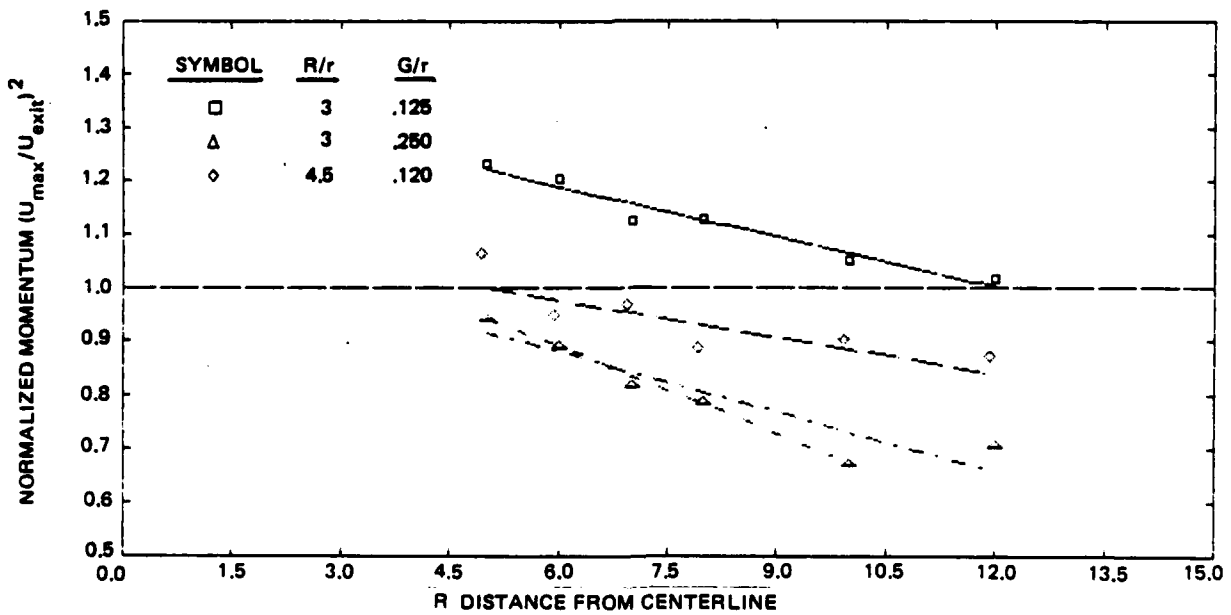
1335-025D

Fig. 40 Radial Wall Jet Exit Profiles



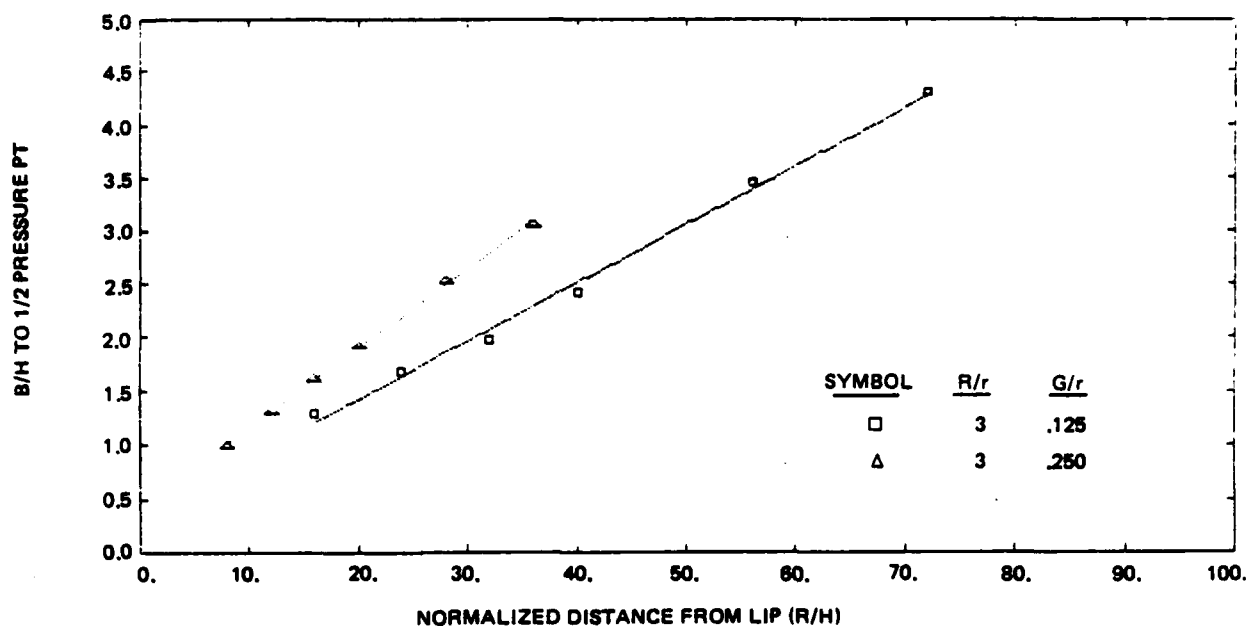
1335-026D

Fig. 41 Radial Wall Jet Mean Velocity Decay Profile



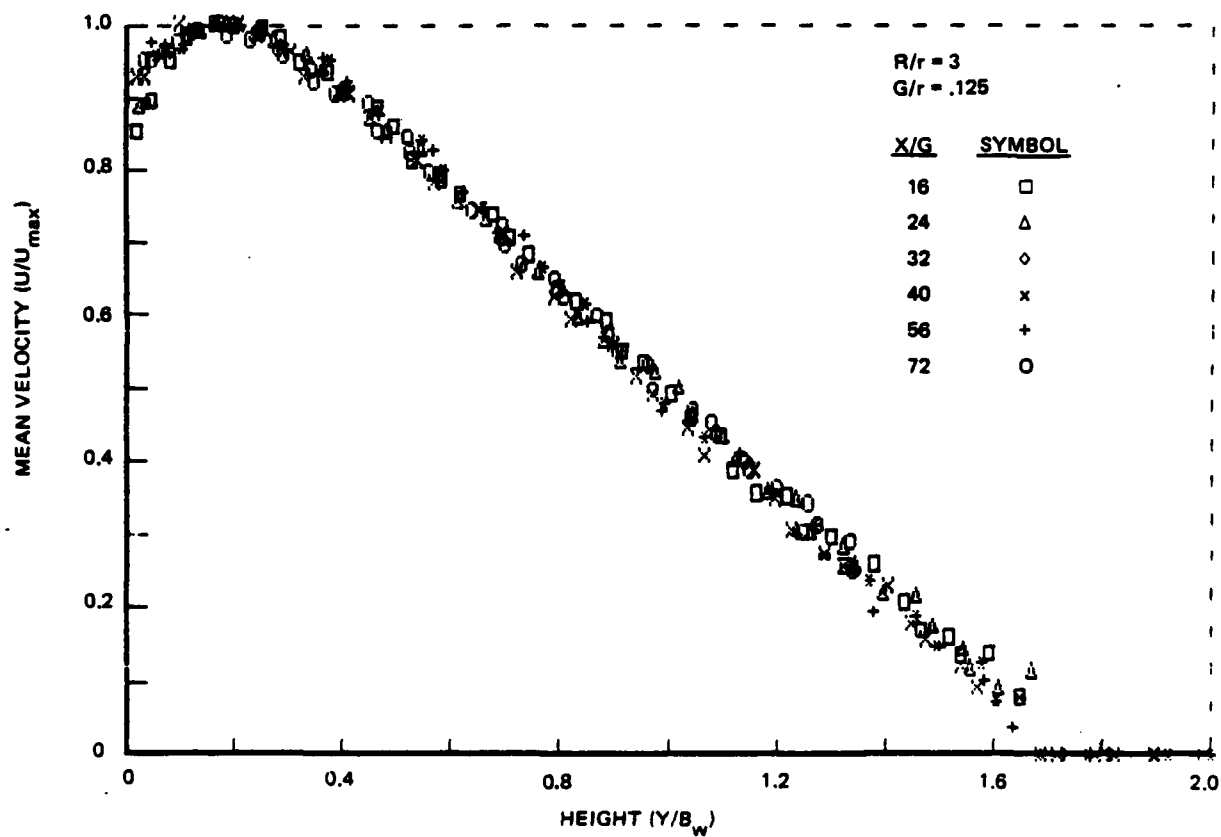
1335-027D

Fig. 42 Radial Wall Jet Momentum for Different Gap Heights



1335-028D

Fig. 43 Increased Mass Flow Rate for Radial Wall Jets



1335-029D

Fig. 44 Radial Wall Jets Mean Velocity Profiles

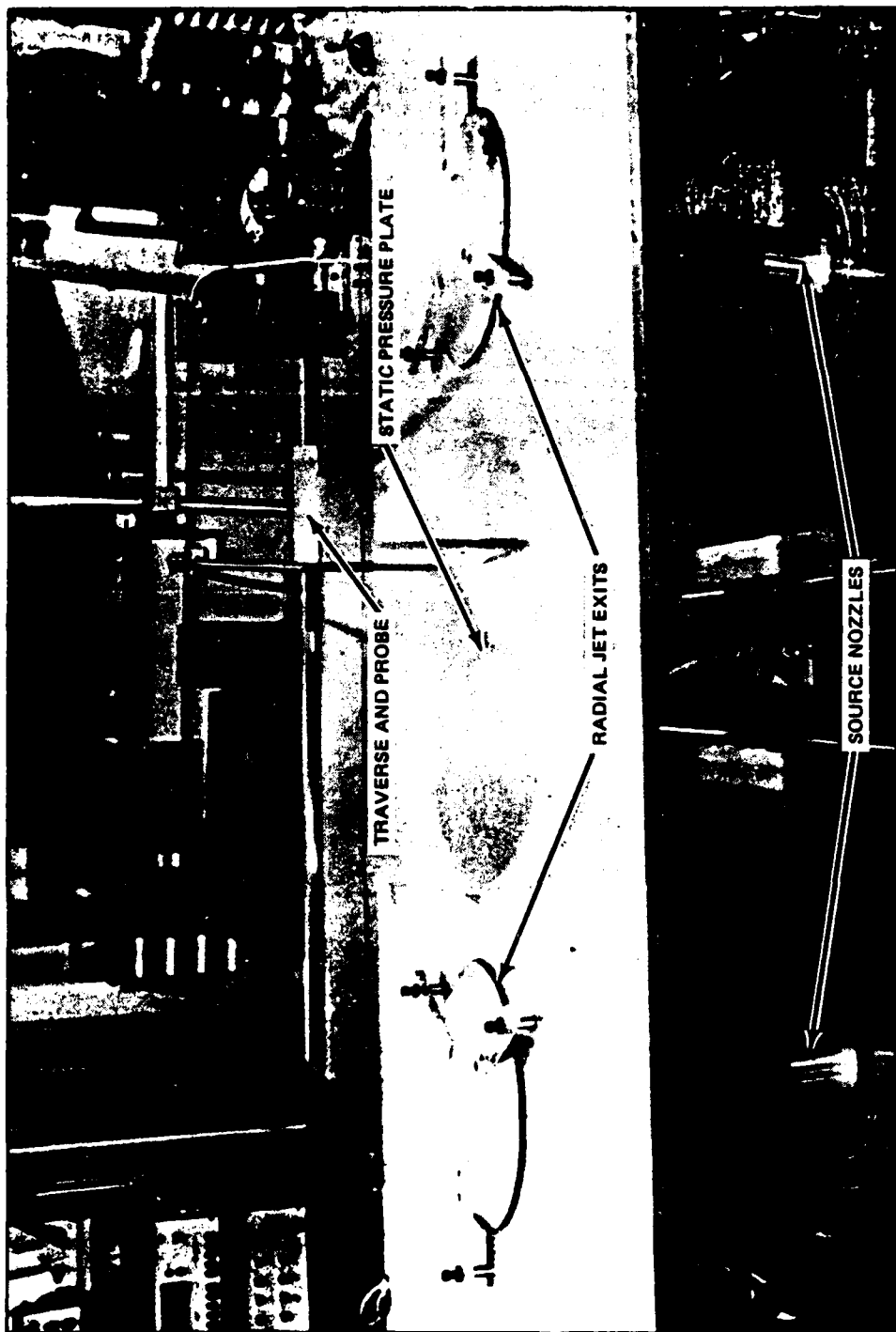


Fig. 45 Photograph of Radial Wall Jet Upwash Facility

3. CONCLUSION

Our experimental investigation of the turbulence mechanisms in a V/STOL upwash field was conducted in a two-dimensional facility to simplify the geometric complexity and interference effects of a real V/STOL flow. The basic turbulence characteristics in the upwash are similar to those found in an ordinary two-dimensional free jet. The most notable differences are the much greater mixing rate and turbulence scale (shown by the intermittency) in the upwash. It was found that as the flow develops downstream, the increased mixing rate starts to decrease, although similarity seems to exist in the turbulence quantities. Measurements here were limited to 12 local wall jet half velocity heights. It is hypothesized that if measurements were taken farther into the upwash, values of mixing layer growth rate would approach 0.1, the value found in free jets. The higher mixing rate is explainable primarily on the basis of the head-on collision and turning effect of the wall jets that form the upwash. These create large turbulent eddies that involve more ambient fluid than normal. Higher rates than these observed by previous investigators are most likely due to a combination of measurement difficulties, poor control of source streams, and measurements taken in the near field. Higher turbulence levels reported by others seem to be due to misinterpretation of the data. However, it should be pointed out that since the intermittency function extends farther into the upwash, and since the time average turbulence energy is approximately the same as a free jet, when the turbulence is present, it is more energetic. Development of an apparatus for the continued investigation of a more complex upwash formed from the collision of radial wall jets is also described. This unique design assures that the upwash may be studied separately from the effects of source jet impingement and secondary flows.

4. REFERENCES

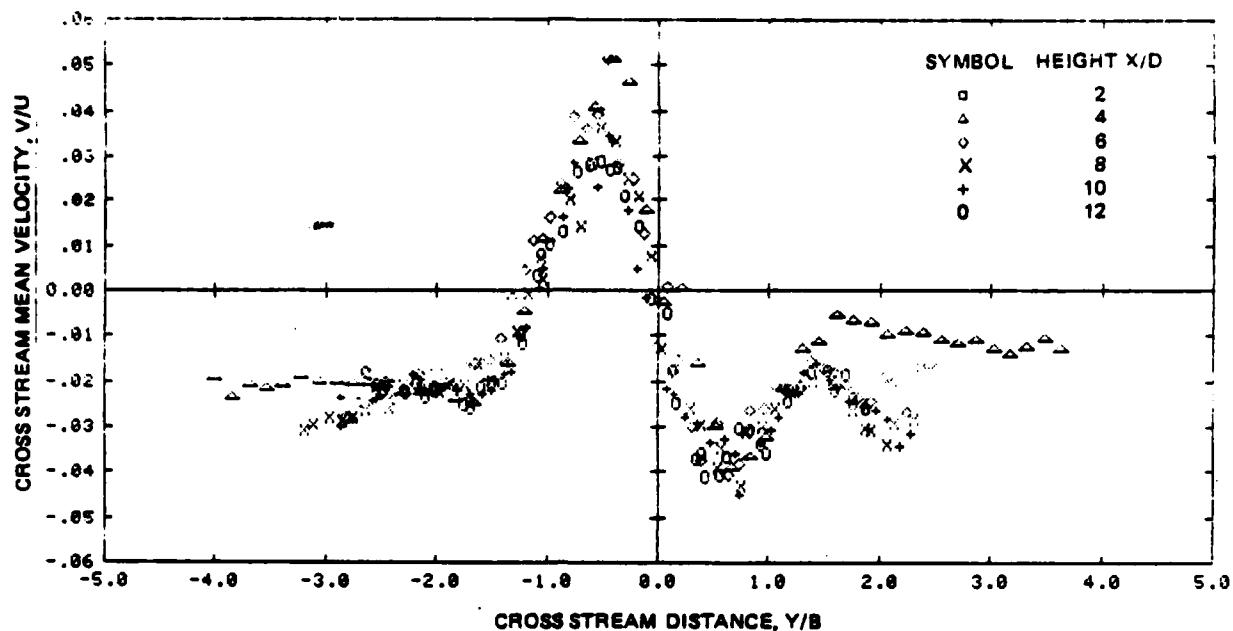
- 1 Kalemari, S.G. and Cea, R.A., "Effects of Technology Level on V/STOL Aircraft," AIAA Paper #77-1238, Aircraft Syst Tech Mtg, Seattle, WA, Aug 1977.
- 2 Kalemari, S.G. and York, P., "Weight Impact on VTOL," SAWE Paper #1326, 38th Annual Conf of SAWE, New York, May 1979.
- 3 Rajaratnam, N., Turbulent Jets, Developments in Water Science, 5. Elsevier Scientific Publishing Co., Amsterdam, 1976.
- 4 Harsha, P.T. "Free Turbulent Mixing: A Critical Evaluating Theory and Experiment," AEDC-TR-71-36, Feb 1971.
- 5 Kind, R.J. and Suthanthiran, K., "The Interaction of Two Opposing Plane Turbulent Wall Jets," AIAA Paper No. 72-211, AIAA 10th Aerospace Sciences Mtg, San Diego, CA, Jan 17-19, 1972.
- 6 Witze, P.O. and Dwyer, H.A., "Impinging Axisymmetric Turbulent Flows: The Wall Jet, The Radial Jet and Opposing Free Jets," Symp on Turbulent Shear Flows, Vol 1, Univ Park, PA, Apr 23-30, 1977.
- 7 Kotansky, D.R., and Glaze, L.N., "The Effects of Ground Wall-Jet Characteristics on Fountain Upwash Flow Formation and Development," AIAA Paper #81-1294, AIAA 14th Fluid & Plasma Dyn Conf, Palo Alto, CA, June 23-25, 1981.
- 8 Foley, W.H. and Finley, D.B., "Fountain Jet Turbulence," AIAA Paper #81-1293, AIAA 14th Fluid & Plasma Dyn Conf, Palo Alto, CA, June 23-25, 1981.
- 9 Jenkins, R.A. and Hill, W.G., Jr., "Investigation of VTOL Upwash Flows Formed by Two Impinging Jets," Grumman Research Department Report RE-548, Nov 1977.
- 10 Gilbert, B.L., "Detailed Turbulent Measurements in a Two-Dimensional Upwash," AIAA No. 83-1678, AIAA 16th Fluid & Plasma Dynamics Conf, Danvers, MA, July 12-14, 1983.
- 11 Gilbert, B.L., "An Investigation of Turbulence Mechanisms in V/STOL Upwash Flow Fields," Grumman R&D Center Report RE-688, Aug 1984.

- 12 Kline, S.J., et al., ed, Proc of the 1980-81 AFOSR-HTTM-Stanford Conf on Complex Turbulent Flows, published by Stanford Univ, 1981.
- 13 Townsend, A.A., The Structure of Turbulent Shear Flow, 2nd ed., Cambridge Univ Press, Great Britain, 1980.
- 14 Bradshaw, P., Private communication, Reno, NV, Jan 1985.
- 15 Hill, W.G., Jr., "A Preliminary Investigation of Two-Jet V/STOL Upwash Flow Control Using Small Ground Obstacles," Grumman Research & Development Center Memorandum RM-784, Nov 1983.
- 16 Hill, W.G., Jr., Jenkins, R.C. and Gilbert, B.L., "Effects of the Initial Boundary Layer State on Turbulent Jet Mixing," AIAA J., Vol 14, No. 11, pp 1513-1514, Nov 1976.
- 17 Hill, W.G., Jr. and Jenkins, R.C., "Effects of Nozzle Spacing on Ground Interference Forces for a Two-Jet V/STOL Aircraft," AIAA paper 79-1856, AIAA Aircraft Syst & Tech Conf, New York, NY, Aug 20-22, 1979. Also J. of Aircraft, Vol 17, pp 684-689, Sept 1980.
- 18 Jenkins, R.C. and Hill, W.G., Jr., "Investigation of the Effects of Close Nozzle Spacing on Upwash and Fountain Formation," Proc of the Workshop in V/STOL Aerodynamics, Naval Postgraduate School, Monterey, CA, May 16-18, 1979.
- 19 deGortari, J.C. and Goldschmidt, V.W., "The Apparent Flapping Motion of a Turbulent Plane Jet," J. of Fluids Eng, Vol 103, pp 119-126, March 1981.

APPENDIX A

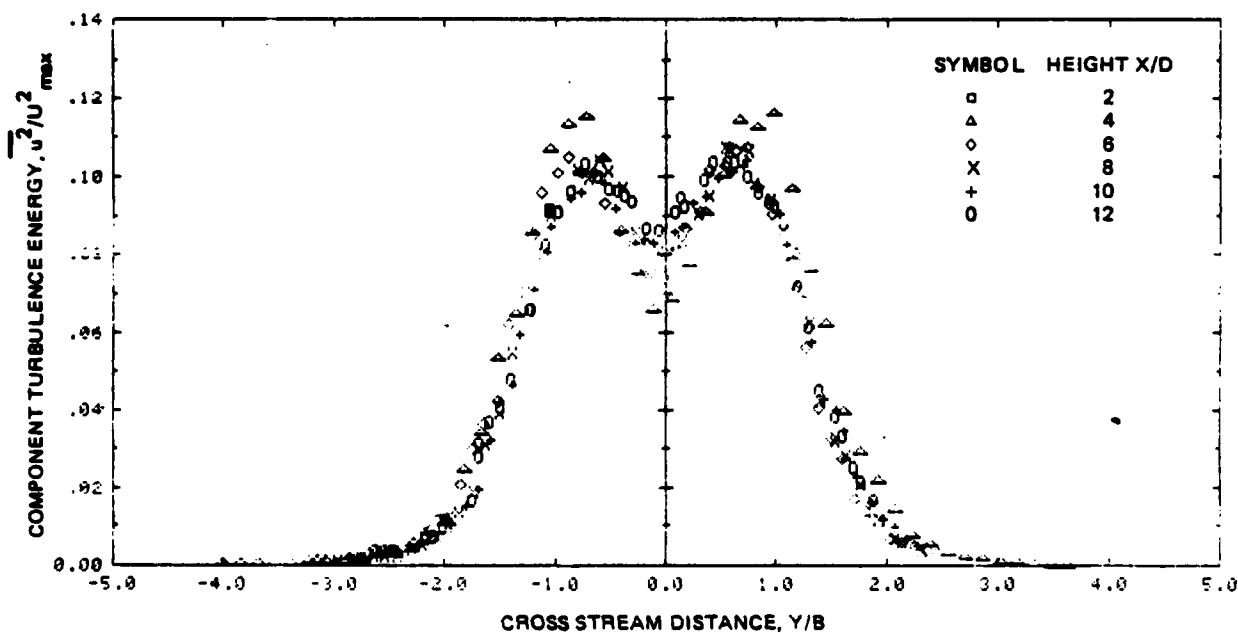
Case A: Short Plate, full speed

These appendices contain the normalized profiles of various turbulence quantities measured with the short plate and are described as Case A and Case B in Table 1. In this form there is not too much to distinguish the differences in the test data. These data are being included for completeness. The real differences are hidden in the normalizing constants and are described in the main text. The data are plotted on the same coordinates for easy comparison. Case A is contained in Appendix A and denoted as Fig. A-n. The corresponding turbulence values for Case B are in Appendix B and denoted as Fig. B-n. The symmetry of the even higher moments and asymmetry of the odd higher moments are very obvious. These moments appear in the turbulent kinetic energy equation.



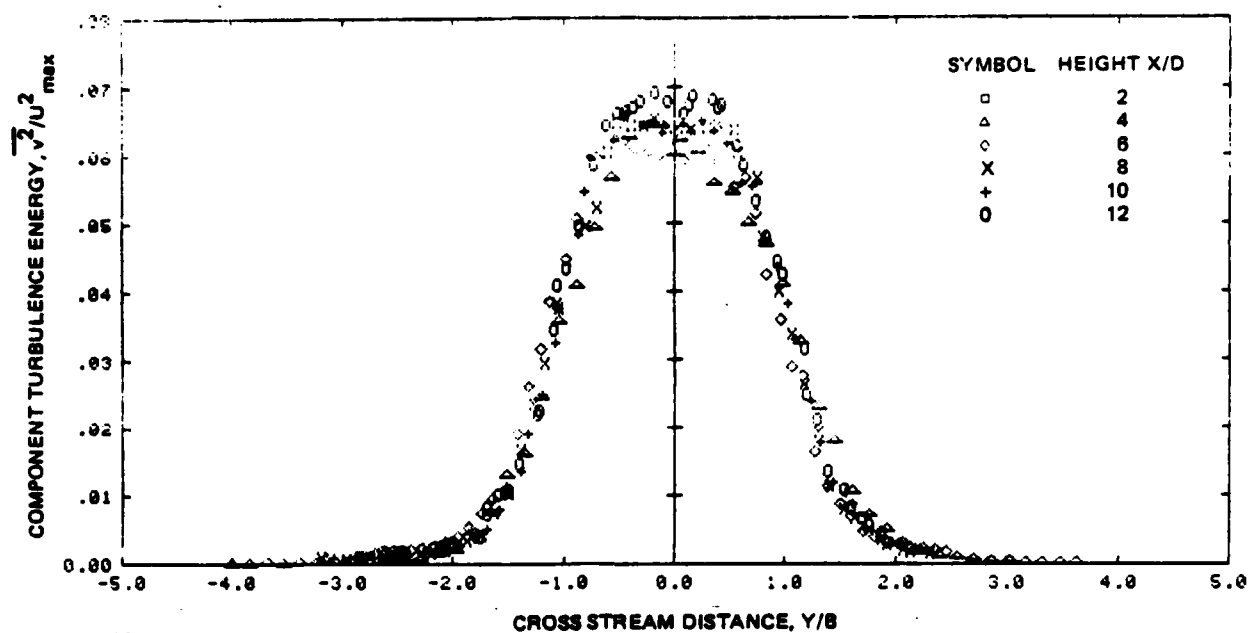
R85-1154-0248

Fig. A-1 Cross Stream Mean Velocity Profiles at Six Heights



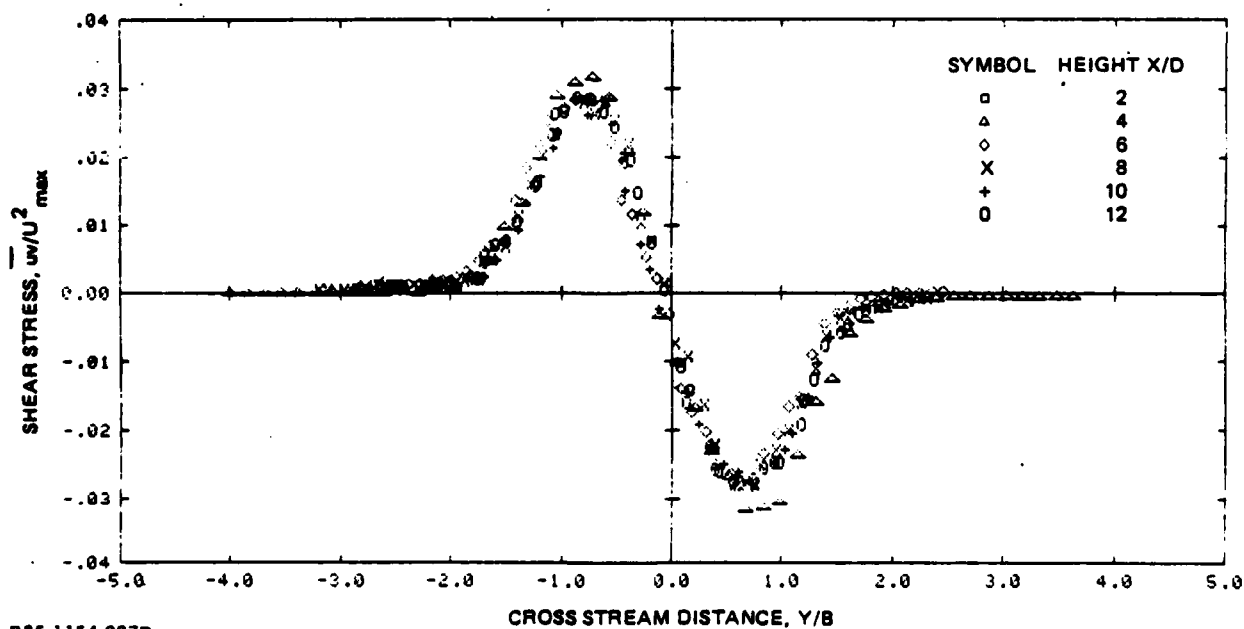
R85-1154-0258

Fig. A-2 Component Turbulent Energy in the Mean Flow Direction at Six Heights



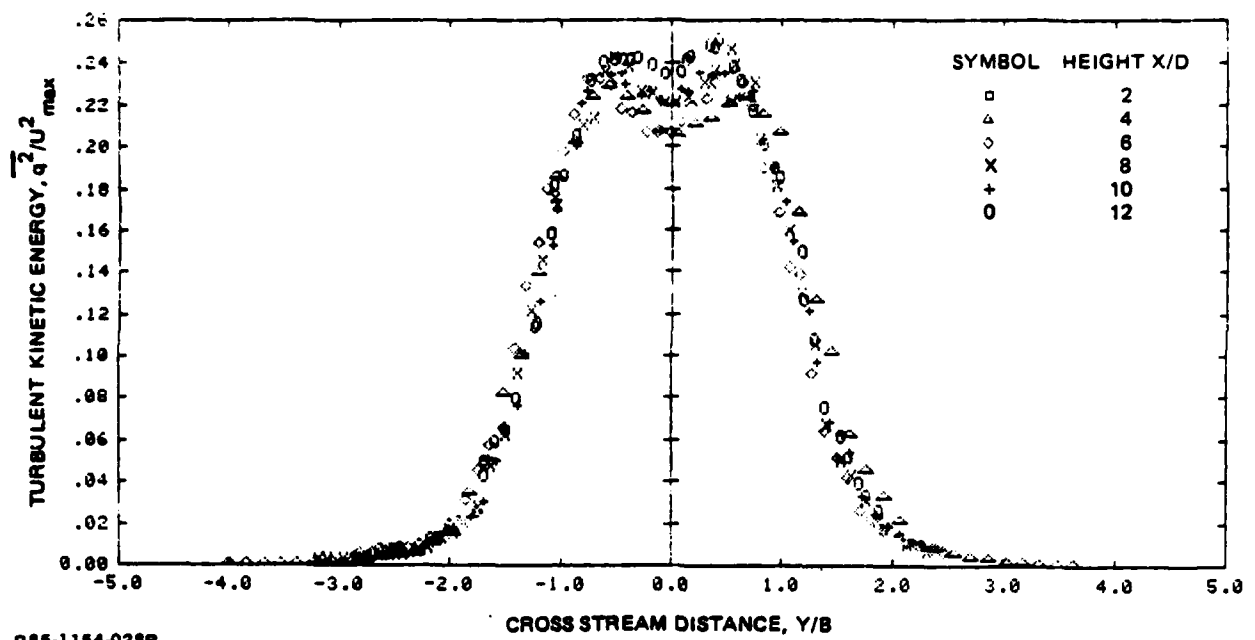
R85-1154-026B

Fig. A-3 Component Turbulence Energy in the Cross Flow Direction at Six Heights



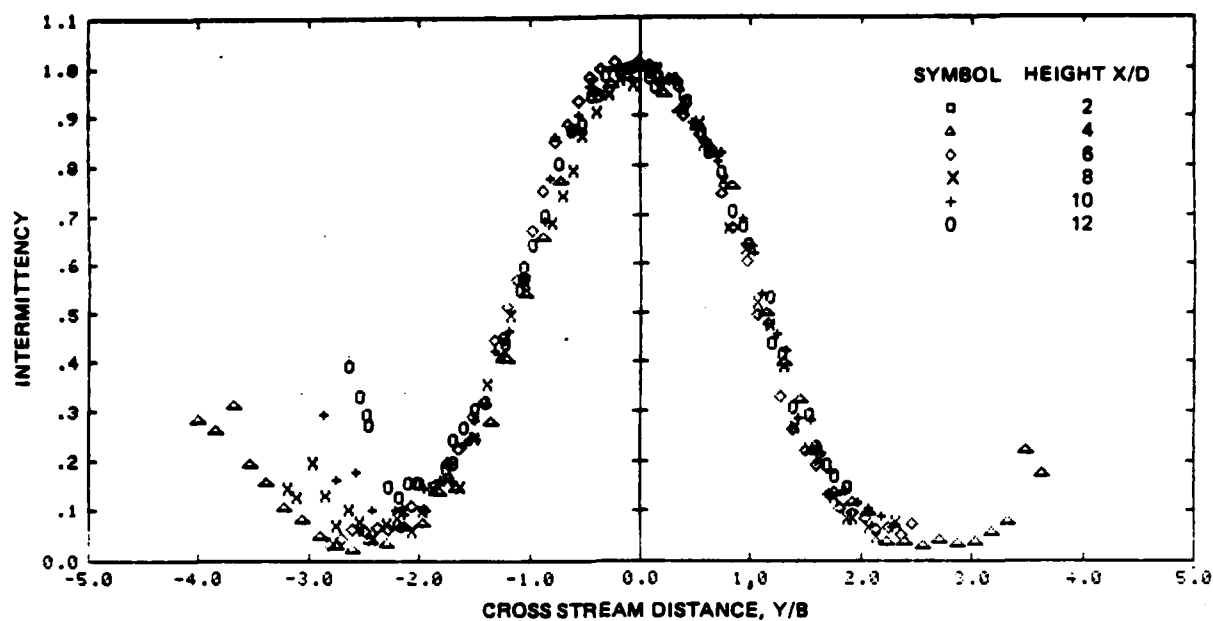
R85-1154-027B

Fig. A-4 Shear Stress Component in an Upwash at Six Heights

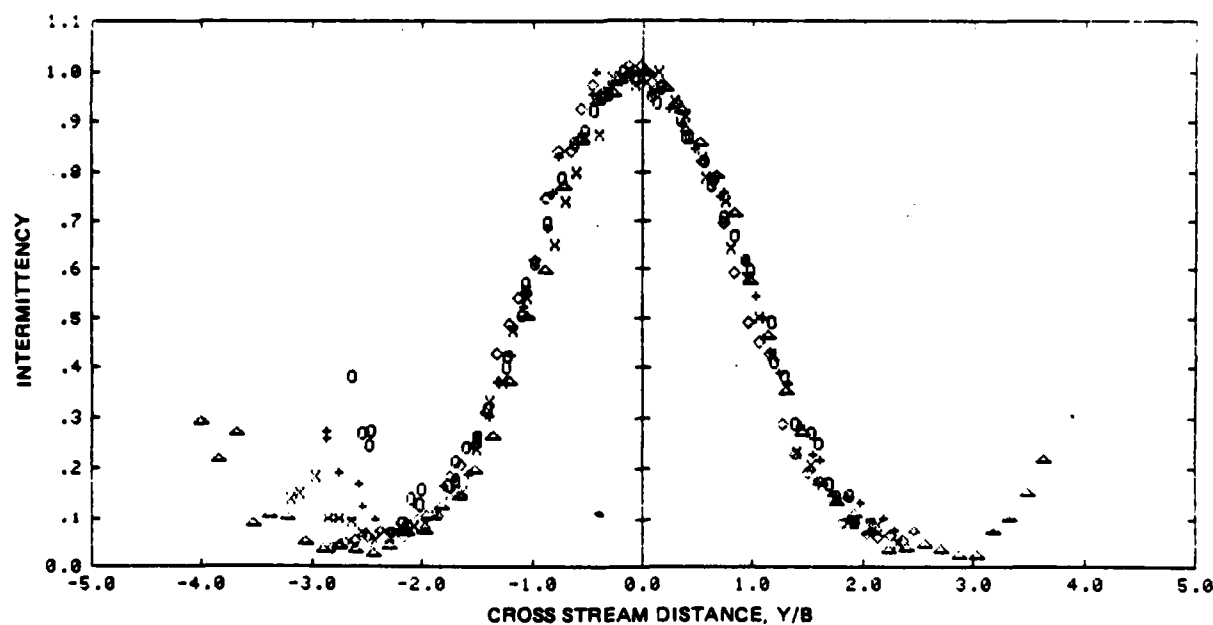


R85-1154-0288

Fig. A-5 Total Turbulence Kinetic Energy in an Equal Wall Jet Upwash at Six Heights



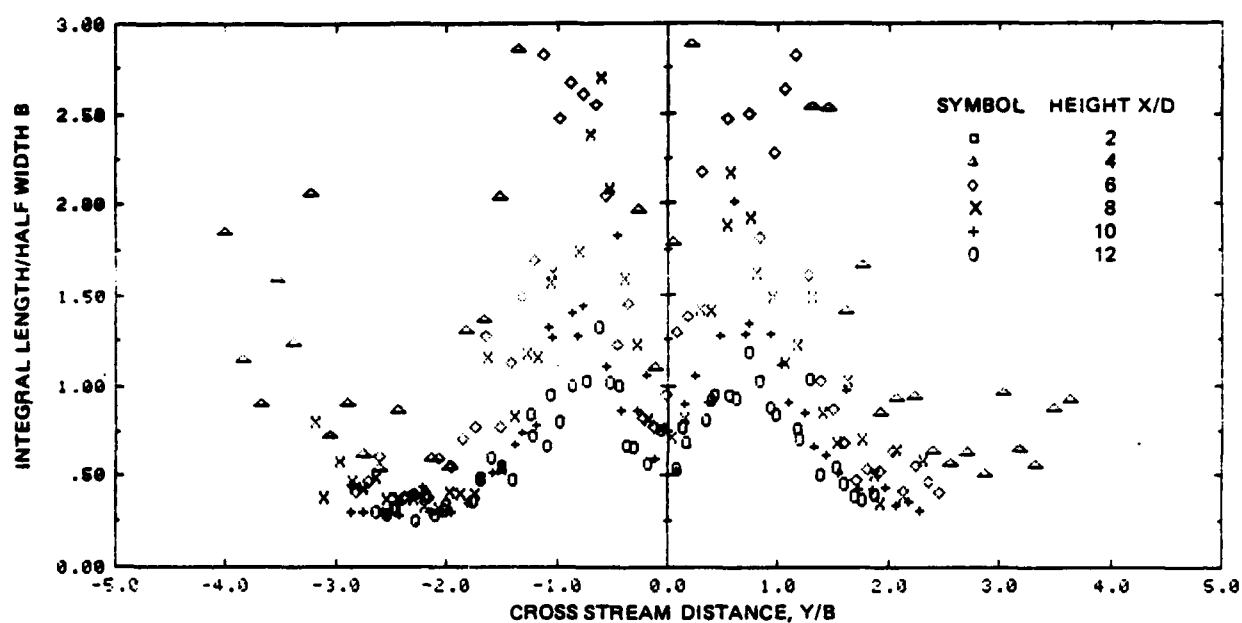
a) MEAN FLOW DIRECTION



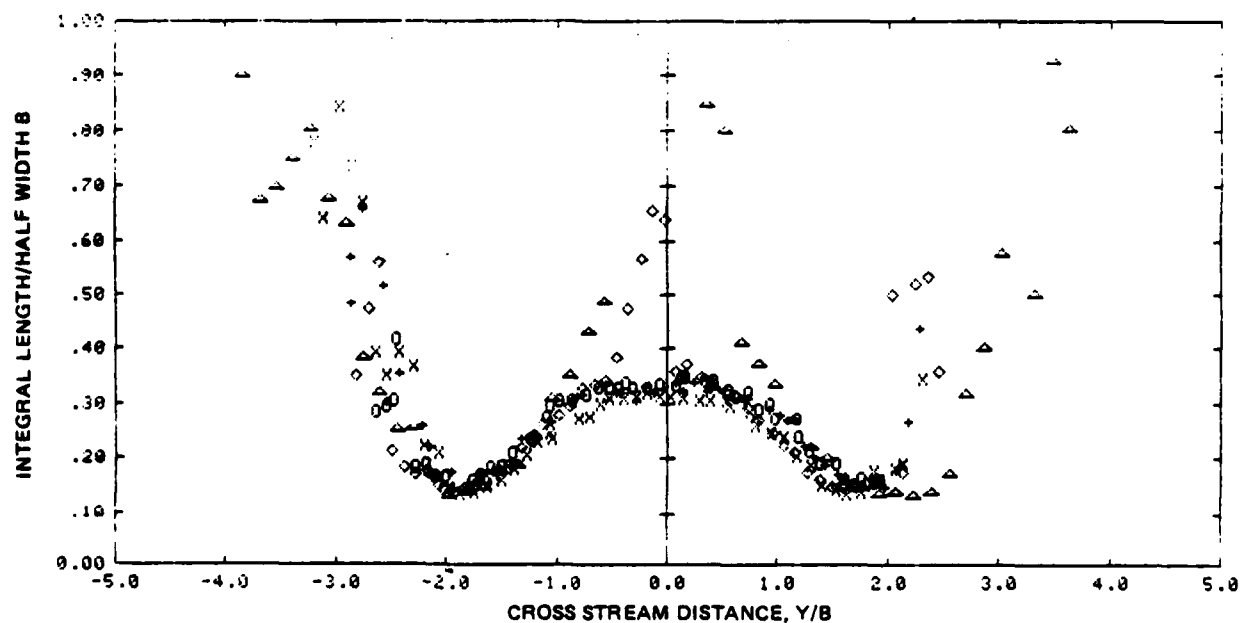
b) CROSS FLOW DIRECTION

R85-1154-0078

Fig. A-6 Intermittency Profiles in an Equal Jet Upwash



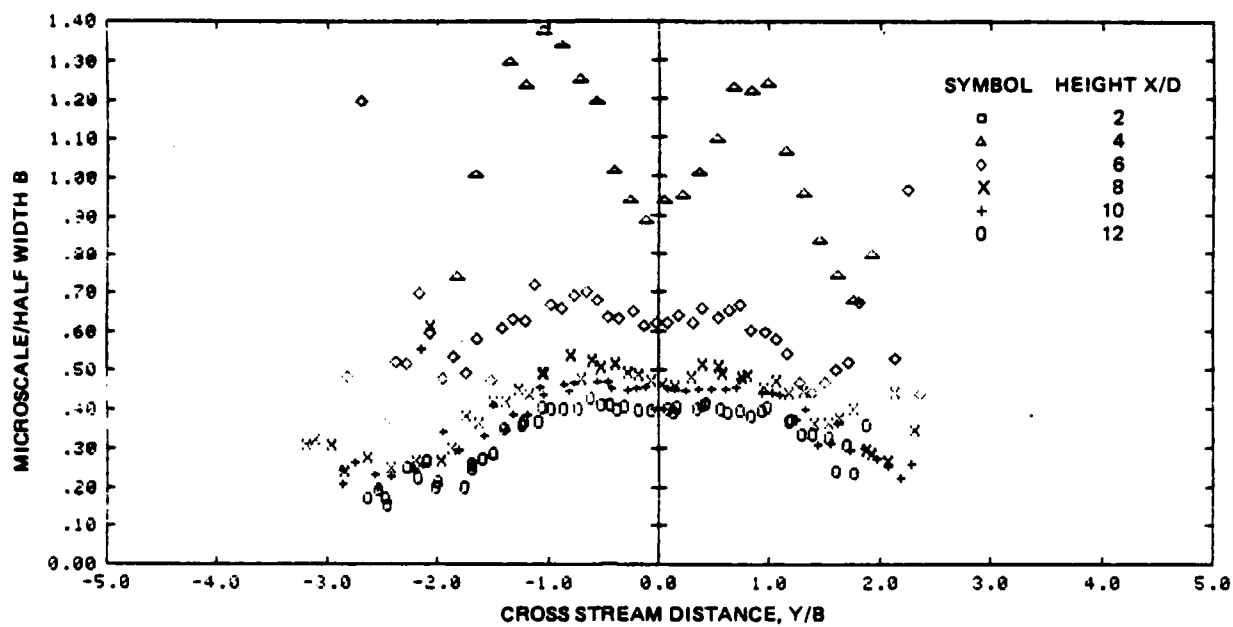
a) MEAN FLOW DIRECTION



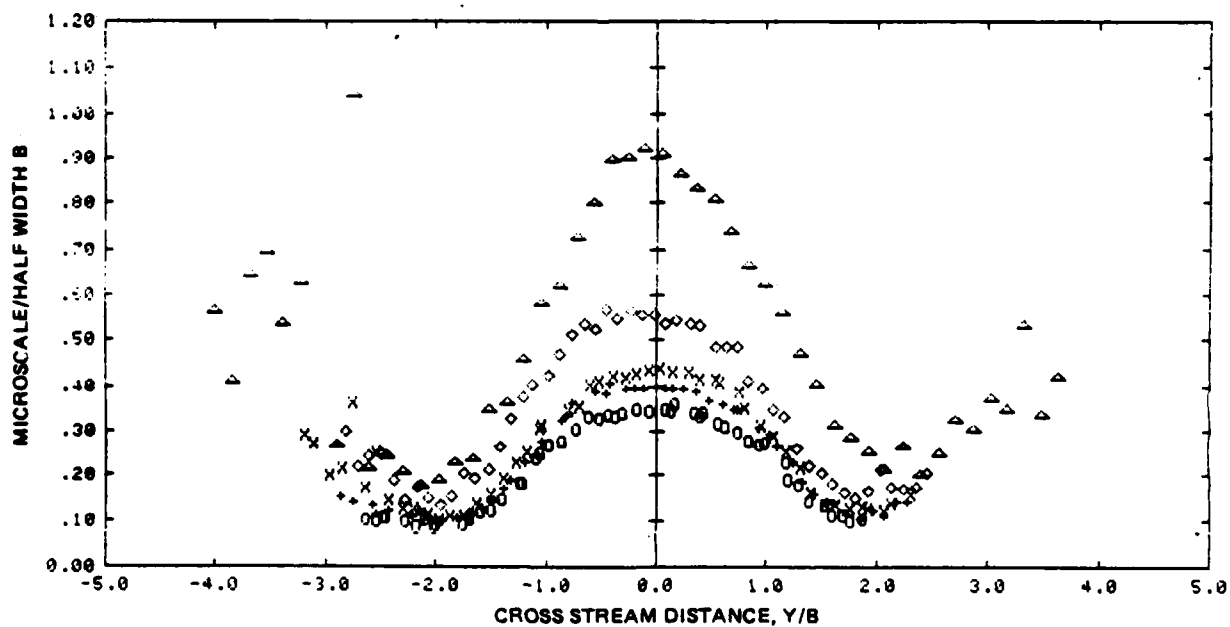
b) CROSS FLOW DIRECTION

R85-1154-008B

Fig. A-7 Integral Scale Lengths Across 2-D Upwash



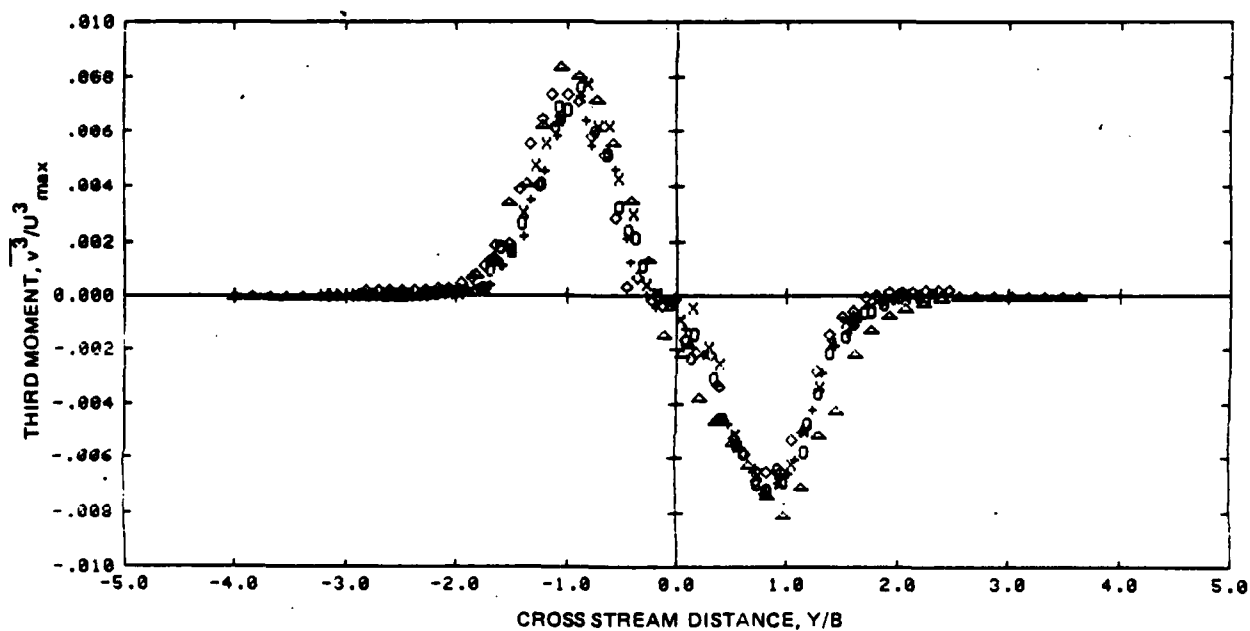
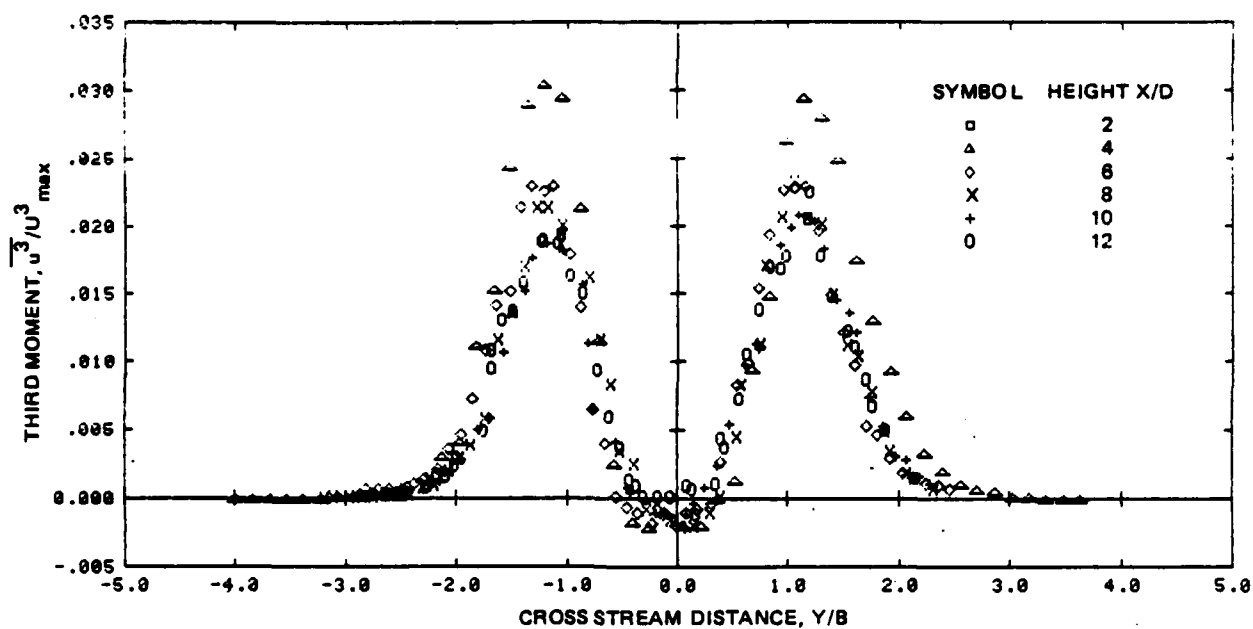
a) MEAN FLOW DIRECTION



b) CROSS FLOW DIRECTION

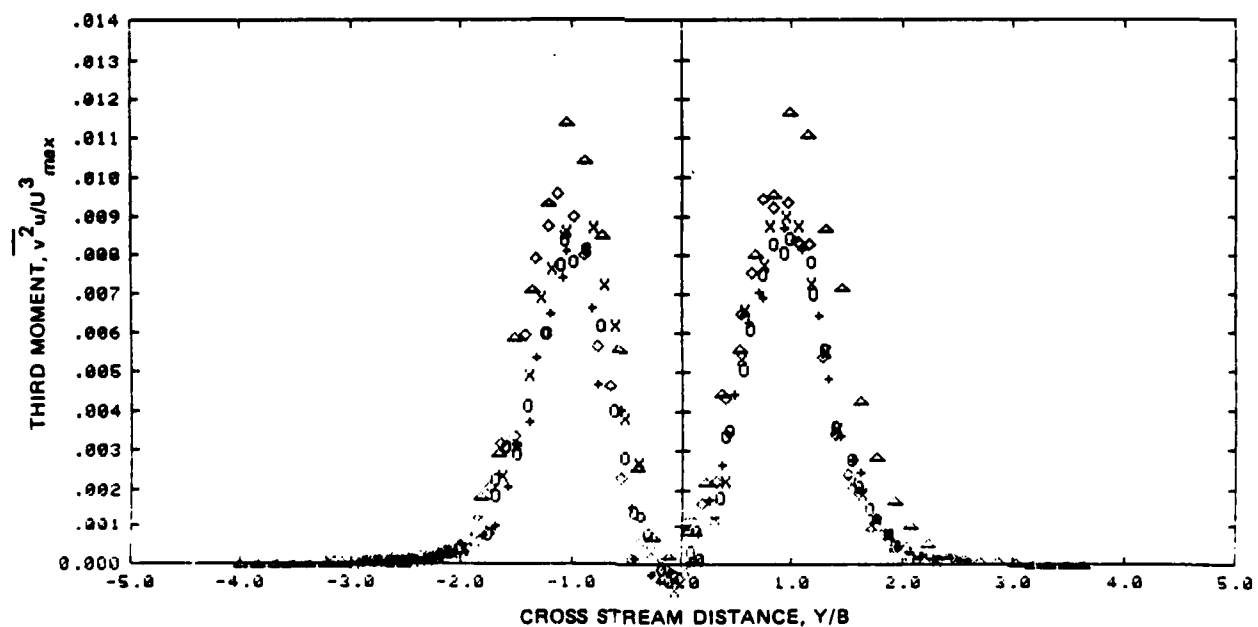
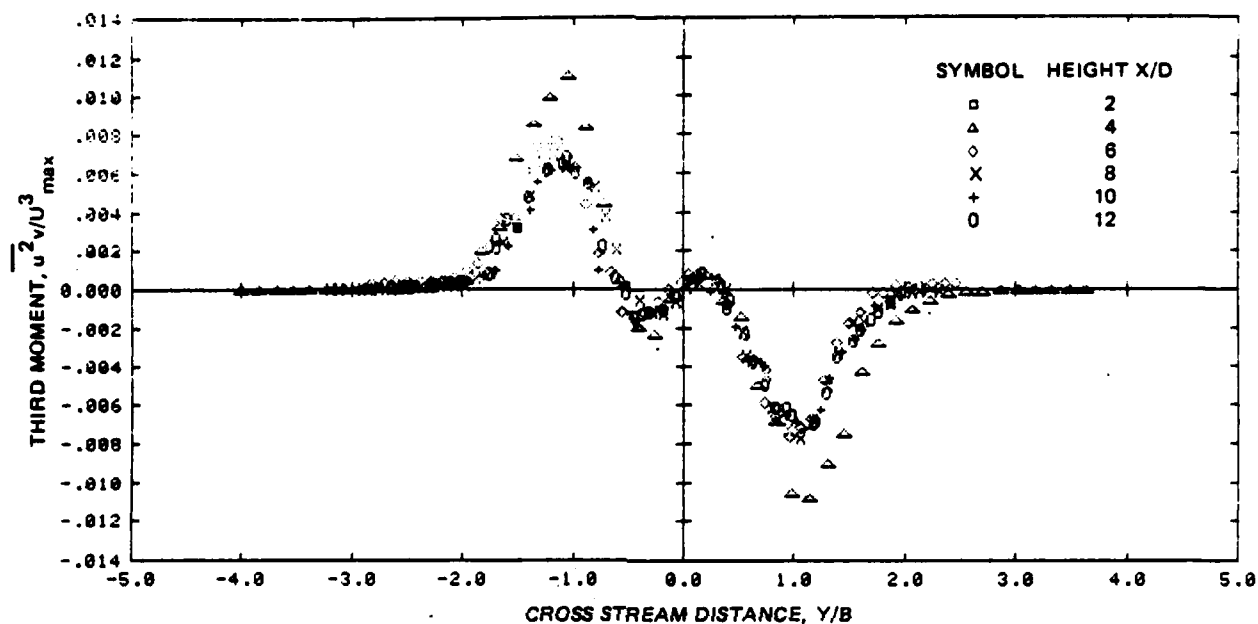
R65-1154-009B

Fig. A-8 Taylor Micro-scale Lengths Across 2-D Upwash



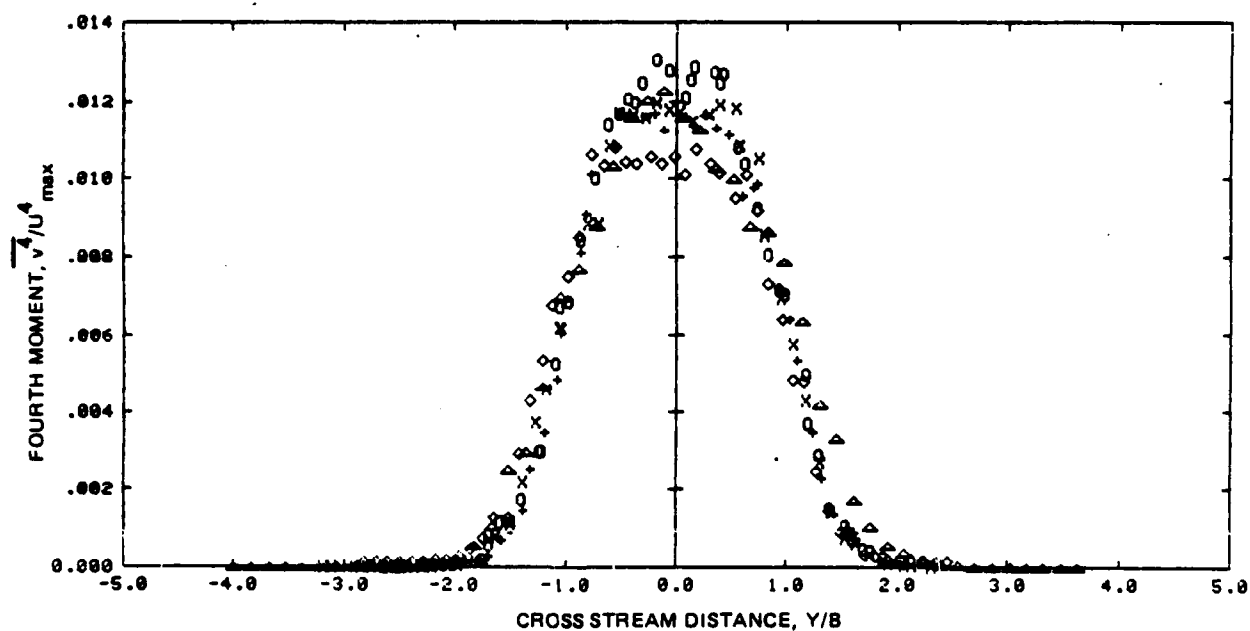
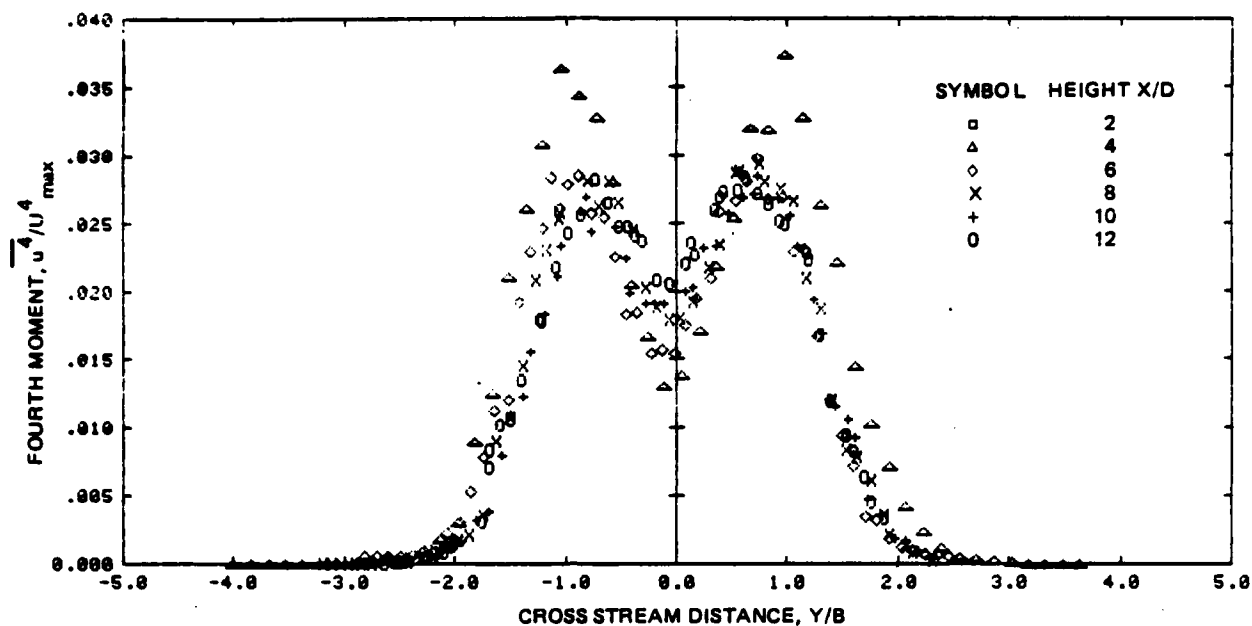
R85-1154-010B(1/2)

Fig. A-9 Third Moments Across 2-D Upwash (Sheet 1 of 2)



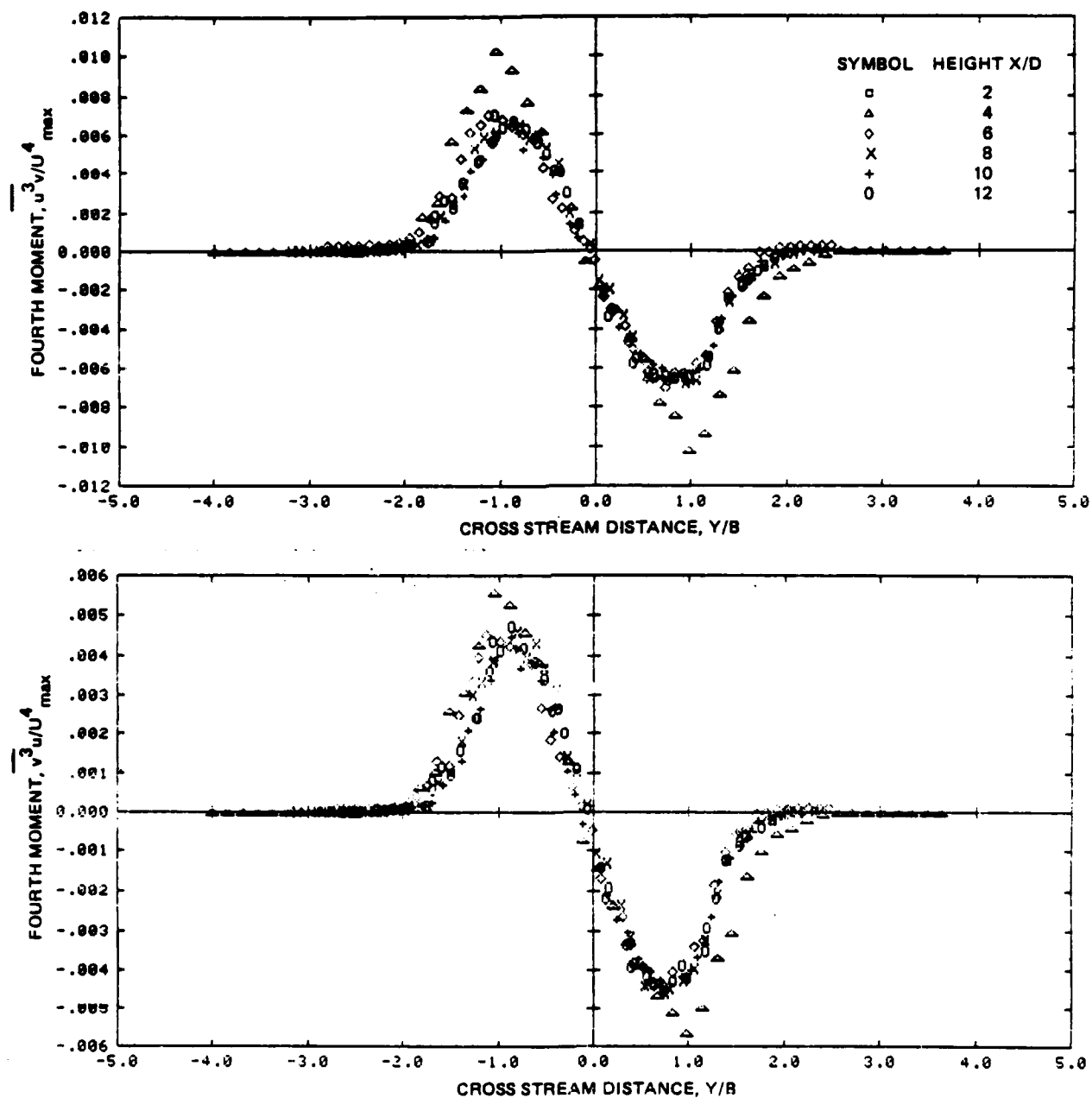
R85-1154-0108(2/2)

Fig. A-9 Third Moments Across 2-D Upwash (Sheet 2 of 2)



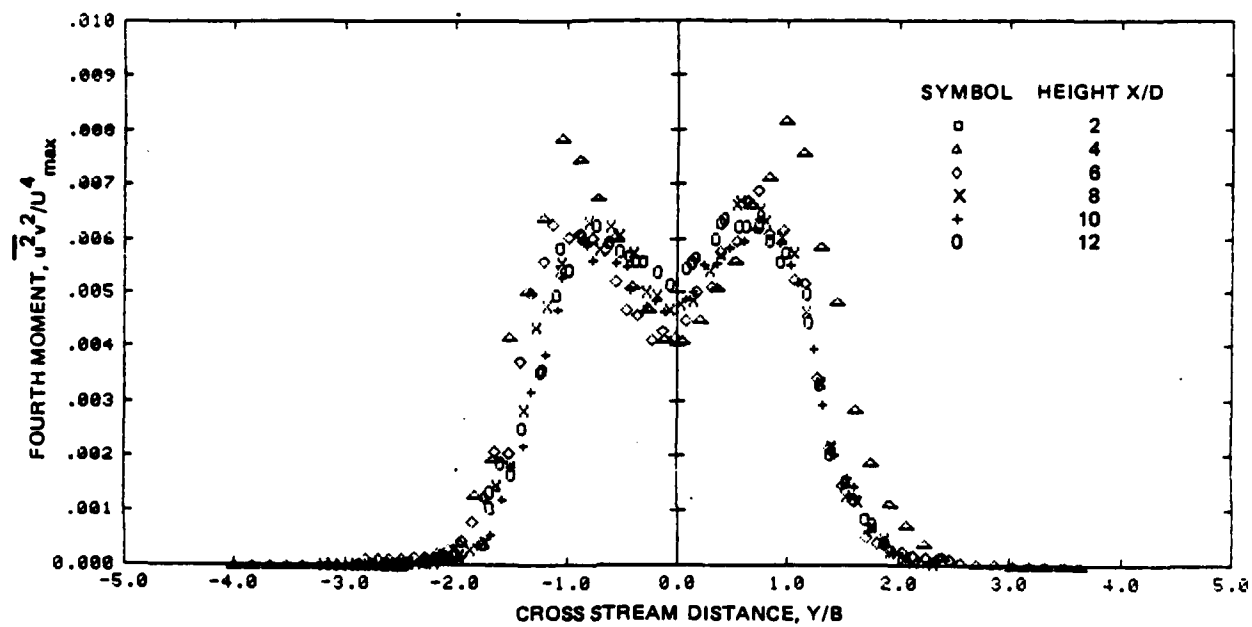
R85-1154-011B(1/3)

Fig. A-10 Fourth Moments Across 2-D Upwash (Sheet 1 of 3)



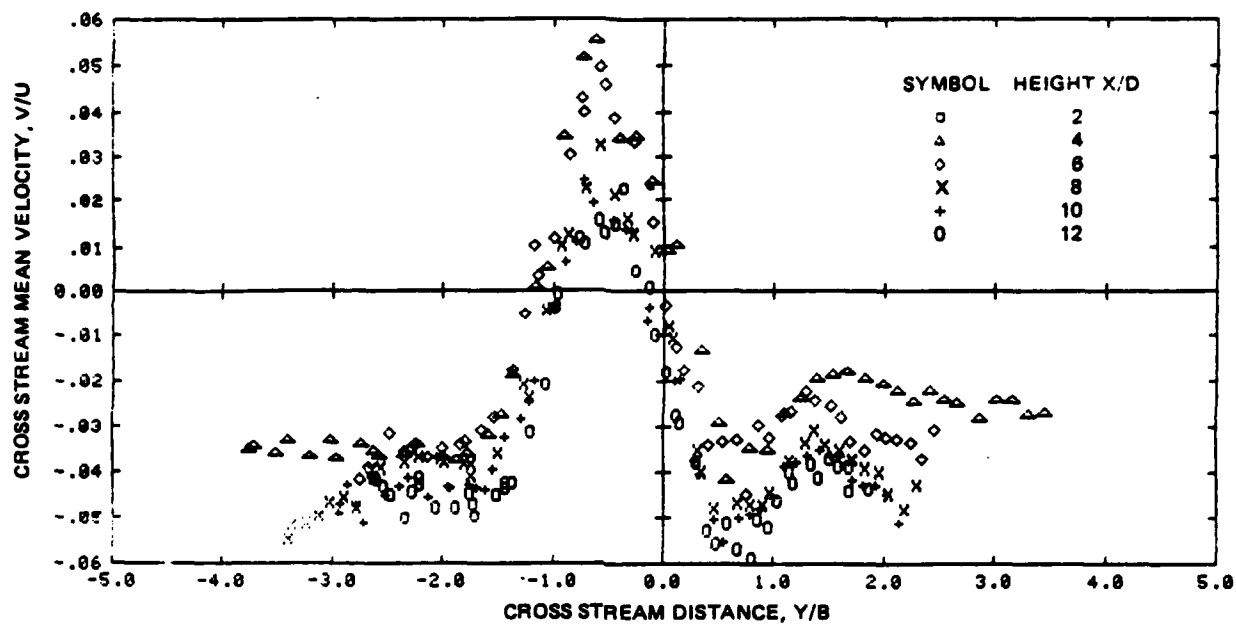
R85-1154-0118(2/3)

Fig. A-10 Fourth Moments Across 2-D Upwash (Sheet 2 of 3)



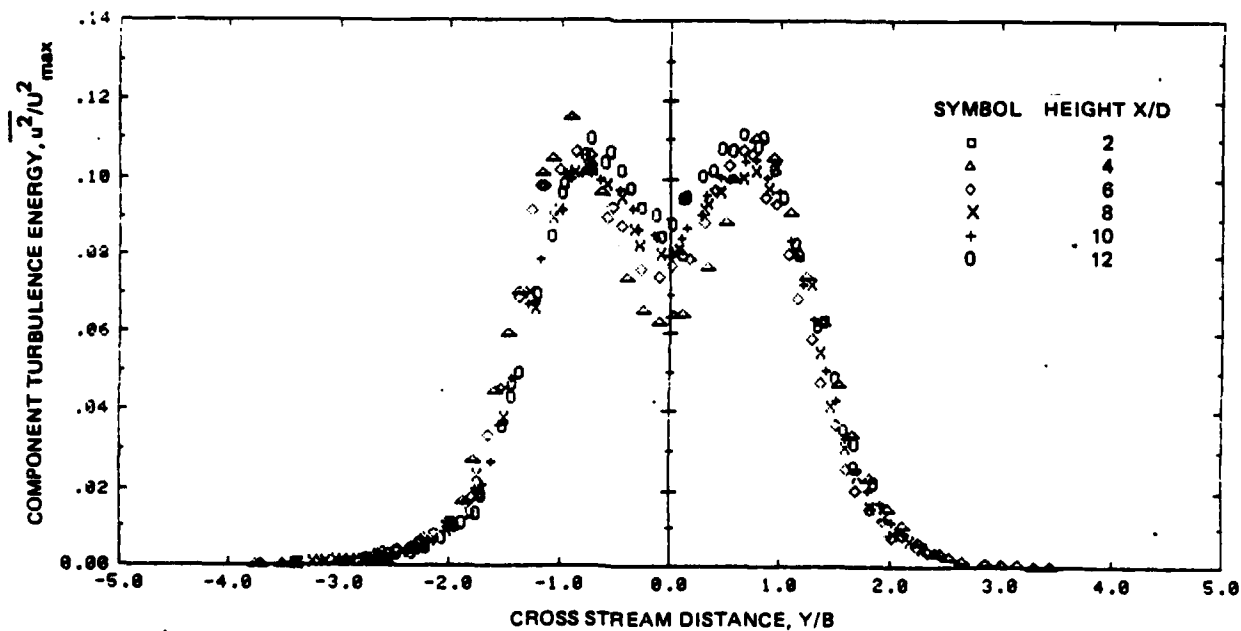
R85-1154-011B(3/3)

Fig. A-10 Fourth Moments Across 2-D Upwash (Sheet 3 of 3)



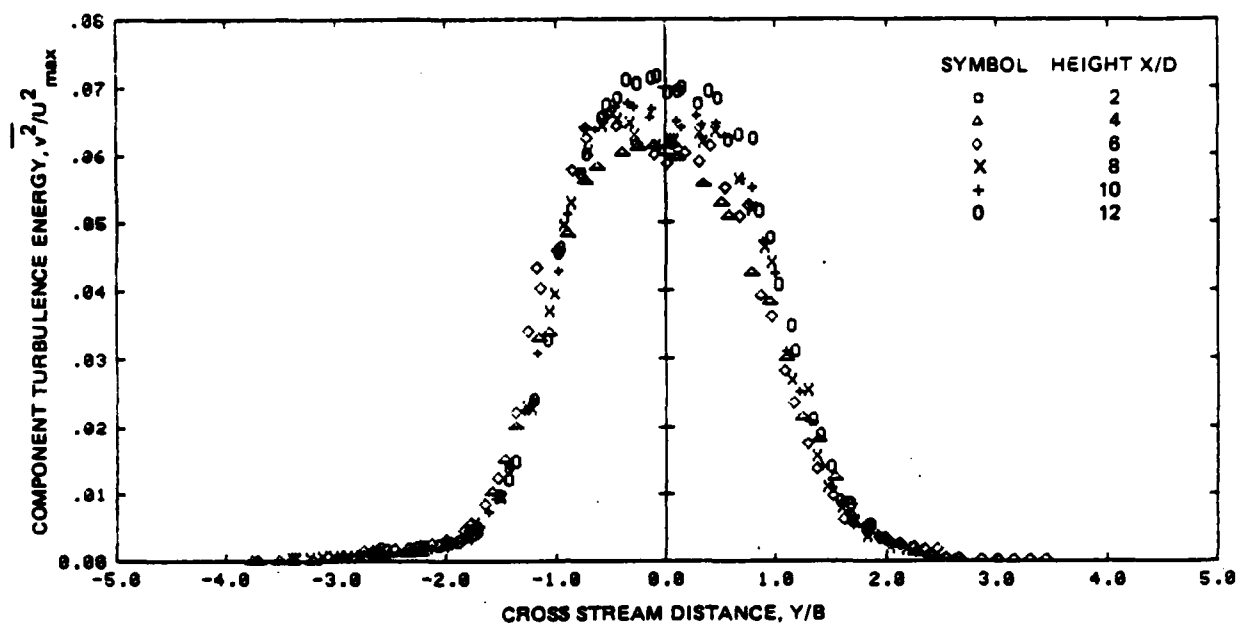
R85-1154-013B

Fig. B-1 Cross Stream Mean Velocity Profiles at Six Heights



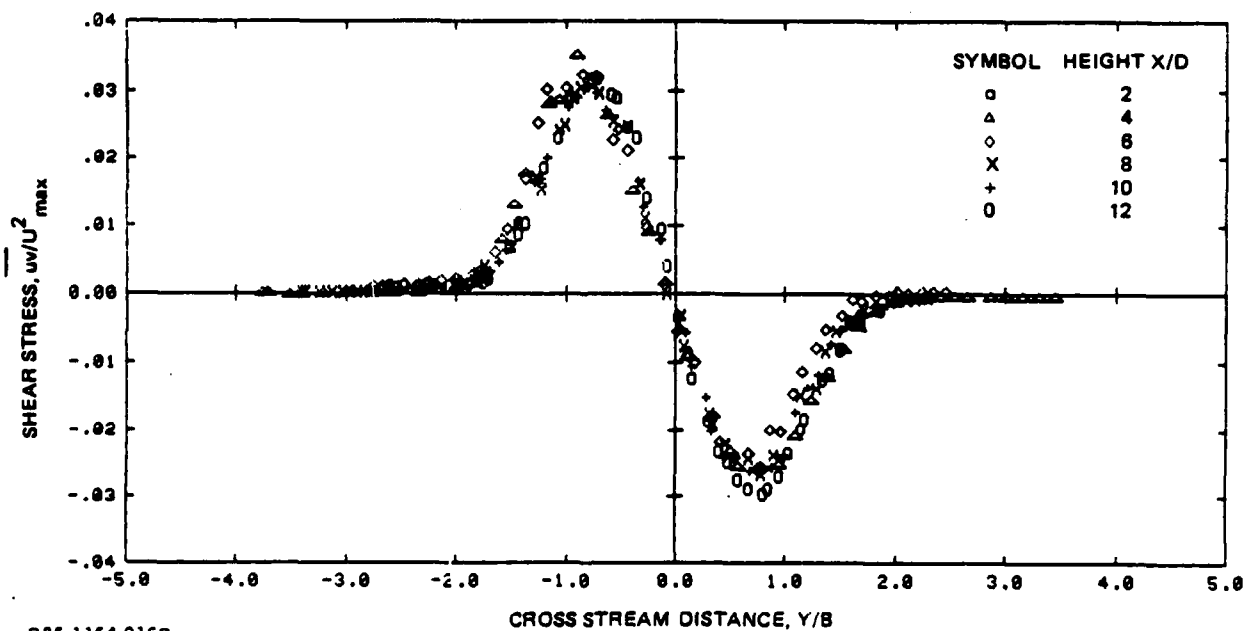
R85-1154-014B

Fig. B-2 Component Turbulent Energy in the Mean Flow Direction at Six Heights



R85-1154-015B

Fig. B-3 Component Turbulence Energy in the Cross Flow Direction at Six Heights



R85-1154-016B

Fig. B-4 Shear Stress Component in an Upwash at Six Heights

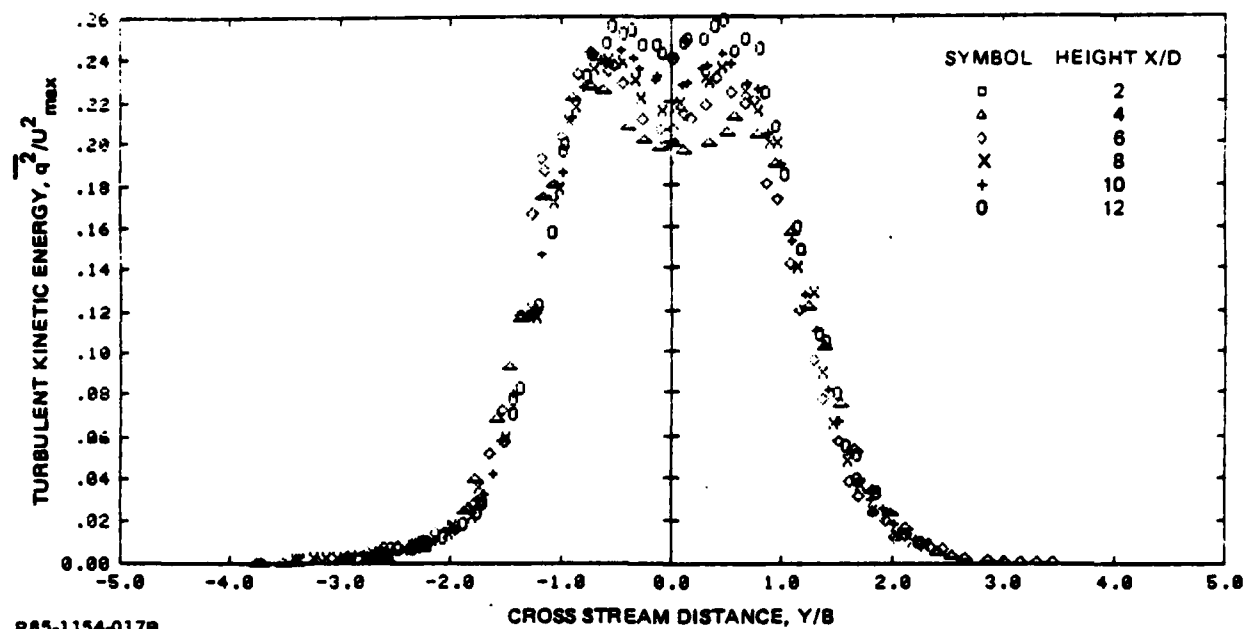
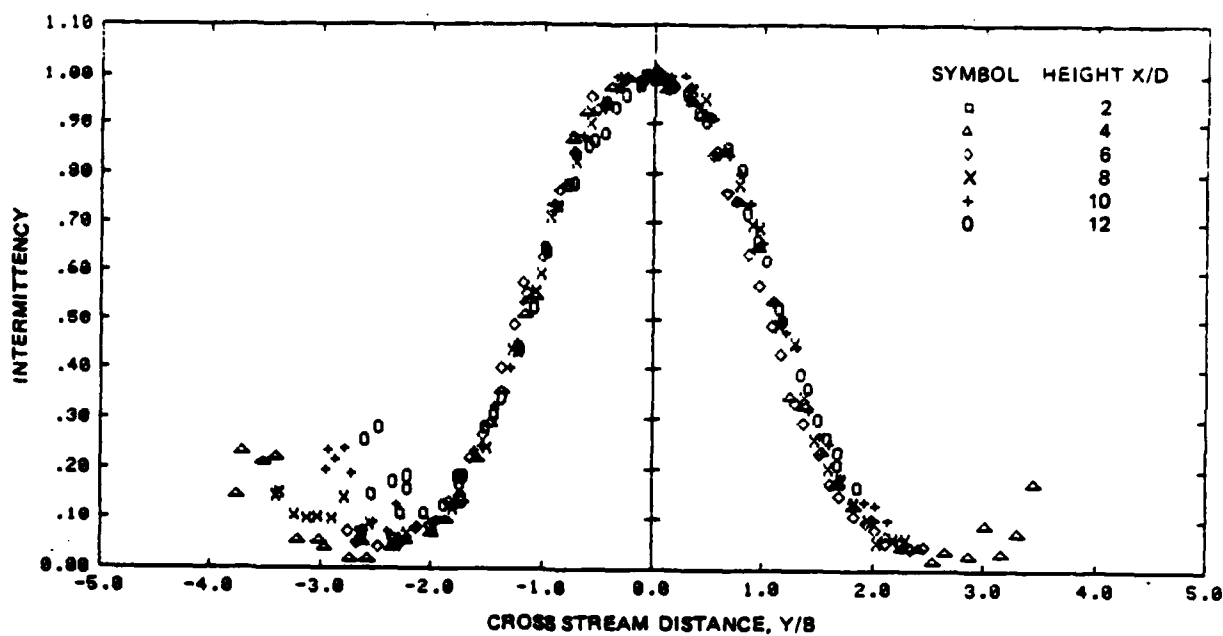
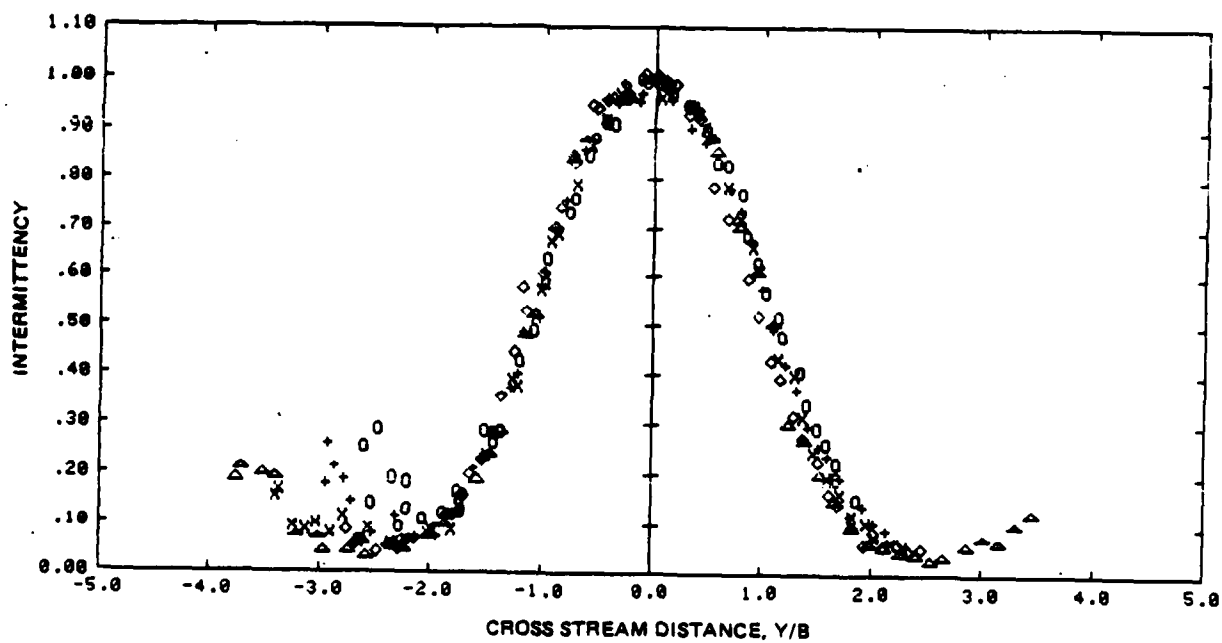


Fig. B-5 Total Turbulence Kinetic Energy in an Equal Wall Jet Upwash at Six Heights



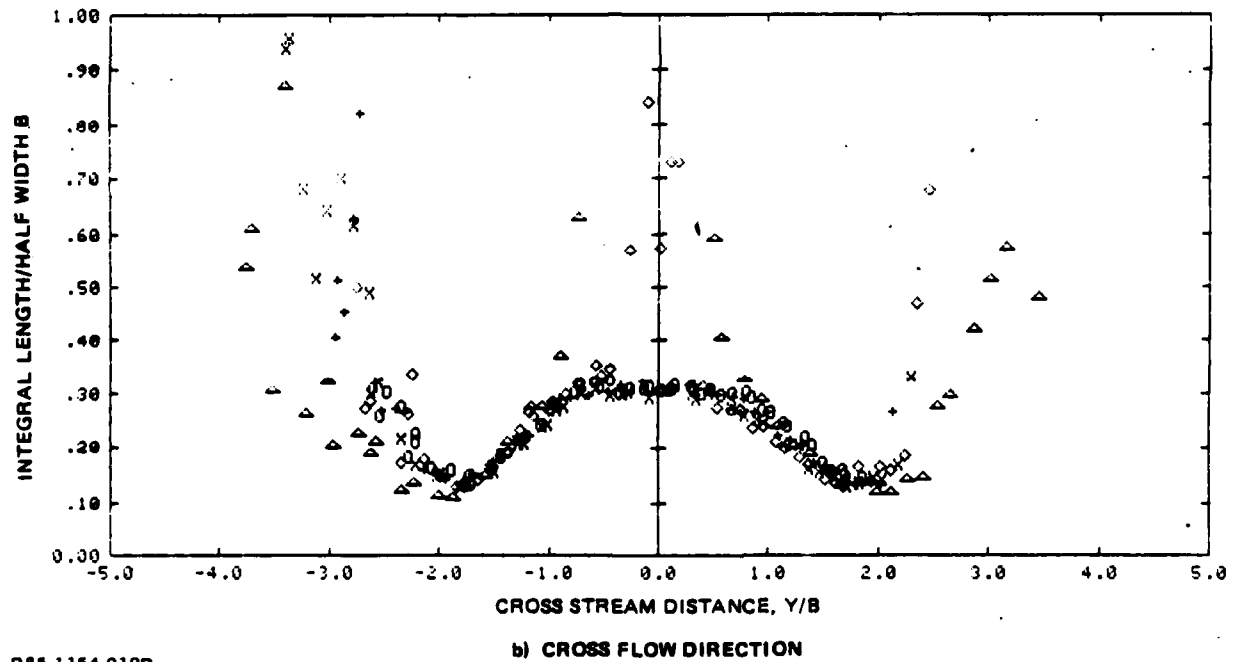
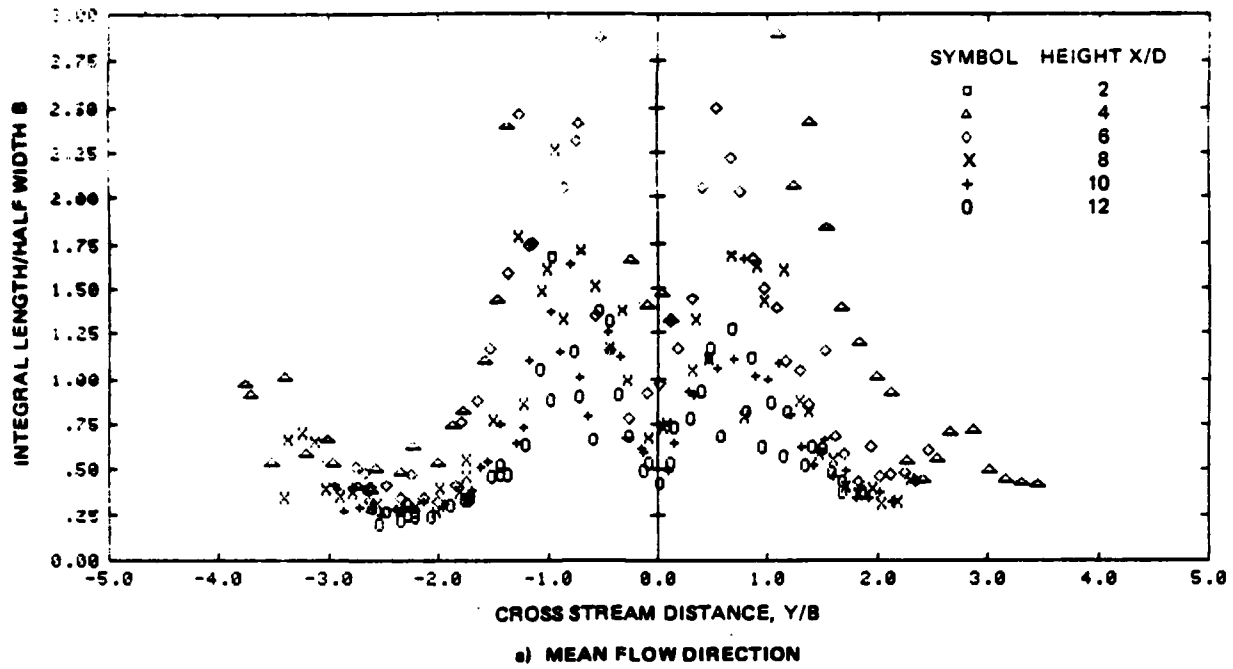
a) MEAN FLOW DIRECTION



b) CROSS FLOW DIRECTION

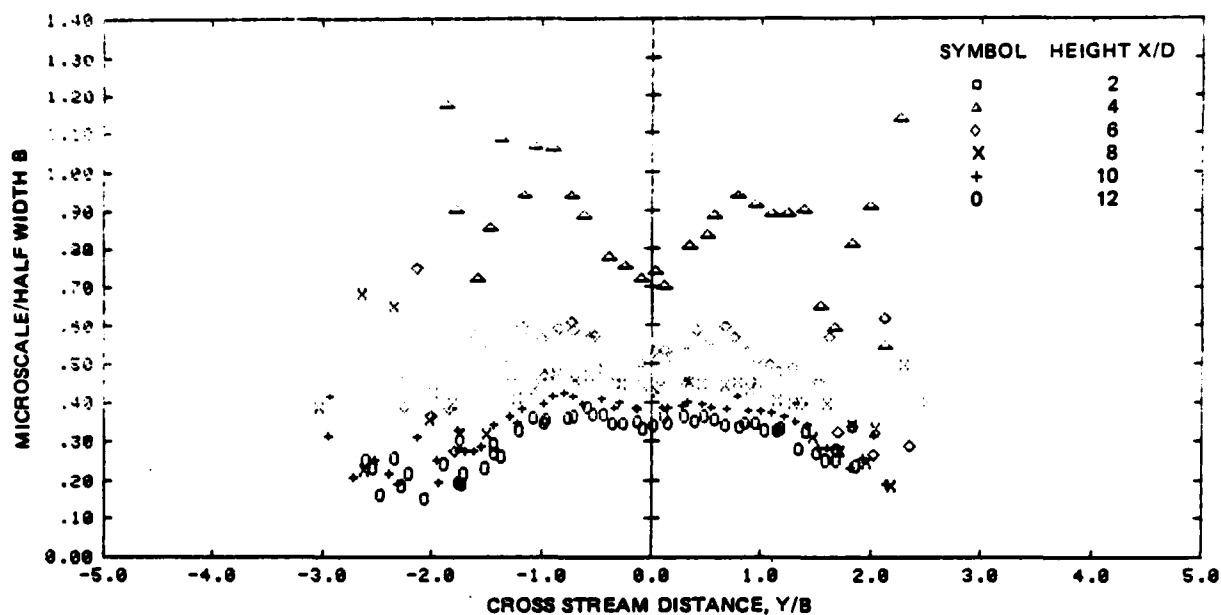
R85-1154-0188

Fig. B-6 Intermittency Profiles in an Equal Jet Upwash

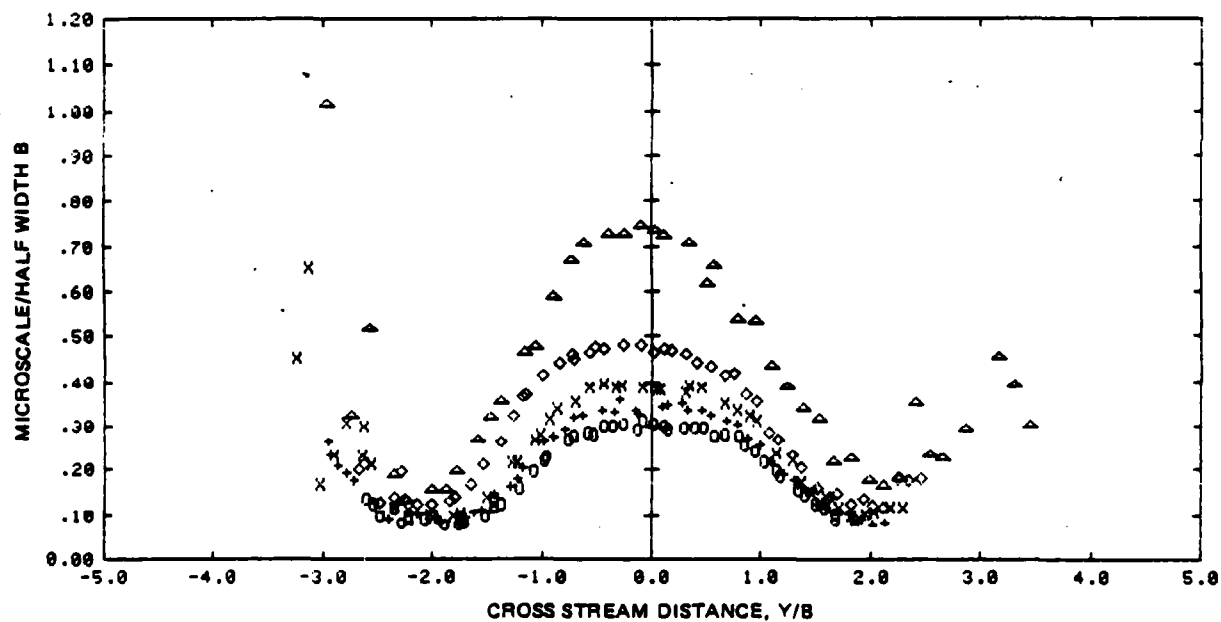


R85-1154-019B

Fig. B-7 Integral Scale Lengths Across 2-D Upwash



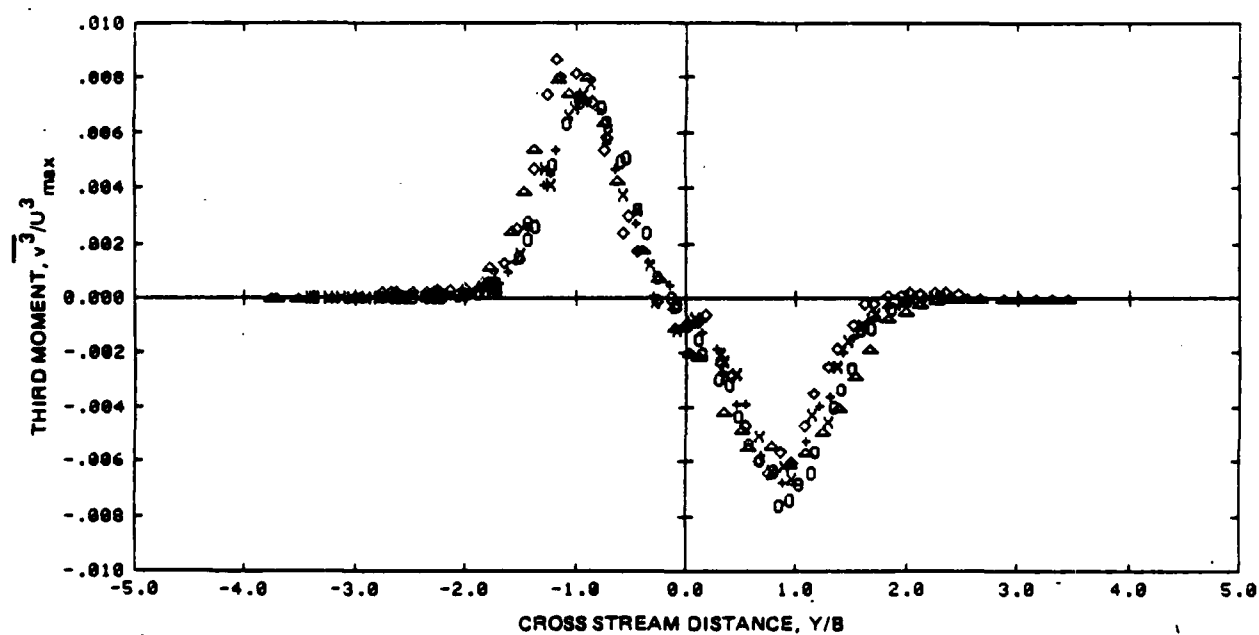
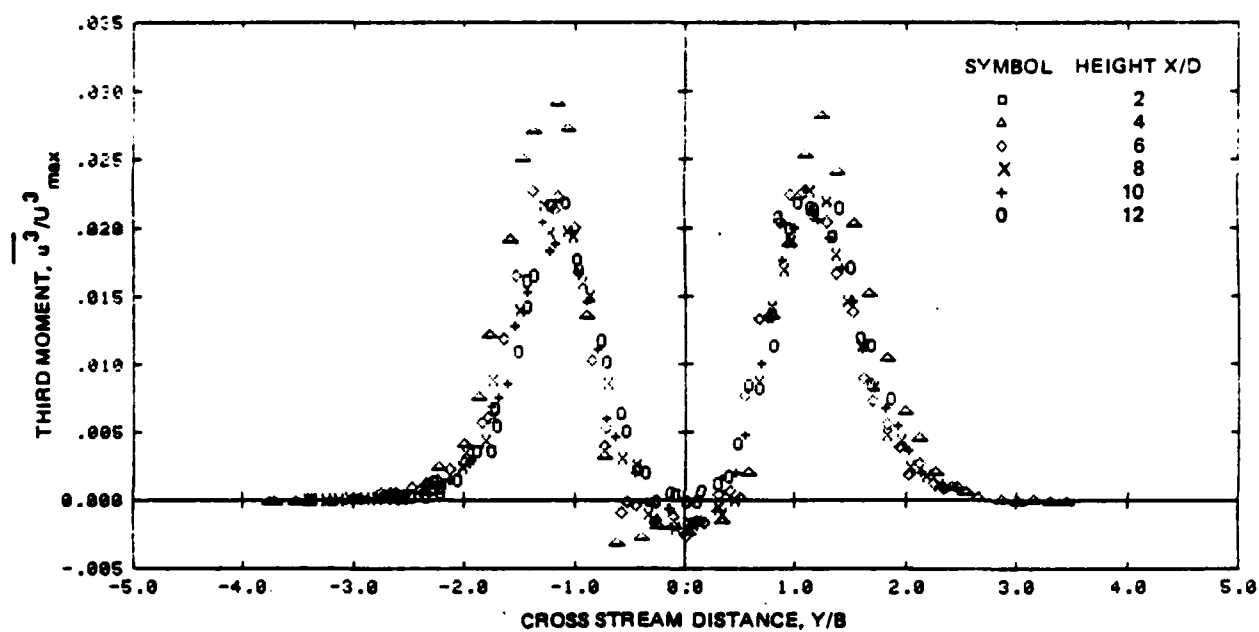
a) MEAN FLOW DIRECTION



b) CROSS FLOW DIRECTION

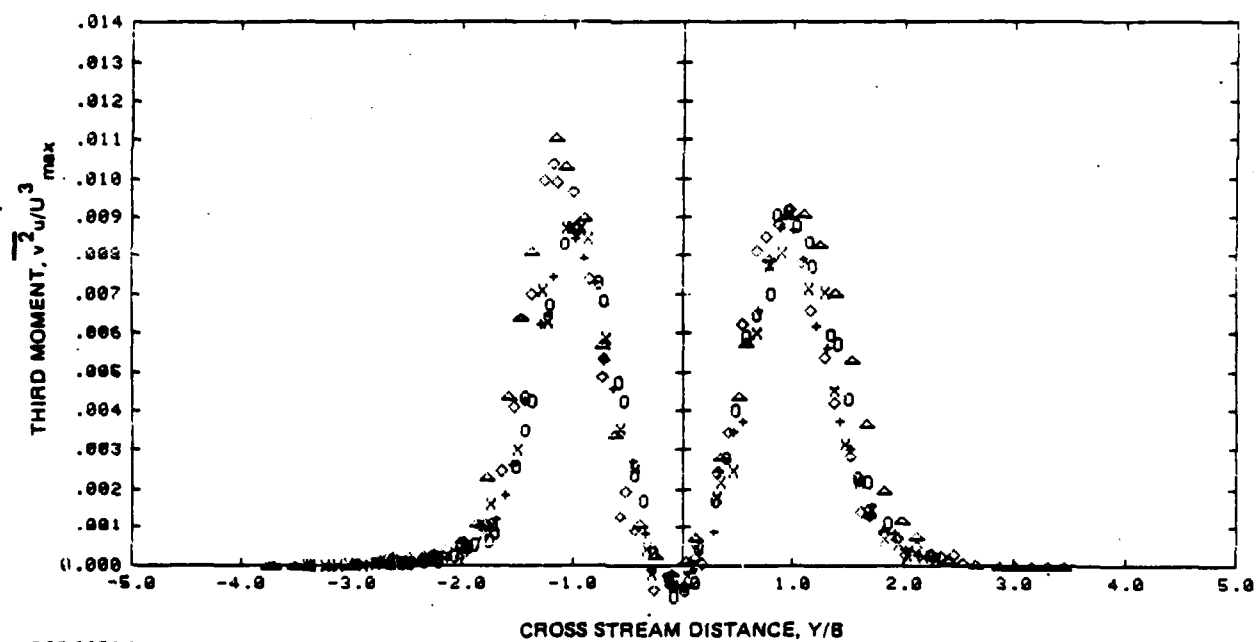
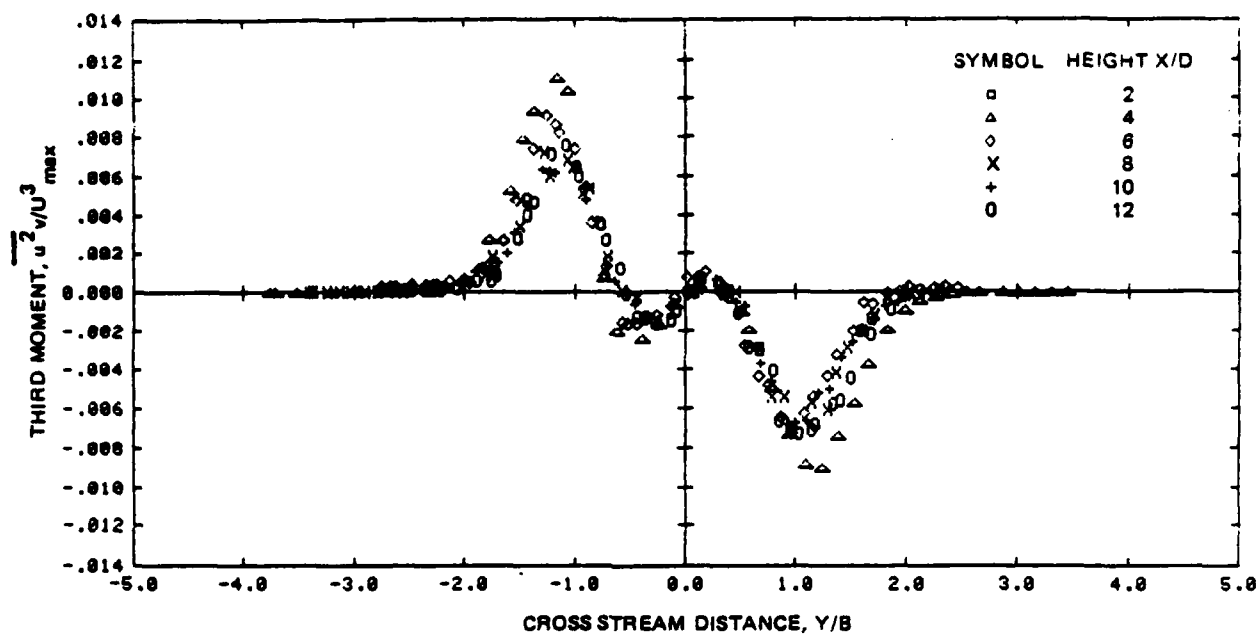
R85-1154-0208

Fig. B-8 Taylor Micro-scale Lengths Across 2-D Upwash



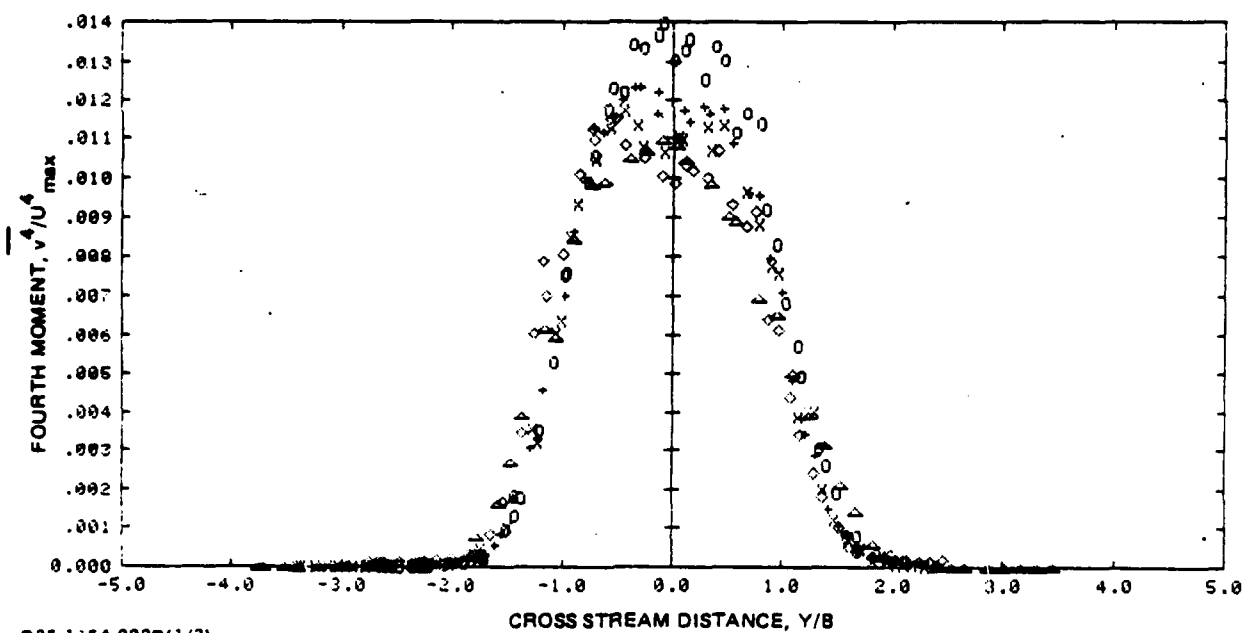
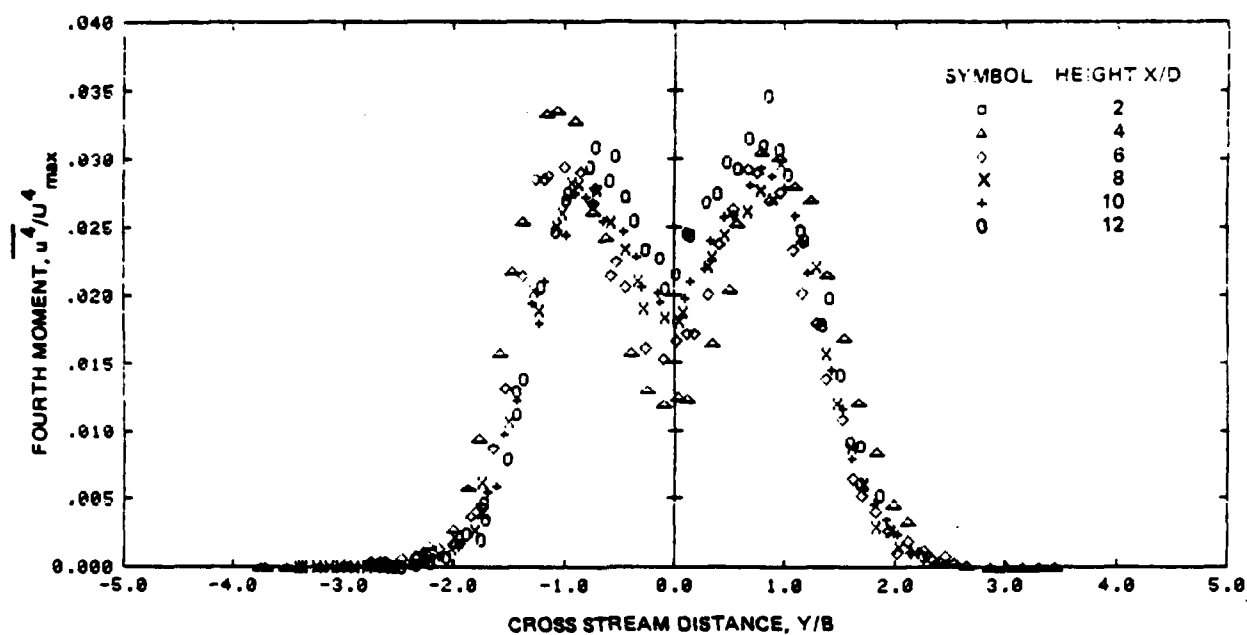
R85-1154-021B(1/2)

Fig. B-9 Third Moments Across 2-D Upwash (Sheet 1 of 2)



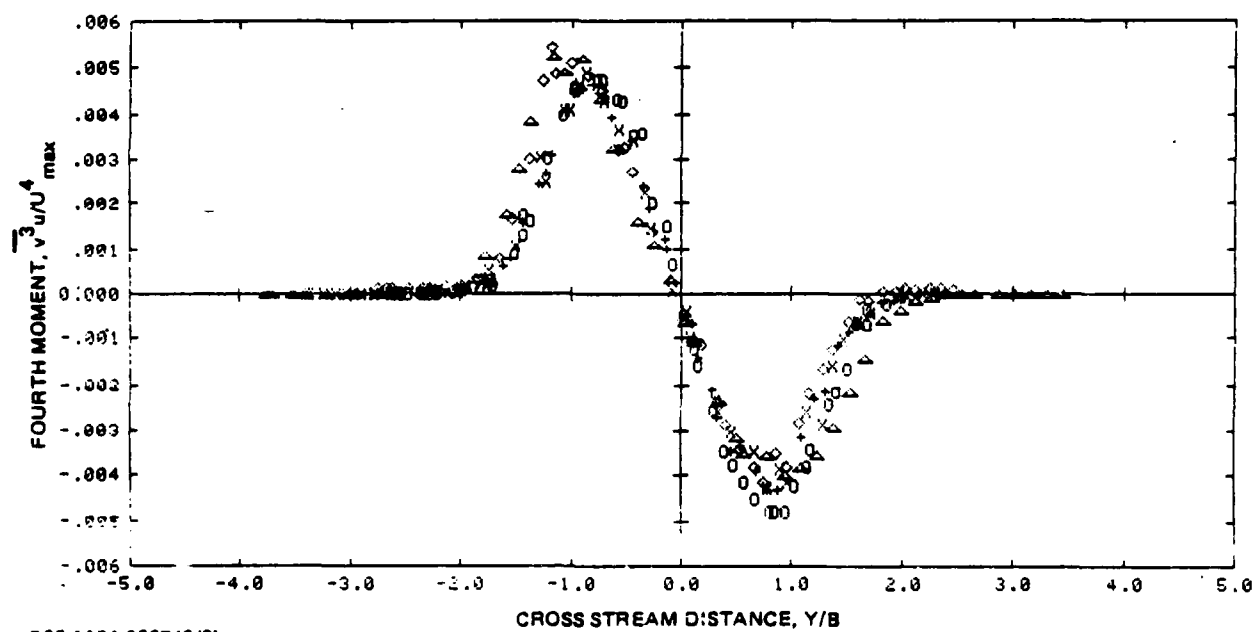
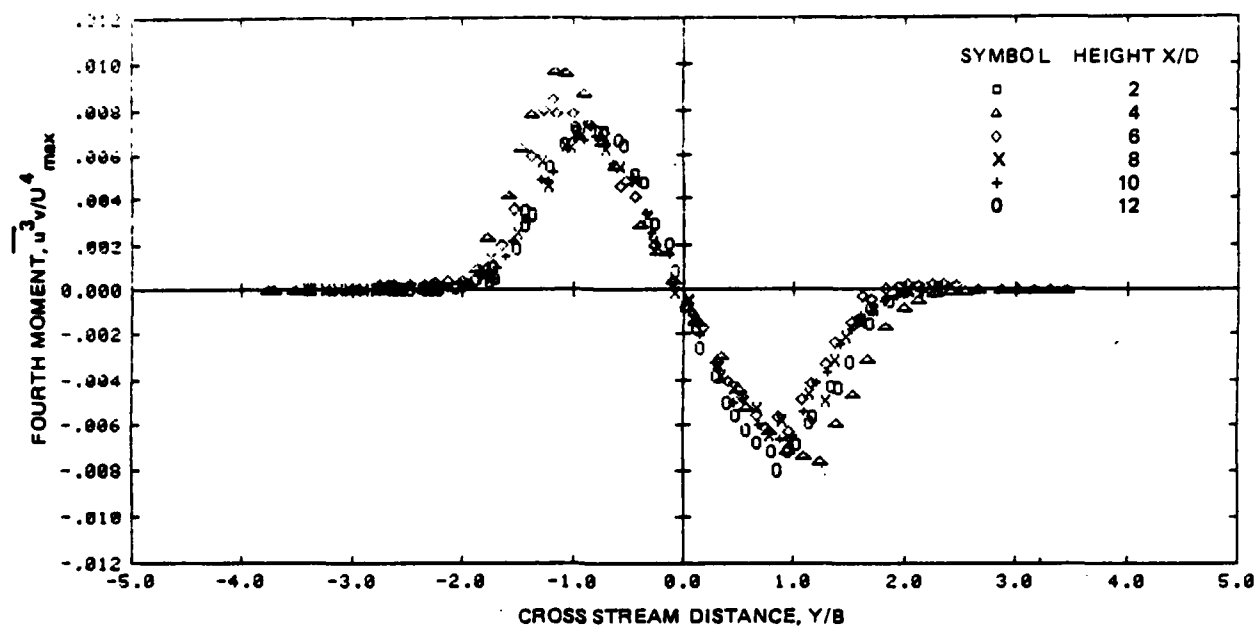
R85-1154-021B(2/2)

Fig. B-9 Third Moments Across 2-D Upwash (Sheet 2 of 2)



R85-1154-022B(1/3)

Fig. B-10 Fourth Moments Across 2-D Upwash (Sheet 1 of 3)

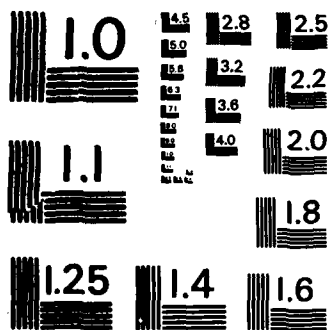


R85-1154-022B(2/3)

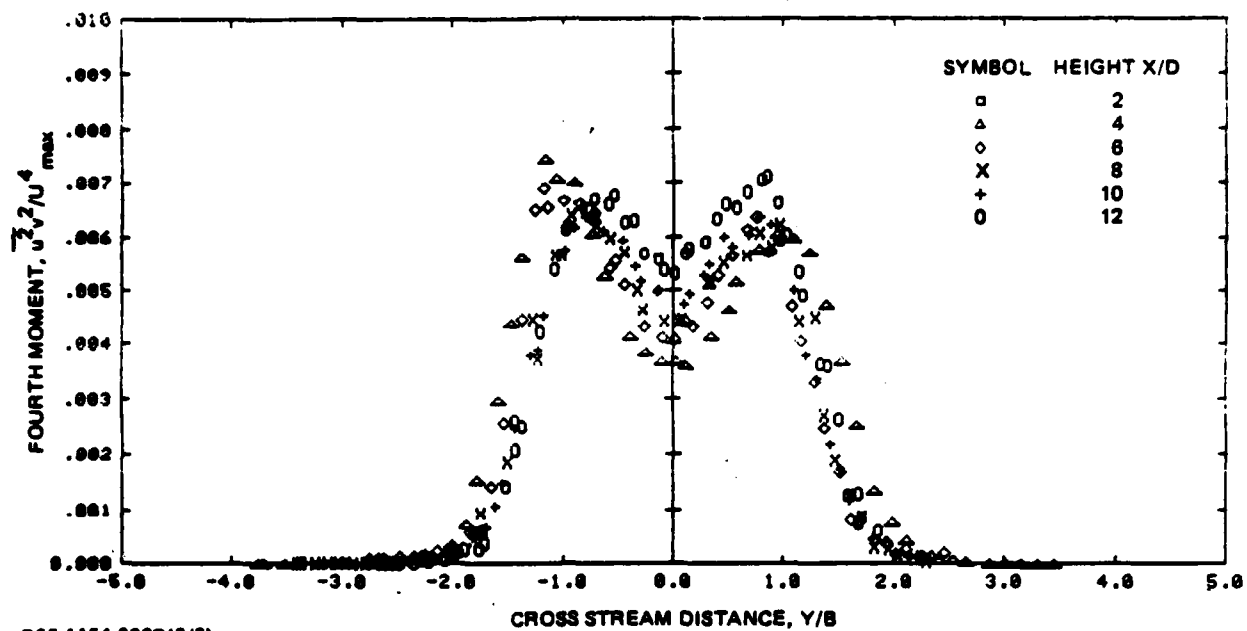
Fig. B-10 Fourth Moments Across 2-D Upwash (Sheet 2 of 3)

AD-A166 286 AN INVESTIGATION OF TURBULENCE MECHANISMS IN V/STOL 2/p
UPWASH FLOW FIELDS. (U) GRUMMAN AEROSPACE CORP BETHPAGE
NY RESEARCH AND DEVELOPMENT C. B GILBERT 15 SEP 85
UNCLASSIFIED RE-707 AFOSR-TR-86-0096 F49620-82-C-0025 F/G 20/4

NL



MICROCOPY RESOLUTION TEST CHART
NATIONAL BUREAU OF STANDARDS-1963-A



R85-1154-022B(3/3)

Fig. B-10 Fourth Moments Across 2-D Upwash (Sheet 3 of 3)

END

Dtic

5-86